REDUCING INFECTION SUSCEPTIBILITY OF TITANIUM PERCUTANEOUS

IMPLANTS: A STUDY OF POROUS AND SMOOTH SURFACES

AND MESENCHYMAL STEM CELL TREATMENTS

by

Dorthyann Isackson

A dissertation submitted to the faculty of
The University of Utah
in partial fulfillment of the requirements for the degree of

Doctor of Philosophy

Department of Bioengineering

The University of Utah

May 2012

The University of Utah Graduate School

STATEMENT OF DISSERTATION APPROVAL

The dissertation of   **Dorthyann Isackson**

has been approved by the following supervisory committee members:

Kent N. Bachus	, Chair	**1/5/2012** Date Approved
David W. Grainger	, Member	**1/5/2012** Date Approved
Linda L. Kelley	, Member	**12/30/2011** Date Approved
Scott Miller	, Member	**1/5/2012** Date Approved
Yan-Ting Shiu	, Member	**1/5/2012** Date Approved

and by   **Patrick Tresco**   , Chair of

the Department of   **Bioengineering**

and by Charles A. Wight, Dean of The Graduate School.

ABSTRACT

Percutaneous osseointegrated prosthetics are a promising limb prosthetic alternative for amputees. Similar to other percutaneous devices that have permanent residence in host tissue, their success is dependent on an impassable attachment between skin and the device. An incomplete attachment greatly increases risk of infection and subsequent device removal. A common failure mechanism of percutaneous devices is the epidermis migrating internally, called "epidermal downgrowth," creating a pocket between the skin and the device. This pocket serves as an access point for microorganisms, contributing to infection and device failure. Thus, there is a need to improve the skin integration with the percutaneous device such that microbial access and infection is prevented.

This first portion of this dissertation work sought to investigate infection vulnerability of porous titanium and smooth titanium percutaneous implants with subcutaneous flanges. In this work, a more relevant small animal model of percutaneous device infection was established. It was demonstrated that porous surfaces significantly decreased risk of infection of percutaneous implants. However, due to epidermal downgrowth in the majority of implants, there was an absence of skin integration with the percutaneous component, thus contributing to increased infection susceptibility and device failure.

It is suggested that epidermal downgrowth may occur because of poor vascularization and/or inadequate soluble signaling factors. To prevent downgrowth and improve the skin-implant seal and integration, the remaining portion of the dissertation work evaluated the contributions of mesenchymal stem cells, as they are known to increase vascularization in wound healing environments and to stimulate tissue repair through paracrine signaling mechanisms. It was demonstrated that mesenchymal stem cells accelerated tissue integration and improved the healing response to porous titanium percutaneous implants. This work also demonstrated that in a bacterial challenged environment, porous titanium percutaneous implants treated with mesenchymal stem cells did not develop infection, attesting to the establishment of a more robust barrier to infection compared to that in untreated implants.

The work described herein provides encouraging data that, upon further evaluation and optimization, could potentially be translated to the clinic to improve tissue integration and reduce infections of percutaneous implants, specifically, percutaneous osseointegrated prosthetics.

To my best friend, Todd

TABLE OF CONTENTS

LIST OF TABLES

LIST OF FIGURES

xi

NOMENCLATURE

(BAHA)	Bone-anchored hearing aid
EGF	Epidermal growth factor
KGF	Keratinocyte growth factor
TGF-α	Transforming growth factor alpha
bFGF	Basic fibroblast growth factor
PDGF	Platelet-derived growth factor
VEGF	Vascular endothelial growth factor
TGF-β1	Transforming growth factor beta 1
MSC	Mesenchymal stem cell
IGF-1	Insulin-like growth factor-1
Ang-1	Angiopoietin-1
MIP-1	macrophage inflammatory protein-1
S. aureus	*Staphylococcus aureus*
S. epidermidis	*Staphylococcus epidermidis*
P. aeruginosa	*Pseudomonas aeruginosa*
Ra	Arithmetical mean roughness
Rq	Root-mean square roughness
CFU	Colony forming units

PMN	Polymorphonuclear leukocytes
FBGC	Foreign body giant cell
CNS	Coagulase-negative *Staphylococcus aureus*
PMMA	Poly(methyl methacrylate)
S/S	Smooth percutaneous post with smooth subcutaneous disk
S/P	Smooth percutaneous post with porous subcutaneous disk
P/S	Porous percutaneous post with smooth subcutaneous disk
P/P	Porous percutaneous post with porous subcutaneous disk
PBS	Phosphate-buffered saline
pTi	Porous titanium
Ti6Al4V	Titanium alloy
sTi	Smooth titanium
rTi	Roughened titanium
ASC	Adipose-derived mesenchymal stem cell
BMMSC	Bone marrow-derived mesenchymal stem cell
MEM α	Minimum essential medium alpha
DMEM/F-12	Dulbecco's minimum essential medium (50%) with Ham's F-12 (50%)
SD	Standard deviation
SE	Standard error
FDR	False discovery rate
FWER	Family-wise error rate
SEM	Scanning electron microscopy

microCT	Micro computed tomography
PBS+/+	Phosphate-buffered saline with calcium and magnesium
PBS-/-	Phosphate-buffered saline without calcium and magnesium
SEM/EBSD	Scanning electron microscopy with electron backscattered diffraction
G6PD	Glucose 6-phosphate dehydrogenase
CM	Complete medium
BM	Basal medium
FBR	Foreign body response
IACUC	Institutional Animal Care and Use Committee
FBS	Fetal bovine serum
MMA	Methyl methacrylate
H&E	Hematoxylin and eosin
MSS	Multiple stain solution
MCP-5	Monocyte chemoattractant protein
IHC	Immunohistochemistry
PCR	Polymerase chain reaction
GFP	Green fluorescent protein
FISH	Fluorescence *in situ* hybridization
BrdU	5-bromo-2'-deoxyuridine
CAD	Computer-aided design

ACKNOWLEDGEMENTS

I sincerely thank all who have helped me along this journey. First, to my advisor, Dr. Kent Bachus. Thank you very much for your continual support, mentorship, patience, questioning, constructive criticism, words of wisdom, and encouragement. I also thank past and present members of the Orthopaedic Research Lab, specifically Kevin Cook, Allison Schoeck, Andrew Guss, Heather Greenwall, and Dr. Nick Brown, for their assistance and willingness to help with anything along the way. I thank my undergraduate research assistant, Kevin Cook, who was an immense help and made a valuable contribution to the work.

I would like to extend my sincerest gratitude to my committee members – Drs. Kent Bachus, David Grainger, Scott Miller, Yan-Ting Shiu, and Linda Kelley – for challenging me, for being a wealth of knowledge, and for providing expert advice. You all have been an invaluable resource, and I sincerely appreciate all of your help and guidance.

I would like to acknowledge a couple labs, as they were extremely gracious and accommodating to my work. (a) The Bone and Joint Research Lab: I thank Dr. Roy Bloebaum for allowing me to use their facility and equipment. I thank Tyler Epperson for originally teaching me PMMA histology processing; and Dustin Williams for his contribution to the microbiology portion of my work. (b) Grainger Research Lab: thank

CHAPTER 1

INTRODUCTION

1.1 Prosthetic Technology for Amputees

Currently, the majority of amputees use a socket-type device to connect their

prosthetic limbs to their bodies. These socket prostheses are designed to fit snugly

around the residual limbs and are held in place mechanically through the use of belts,

cuffs, or suction. Over the years, technological advancements with socket prostheses

have greatly improved the lives of amputees, allowing them to be more mobile and to

better engage in an active lifestyle. However, socket prostheses are not without

limitations, including, but not limited to overload and irritation of the adjacent soft tissues

[1-6], disuse osteoporosis in the residual limb [7], difficulty in ongoing socket fit due to

weight fluctuations and muscular atrophy [2, 5, 6], and challenges in fitting individuals

with short residual limbs [8].

To overcome these limitations, percutaneous osseointegrated prosthetics are being

developed as an alternative to socket-type devices [9-17]. Similar to dental implants,

percutaneous osseointegrated prosthetics are anchored to the bone and pass through the

skin, resulting in an abutment to which a limb prosthetic attaches (Figure 1.1) [9, 11, 15,

18, 19]. These unique prosthetics are not for every amputee. Rather, the primary

amputee population to use these prosthetics includes those that have good vascular supply, appropriate bone density, normal wound healing abilities, and overall are healthy individuals. In Europe, patients receiving these implants report improvements in mobility [20, 21], activity levels [20, 21], gait performance [20, 21], and "osseoperception," a sensory feedback in the amputated limb from the surrounding environment [9, 21, 22]. While percutaneous osseointegrated prostheses show great promise for a select amputee population, they permanently disrupt the skin barrier and are at constant risk of infection [15, 21].

1.2 Percutaneous Implant Infection Rates

It is well established that medical device implantation is accompanied by an increased risk of infection [23, 24]. Percutaneous osseointegrated prosthetics currently have a reported 18% infection rate, with most infections developing within the first 3 years of implantation [15, 21]. Similarly, other percutaneous devices, such as central venous catheters, have a reported 3-8% infection rate; heart assist devices, a 25-50% infection rate; and dental implants, a 5-10% infection rate [23]. Bone-anchored hearing aids (BAHAs) have a 23.9% failure rate, including both device infection and other soft tissue problems that typically present within the first year of implantation [25, 26].

The cost for treating these infections is considerable, ranging $40,000 - $70,000 per patient [27]. Treating infections of percutaneous implants typically requires a regimen of antibiotic therapy, and if that is unsuccessful, the next treatment strategy is surgical removal of the device and infected peri-implant tissue [28]. Concerns arise regarding antibiotic therapy as it is well known that once a biofilm is formed on the

implant, it is extremely difficult, if not impossible, for an antibiotic regimen to eradicate the chronic inflammation and subsequent infection [29, 30]. An additional concern is that overuse of antibiotics increases the ability of bacteria to develop resistance to these antibacterial interventions, thus encumbering treatment strategies and perpetuating implant infection [31].

1.3 Cause of Percutaneous Device Infections

Several factors are involved that may determine if and when a percutaneous device will get infected. For example, some more obvious factors include improper surgical implantation, introduction of microorganisms during surgical procedures, poor healing abilities, lack of routine cleaning of the device, misuse of the device, etc. Additional modes of failure as described by Andreas F. von Recum include marsupialization, permigration, mechanical avulsion, and infection unrelated to the other modes of failure [32]. These percutaneous device failure modes will be discussed in more detail later.

All failure mechanisms of percutaneous devices ultimately result in a poor seal between the skin and the device. The interrupted skin-implant seal provides an access point for commensal and noncommensal microorganisms, which, after migration and colonization, will most likely lead to chronic inflammation and/or infection of the peri-implant tissue. Studies evaluating microorganism colonization at the skin-implant interface of percutaneous osseointegrated prosthetics report that *Staphylococcus aureus* and coagulase-negative staphylococci are the most commonly isolated microorganisms [15].

The ideal situation is that the skin with underlying soft tissues acts as the primary barrier to infection through a complete integration and attachment with the percutaneous implant. Numerous studies over the years have acknowledged this, and as such, have presented data addressing potential improvements of skin-implant attachment. Yet, when reflecting over the last 40+ years of studies, development of an infection-free, long-term skin-implant integration has still proved to be a challenge.

1.4 A Walk through the Decades of Percutaneous Implant Studies

In reviewing literature at what has been done to improve percutaneous device residence in host tissue, much of the work that is of relevance to our ultimate goal of infection-free percutaneous osseointegrated prosthetics is that pertaining to dental implants and bone-anchored hearing aids. These devices are typically composed of metal and are implanted for the lifetime of the individual. Thus, this section will primarily review that literature, though with some exceptions.

1.4.1 Related work from the 1800s

Beginning in the mid 1800s, Malgaigne was reported to be the first to use external fixation for fractures [33]. External fixators are similar to percutaneous osseointegrated devices in that they are inserted into the bone and proceed to exit through the skin. With fairly good success, he and others concluded that inflammation and infection around these percutaneous devices were most likely to occur if there was repeated gross motion of the skin around the external fixation pin [33]. Eugene Murphy makes a very interesting statement in his review of Malgaigne's work, regarding positive outcomes of

the percutaneous devices despite aseptic technique and antibiotics. He states,

"…infection-free passage through the skin for weeks or months is not completely

impossible, even with unsophisticated materials and <u>absence of aseptic surgery and of</u>

<u>antibiotics</u>… Malgaigne made a point of <u>avoiding relative motion between skin and</u>

<u>device"</u> [33].

1.4.2 Previous work in the 1900s

In the early to mid 1900s, there were many attempts of prosthetic skeletal

attachment for amputees, especially during and after World War II [33]. In 1946, Dr.

Dümmer, a general surgeon in Pinneburg, Germany, fitted four human subjects with

prostheses attached to the skeleton. These prostheses were later removed (length of time

not mentioned) from all individuals as a result of one individual, termed "a dirty man",

that developed implant infection [33]. Note though, that the other three individuals did

not develop infection.

1.4.2.1 The 1950s

In 1952, Per-Ingvar Brånemark discovered the phenomenon of

"osseointegration," and in the mid 1960s, he and his team in Sweden combined this

concept with that of a percutaneous device and developed the dental implant as a tooth

replacement [9]. Since then, they have used this technology for bone-anchored hearing

aids [9], plastic reconstructive surgery applications [19], thumb replacements [9], and

limb prosthetics [9]. In the 1990s, they began fitting trans-femoral amputees with

osseointegrated limb prosthetics; and, to this day, they have treated over 100 amputees with osseointegrated prosthetics [9, 15].

1.4.2.2 The 1970s

In the 1970s, George D. Winter performed some preliminary experiments in a pig model to study the skin reactions around porous and nonporous implants "sticking" out of the skin surface [34]. His team harvested implant specimens at several time points up to 10 weeks post implantation. Winter concluded that the epidermis will migrate internally along a nonporous implant, creating an unstable skin-implant junction that becomes infected; thus, he concludes that the percutaneous component of a prosthesis should be porous to allow ingrowth of fibrous tissue that results in a stable skin-implant attachment [34]. C.W. Hall also looked at several materials exiting the skin in a goat model that were implanted up to 14 months [35]. Out of the materials evaluated, a nylon velour on the percutaneous component allowed soft tissue ingrowth which eliminated problems of marsupialization and created a "bacteriostatic" seal with the skin [35].

In the late 1970s, Mooney and colleagues investigated stainless steel osseointegrated percutaneous prosthetics with an unpolished carbon surface on the percutaneous component [36]. Three human amputees received these prosthetics; unfortunately, six months later, the prosthetics were removed due to chronic infection [36]. They reported that a good seal at the skin-implant interface never developed, which resulted in serous drainage and/or infection [36]. They concluded that mechanical factors and poor vascularization in the tissue were primarily responsible for percutaneous device failure [36].

1.4.2.3 The 1980s

Now moving into the 1980s, Squier and Collins evaluated soft tissue attachment and epithelial downgrowth as a response to the pore size of Millipore filters (cellulose ester material) using a porcine model [37]. The following pore sizes were analyzed over an 8 week period: 0.025 μm, 0.65 μm, 1.0 μm, 1.2 μm, 3.0 μm, 2.2 μm, 7.0 μm, and 8.0 μm. Though the rate of epidermal downgrowth was more rapid during the first 2 weeks of implantation, it was significantly decreased with larger pore sizes (3.0-8.0 μm), compared to smaller pore sizes (< 3.0 μm) [37]. Their explanation for this observation was that the larger pore sizes allowed for a greater amount of soft tissue ingrowth which acted as a restrictive barrier to any further downward migration of the epidermal tissue [37].

Also in the 80s, some excellent reviews were written on percutaneous device failures and device design parameters [32, 38]. As mentioned previously, Andreas F. von Recum described five principle failure modes of percutaneous implants: marsupialization, permigration, mechanical avulsion, infection and abscess formation, and, lastly, failure due to a combination of mechanisms [32]. He describes these mechanisms based on his research of Dacron velour percutaneous implants in dogs, rabbits, and goats. Briefly, marsupialization is when the epidermis grows internally along the percutaneous component (this process is often called "epidermal downgrowth") creating a sinus tract or a gap between the skin and the implant surface (Figure 1.2). Thus marsupialization is epidermal downgrowth with a sinus tract between the tissue and percutaneous element. Permigration is similar to marsupialization and epidermal downgrowth, but is specific to

completely porous percutaneous elements. Permigration is when the skin migrates inward and then completely through a porous percutaneous component. The completely porous percutaneous component fills with keratinized, non-viable epidermal cells, which over time, leads to extrusion of the implant filled with cell debris. Mechanical avulsion is the extrusion of the device due to mechanical forces. Infection and abscess development at the skin-implant interface is a separate occurrence unrelated to the above described failure modes. And lastly, it is generally agreed upon that percutaneous implant failure is typically a result of a combination of these described mechanisms.

Grosse-Siestrup and Affeld wrote an interesting review on design of percutaneous devices, highlighting the importance of stress reduction at the "three-phase junction," which is the point at which the air, artificial material, and skin tissue meet [38]. Based on their investigations of some naturally found percutaneous devices such as antlers, horns, hair, feathers, fingernails, hoofs, and teeth, they suggested a few implant design parameters intended to reduce stress at the skin-implant interface. For example, one such design was to modify the percutaneous component at the "three-phase junction" by adding a cone or cylinder cuff, or a corrugated elastic cuff. The purpose of these cuffs was to place the skin attachment site at a distance from the central percutaneous component, thus shifting interfacial mechanical stresses [38]. They also suggested that the subcutaneous component should be a flange design that could accommodate tissue ingrowth and impact of external forces. Some designs or geometries of a subcutaneous flange included circular discs with small and large holes, discs with meshwork, discs that appeared as a spoked wheel, discs in the shape of a leaf, and flanges designed like a snowflake [38].

A few years later, Von Recum published his work investigating species-related differences in percutaneous device healing [39]. He examined a Dacron® mesh percutaneous implant in dogs, goats, and rabbits, and found that there were no substantial differences in the tissue response between the three animals, though no statistical evaluations were performed on the histology data. Regarding epidermal downgrowth, he concluded that the rate of downgrowth was significantly increased in the rabbit as opposed to that observed in dogs or goats [39].

1.4.2.4 The 1990s

The field expanded in the 1990s with more groups entering the scene, particularly, John A. Jansen's group at the University of Nijmegen in the Netherlands. A selection of their percutaneous device studies are as follows: evaluations of percutaneous implant location (cranium vs. bone-anchored in tibia) and implant coating (i.e., hydroxyapetite, titanium, and carbon) in a rabbit model [40]; comparisons between a subcutaneous titanium mesh flange and a Dacron velour flange [41, 42]; comparisons between a one-stage surgery (subcutaneous and percutaneous components implanted in a single surgery) versus a two-stage surgery (subcutaneous component in one surgery, allow time for healing, then in second surgery attach percutaneous component to subcutaneous component) [43]; investigations of percutaneous implant tissue reactions in normal and diabetic goat and rabbit models [44-46]; and studies of microgrooved surfaces on percutaneous implants to improve tissue attachment [47]. Though many of these studies were relatively simple and similar, some take home messages are that (1) a sintered titanium mesh as a subcutaneous flange proved to allow better tissue ingrowth with

decreased inflammation compared to a Dacron velour flange [42, 48]; (2) two-stage surgeries had better outcomes than one-stage surgeries [43]; (3) severe, uncontrolled diabetes resulted in increased infection rate and poor healing around soft tissue-anchored percutaneous devices, though, interestingly, bone-anchored percutaneous devices healed uneventfully in both normal and diabetic animals [45, 46]; and (4) microgrooves on catheter-like implants did not inhibit epidermal downgrowth, with similar tissue reaction to both grooved and smooth surfaces [47].

In the 1990s, K.M. Holgers from the Brånemark group in Sweden published a couple articles looking at the microbial flora and the inflammatory cell repertoire at the skin-implant interface of percutaneous implants in humans [49-51]. They showed that the main bacterial isolate was coagulase-negative Staphylococci [51]; and, as one would expect, inflammatory cell infiltrates, specifically lymphocytes, were greater around clinically irritated percutaneous implants compared to nonirritated implants, and were more pronounced around the implant interface compared to distant skin sites with no implant [49, 52]. Like previous groups, they also acknowledged that percutaneous implant success was increased when interfacial motion between the skin and implant was reduced [9, 19].

Chehroudi, Brunette, and colleagues evaluated surface topography of both the subcutaneous and percutaneous components, showing that micromachined grooved surfaces can promote tissue integration and can inhibit epithelial downgrowth; and further, a two-stage surgery improves device performance compared to a one-stage surgery [53-55]. The difference between these studies and the Jansen studies mentioned above are that Chehroudi et al. had very different implant designs, and they studied the

effect of textured surfaces separately on the percutaneous and subcutaneous components (meaning percutaneous component was textured while the subcutaneous was not, and then vice versa) [53-55].

The field kept progressing in the 90s. Fine trabecularized carbon was compared to Dacron concluding the epidermal seal was better around a carbon material than Dacron, though the seal was not durable enough to withstand shear forces at the interface [56]. Knabe et al. highlighted epidermal downgrowth as a failure mechanism by demonstrating downgrowth in all continuous ambulatory peritoneal dialysis catheters that were explanted from humans [57]. Heaney evaluated marsupialization in a murine model, and demonstrated variable data regarding epidermal downgrowth and sinus tract formation, concluding that it reaches its maximum migration distance at 1 week post-operation (note this is contrary to above data from Squier and Collins and many others), and that underlying muscle or granulation tissue can act as a barrier to the migrating epidermis [58]. Okada and Ikada evaluated collagen-immobilization on silicone percutaneous implants. They showed that the tissue pull-out force was much greater for collagen-immobilized implants compared to untreated, and infection and epidermal downgrowth rates were decreased for collagen-treated percutaneous implants [59].

1.4.3 Previous work in the 21st Century

From the year 2000 and on, studies began to be a bit more elaborate. Pendegrass, Blunn, and colleagues studied hydroxyapetite coatings, diamond-like carbon, grooved and porous implants, and percutaneous osseointegrated implants with subcutaneous flanges [10, 60]. They concluded that (a) surface texturing did not have significant

effects on epidermal downgrowth, (b) a subcutaneous flange was important in reducing epidermal downgrowth and interfacial motion, and (c) diamond-like carbon may potentially reduce biofilm formation on percutaneous implants [10, 60]. More recently, they evaluated covalently attached laminin, fibronectin adsorbed to silanized titanium, and fibronectin adsorbed to hydroxyapetite on implants in subcutaneous tissue. They demonstrated that dermal tissue attachment is enhanced around implants with fibronectin adsorbed to silanized tianium and in implants in which fibronectin was adsorbed onto a hydroxyapetite coating [61-63]. Very recently in 2010, Pendegrass, Blunn, and colleagues published a 2-year follow-up report on their first human patient who received a transhumeral bone-anchored prosthesis with a porous subcutaneous flange that was coated with hydroxyapetite [64]. The hydroxyapetite coating, they believed, encouraged soft tissue attachment to the implant achieving what they have coined "osseocutaneous" integration [64].

Over the last few years, Olerud and Fleckman at the University of Washington have produced some work in a murine model evaluating porous poly(HEMA) percutaneous devices, with the goal of establishing an optimal pore size that maximizes epidermal and dermal tissue integration [65-67]. Most recently, they concluded that a 40 μm pore size was the most optimal for skin integration, and that the epidermis halts migratory behavior after 3 days, with no further epidermal downgrowth, marsupialization, or permigration [67]. As a side note, neither larger pore sizes or longer implantation times over 14 days were investigated, among other limitations in the study design [67].

Locally in Salt Lake City, Bloebaum and colleagues have evaluated animal implant infection models and the use of antimicrobials in preventing infection of percutaneous osseointegrated implants, though they have met with minimal success [12, 14, 68]. Bachus and colleagues have demonstrated that porous surfaces can reduce infection rate in a small animal model [16]; and further, they have established a large animal model to study long-term limb compensation of animals with percutaneous osseointegrated prosthetics [17].

1.4.4 Literature summary

In summary, a few recurrent themes are that motion at the skin-implant interface is not conducive to development of an impenetrable seal, porous surfaces appear to improve the likelihood of a functional barrier to form between the skin and implant, and biological coatings are a promising treatment in creating a skin-implant seal. However, it still seems as though progress in research and technological advancement from the early 1900s until now has been slow. Perhaps this is due to extreme variance in study designs, such as use of different animal models, incorporation of various implant designs and diverse materials, different implant placement locations in animal models, and various outcome measurements that are rarely similar between studies. All of these variables create difficulty in formulating concrete comparisons and contrasts between studies. Subsequently, this creates challenges in establishing conclusions regarding improvements of percutaneous device functionality and residence in host tissue. On the other hand, perhaps an incomplete knowledge of the precise reactions and mechanisms involved between the host skin tissue and the implant surface limits development of an

optimal implant design or optimal treatment for successful percutaneous device residence in host tissue.

In any event, while the previously discussed strategies show moderate improvements, most of these modifications consist of a static treatment with little interaction or direct involvement in host tissue healing and integration with the implant surface. A treatment or modification that dynamically interacts with host tissue is an approach that has not yet been pursued. One such strategy is to utilize the body's own wound healing cells to stimulate tissue repair and integration with the implant surface.

1.5 Skin Physiology

It is important to review basic cutaneous physiology, and the general processes that occur during wound healing to fully appreciate the complexity of the dynamic *in vivo* environment that hosts percutaneous implants. Because *in vivo* studies are typically performed in small and large animal models, as opposed to humans, this section will also briefly discuss relevant differences in skin structure between common animal models and humans.

The skin is composed of three basic layers: the epidermis, dermis, and the hypodermis. Beginning from the bottom, the hypodermis is mainly composed of adipose tissue, with the adipocyte being the primary cell. The hypodermis contains blood vessels, nerves, lymphatics, and epidermal appendages. It functions to insulate the body, serve as an energy source, cushion and protect the skin, and aid in skin mobility over underlying structures [69].

The dermis functions to protect, provide elasticity and tensile strength, and aid in thermal regulation, among many other functions. The main types of connective tissue in the dermis are collagen and elastin, with collagen accounting for 75% of the dry weight of skin [69]. The primary cell of the dermis is the fibroblast. The dermis is divided into two parts, the papillary dermis and the reticular dermis. The papillary dermis is adjacent to the basement membrane, hosts the highest concentration of fibroblasts, and is characterized by small-diameter collagen fibrils [69]. Between the papillary dermis and the reticular dermis lies the subpapillary plexus which is a horizontal plane of blood vessels. The reticular dermis is characterized by large-diameter collagen fibrils with elastic fibers surrounding the collagen bundles [69].

Between the epidermis and dermis is the basement membrane, which is important in regulation of cell adhesion, differentiation, cell motility, and in the transmission of extracellular signaling factors [70]. Since the epidermis is avascular, the basement membrane, with vasculature residing just underneath it in the papillary dermis, is a source of oxygen and nutrients for the very active epidermis [69].

The epidermis is a stratified, continually renewing epithelium that is composed of approximately four cell layers characterizing differentiation stages of keratinocytes, which account for 90-95% of all epidermal cells [69]. Adjacent to the basement membrane is the stratum germinativum, or the basal cell layer, consisting of mitotically active keratinocytes and other cells such as melanocytes, Langerhans cells, and Merkel cells. Keratinocytes from the basal layer then differentiate into cells of the stratum spinosum, which then differentiate into keratinocytes of the stratum granulosum, or the granular layer. From the granular layer, keratinocytes terminally differentiate into a

cornified cell of the stratum corneum. The stratum corneum is composed of multiple layers of non-viable corneocytes, the largest cell in the keratinocyte family. The time it takes for keratinocytes in the basal layer to transition to the corneum is termed the "transit time." In normal human skin the transit time is approximately 14 days [69]. The epidermis functions to prevent dehydration and absorbance of environmental substances, and acts as the first layer of mechanical protection [69]. This effective barrier function of the stratum corneum is due to its "brick and mortar" structure in that the corneocytes (bricks) are surrounded by an extracellular lipid matrix (mortar) [69].

Even with this simple, brief review of skin morphology, we can see that the skin is quite complex. So how does human skin morphology differ from other animal skin morphology? Most studies evaluating skin wound healing or percutaneous implant behavior in skin are performed in small animals or other larger vertebrates. This makes it necessary to not only appreciate human skin, but also appreciate the differences in small and large animals.

In Table 1.1, the major differences in skin physiology between humans and other vertebrate animals are outlined. An important difference between man and other vertebrates is that man, and to a certain extent pig, does not have a panniculous carnosus. As a result, man and pigs heal by an epithelialization mechanism as opposed to a contraction mechanism found in small animals [71-73]. This has an impact on wound closure rate as contraction is a faster mechanism of closing wounds compared to epithelialization [74]. In addition, humans and pigs are considered "tight-skinned" mammals as their skin tissues are well attached to underlying fascia and muscles. On the other hand, "loose-skinned" small animals lack attachment between the skin layers with

underlying fascia and muscle, and thus rely on the panniculus carnosus and skin

contractility to produce skin closure when wounded.   In full thickness wounds, as

opposed to partial thickness wounds, wound closure is relatively similar in humans and

animals as it is by epithelialization, contraction, and filling of granulation tissue in the

void space, though keep in mind that small animals additionally have the assistance of the

panniculus carnosus [74].

To further understand the *in situ* environment of percutaneous implants, the next

section will discuss general mechanisms involved in the wound healing process, with

focus on human skin.

1.6 Basic Overview of Wound Healing and Foreign Body Response

The skin is the largest organ in the body, and serves as our first line of protection

against the environment.   When the skin barrier is breached, what follows is an intricate,

complex orchestration of many cell types and soluble factors working in synchrony to

bring wound closure. Wound healing of the skin can be divided into three overlapping

phases: inflammation, new tissue formation, and tissue remodeling.

During the first phase of healing, tissue injury causes blood vessel disruption and

extravasation of blood components. A blood clot provides a provisional extracellular

matrix for cellular migration; and platelets, through release of alpha granules, secrete

multiple wound healing signaling factors that attract cells to the site. Neutrophils are

recruited to begin cleaning, and they in return recruit macrophages to assist in debriding

the wound of bacteria and cellular debris through phagocytosis [75].   Within hours of

injury, keratinocytes through expression of integrin receptors begin to migrate over the

wound bed, interacting with extracellular matrix proteins, such as fibronectin, vitronectin, and type I collagen [76].

The second stage of wound repair begins 2-10 days after injury and is characterized by increased cellular proliferation and migration of a variety of cells [77]. The epidermal cells behind the migrating margin continue to proliferate and produce extracellular matrix components, including typeV collagen, type VII collagen, and laminin, all of which will reconstitute the basement membrane zone, the source of oxygen and nutrients for the epidermal cells [69]. The exact mechanism behind epidermal cell migration is not fully understood, but in simplicity is thought to be attributed to (a) the "free edge" effect and the need to be in contact with neighboring cells; and (b) a response to chemotactic factors, such as epidermal growth factor (EGF), keratinocyte growth factor (KGF), and transforming growth factor α (TGF-α) [69, 75, 78-81]. Epidermal cells eventually transform back to their original phenotype and reestablish their connection with the basement membrane and dermis [75]. The second stage of healing is also characterized by replacement of the fibrin matrix with granulation tissue, which is composed of many capillaries, macrophages, and fibroblasts [75, 77]. Macrophages release growth factors that stimulate fibroplasia and angiogenesis; fibroblasts synthesize, deposit, and remodel the extracellular matrix; and blood vessels provide the oxygen and nutrients to sustain cellular activity [69, 75].

The third stage of healing, beginning 2-3 weeks after injury, is characterized by the transformation of granulation tissue into mature scar tissue [69]. The fibroblast is the primary player in the third phase, producing fibronectin, hyaluronic acid, proteoglycans, and collagen, all important in cellular migration and tissue support [69]. The fibroblast

also changes phenotype to a myofibroblast configuration which influences contraction of the wound edges [69, 75, 77]. After the collagen matrix is deposited, endothelial cells, macrophages, and myofibroblasts undergo apoptosis and a number of newly formed blood vessels disintegrate, leaving behind an acellular, reduced vasculature stroma [75, 77]. Final wound closure is a synchrony between re-epithelialization and myofibroblast contraction of the wound region, and over time, the acellular matrix which mainly consists of type III collagen is remodeled back to type I collagen [69, 75, 77].

In summary, during wound repair, immune cells (e.g., macrophages, lymphocytes, polymorphonuclear cells, etc.), fibroblasts, keratinocytes, endothelial cells, and stem cells interact with the extracellular matrix. These cells secrete and respond to growth factors, cytokines, chemokines, and proteinases; and together they bring skin closure and tissue restoration [82]. Among the key growth factors present are basic fibroblast growth factor (bFGF), EGF, platelet-derived growth factor (PDGF), vascular endothelial growth factor (VEGF), and transforming growth factor (TGF-β1) [75, 77]. These soluble signaling factors are critical in angiogenesis; and in recruiting mesenchymal stem cells, macrophages, and fibroblasts. Soluble signaling factors stimulate fibroblasts to synthesize collagen matrix, epidermal cells to migrate over the wound bed, and macrophages to debride the wound tissue and release additional signaling factors.

In addition to understanding the general mechanisms of wound healing, it is also necessary to appreciate the tissue response that evolves when a biomaterial is implanted in the body. When a medical device is implanted, mechanisms of the wound healing cascade occur; however, in addition, a foreign body response will develop. In the first few seconds of device implantation, proteins adsorb to the implant surface and cells

subsequently adhere to this adsorbed protein layer [83]. Protein adsorption is greatly influenced by the surface characteristics of the material. Surface chemistry, hydrophobicity, and charge all influence adsorbed protein structure [84]. When inflammatory cells reach the implant, they will react to the adsorbed proteins and will release signaling factors in response to the protein configurations [85]. The signaling factors that are released may recruit more cells, or may increase phagocytosis attempts of the implanted biomaterial [85, 86].

During the second stage of wound repair, a chronic inflammation develops, which is characterized by macrophages, monocytes, foreign body giant cells, and lymphocytes at the implant surface. Further, there is an increase in vasculature and connective tissue in the surrounding stroma [85, 86]. Following the granulation phase and chronic inflammatory phase of healing, a fibrous capsule will form around the biomaterial. The purpose of which is to isolate the foreign material from the *in vivo* tissue environment [87]. The fibrous encapsulation is accompanied by macrophages and foreign body giant cells that line the implant surface [87]. The shape, surface texture, and surface chemistry of the implant will determine the extent of the foreign body reaction and fibrotic response. For example, porous materials will typically have an increased presence of macrophages and foreign body giant cells, but often will have decreased fibrous encapsulation compared to smooth surface implants [85, 87].

To this day, our understanding of the exact details involved in wound repair and the foreign body response is limited. Nonetheless, it is important to appreciate what is known and apply this knowledge to improvement of the healing process involved with

percutaneous implants. The field of wound healing therapeutics provides many examples of applying wound healing biology to assist the body in restoring the skin as the barrier.

1.7 Wound Healing Therapeutics

Chronic, nonhealing wounds present challenges in the clinic. Wound healing therapeutics are intended to treat chronic wounds by stimulating the wound tissue bed through appropriate biological cues to bring restoration of the skin barrier. Some of the more commonly used therapeutics include occlusive dressings (Tegaderm™, 3M™, St. Paul, MN), antimicrobial dressings (Silvercel®, Systagenix, Quincy, MA), collagen dressings (Skin Temp II™, Human BioSciences, Gaithersburg, MD), bioengineered skin grafts composed of fibroblasts, collagen, and a synthetic scaffold (Dermagraft®, Advanced BioHealing, La Jolla, CA), bioengineered skin grafts composed of fibroblasts and keratinocytes seeded on a collagen scaffold (Apligraf®, Organogenesis, Canton, MA), gels containing PDGF-BB (Regranex®, Johnson and Johnson, New Brunswick, NJ), vacuum-assist devices, honey treatments, and laser therapies, among many other therapeutics [88, 89]. Because of the necessity for growth factors to be present in order for a wound to heal properly, growth factor delivery is a prime candidate as a regenerative therapeutic for chronic wounds. Currently, PDGF-BB is the only FDA-approved growth factor to be used as a therapeutic (Regranex®, Johnson and Johnson Wound Management-Ethicon; GEM 21S®, Osteohealth®) [90]. Unfortunately, use of growth factor treatments has proved to be discouraging in the remedy of chronic wounds. This is most likely due to the complex set of interactions among many (not just one)

growth factors and cytokines, blood elements, extracellular matrix components, and multiple cell types [75, 77].

A relatively newer market in regenerative medicine and wound healing therapeutics is that encompassing adult mesenchymal stem cell therapy [91-93]. Adult mesenchymal stem cells (MSCs) can be derived from bone marrow, adipose tissue, umbilical cord blood, placenta, among many other niches in the body. Due to their immunomodulatory properties, MSCs are attractive in that they can be an autologous, allogeneic, or even a xenogeneic source [94]. In addition to the treatment of chronic wounds, MSCs are currently being investigated for treatment of other clinical pathologies in the fields of cardiology (myocardial infarction, heart failure [95]), orthopaedics (critical-size bone defects, cartilage regeneration [96-98]), gastroenterology (Crohns disease [99]), and nephrology (acute kidney injury[100]). The stem cell therapeutic market, though in its infancy, is expected to be a viable, growing market. Currently, sales of stem cell therapeutics are ~$21.3 million and are likely to have an annual growth rate of 29.2% reaching more than $11 billion by 2020 [89].

1.8 Mesenchymal Stem Cells

Why would MSCs be an attractive therapeutic for wound healing, and even further, for percutaneous device applications? First, for wound healing applications, MSCs are fundamental in the wound repair process [82], and they have been shown to contribute significantly to re-establishing the dermal tissue barrier [101]. Studies through the years have published very promising results regarding the ability of MSCs to accelerate wound healing [92, 102-104], increase vascularization [92, 103, 104], increase

cellularity [92, 103, 104], and increase collagen content and wound strength [102, 104, 105]. It is suggested that MSCs produce these effects through two possible mechanisms: (1) through paracrine signaling mechanisms, releasing soluble signaling factors, including EGF, KGF, insulin-like growth factor-1 (IGF-1), VEGF-α, angiopoietin-1 (Ang-1), macrophage inflammatory protein (MIP-1a and MIP-1b), PDGF-BB, FGF, among others [106-108], and/or (2) through differentiation into resident cells [103, 109]. Though in early stages, mesenchymal stem cell therapy holds great promise for chronic wound healing conditions and diverse tissue repair applications, including applications that involve implants, devices, or scaffolds.

1.9 Mesenchymal Stem Cell Treatments for the Improvement
of the Skin-Implant Interface

Mesenchymal stem cells are an attractive therapeutic for improving the skin-implant interface of percutaneous devices because of the above stated properties in that they are an important native cell in the wound healing process, and they are a source of biochemical signaling factors important in skin tissue growth, repair, and closure. Specifically, for the epidermis to close, it needs proper wound signaling cues, appropriate cellular proliferation and activity, and sufficient blood supply to provide nutrients and oxygen [75, 77]. MSCs are capable of providing the soluble signaling factors, of stimulating resident cells, and of promoting vascularization [110]. Results from recent studies looking at the application of MSCs to influence healing around biomaterials [111-114] are encouraging and suggest that these cells stimulate vascularization and decrease the foreign body response around implanted biomaterials. Thus, MSCs possess potential

to stimulate neovascularization for the migrating epidermis and dermis, and to promote a rapid restoration and integration of the epidermal and dermal tissues with a percutaneous device.

As mentioned in sections 1.3 and 1.4 above, it is thought that epidermal downgrowth, marsupialization, and poor vascularization are attributed to percutaneous device failure and increased infection risk [10, 32, 34, 48, 57, 115]. The explanations for these phenomenons are not entirely clear. Possible explanations could include insufficient wound healing signaling cues and lack of cell contact inhibition in the epidermal and dermal tissues [78, 80, 116]; in addition to insufficient vascularization of the dermal tissues in providing nutrients for the restoration of the epidermal and dermal barrier [32, 34, 69]. To address these possible mechanisms, the proven results of mesenchymal stem cells in wound repair applications may transfer to this situation in which the epidermal and dermal tissues need appropriate cellular activity, biochemical signaling cues, and vascular supply to produce a timely closure and seal between the device and the skin.

1.10 Conclusions

In summary, the motivation for this dissertation work is to improve tissue integration with percutaneous devices such that a durable, formidable seal is created between the implant and host tissue thereby preventing infectious complications. The long-term motivation for this work is to develop a strategy that could potentially be used to improve the long-term residence of percutaneous osseointegrated prosthetics in human patients.

To briefly recapitulate what this introduction has covered, first, the concept of a percutaneous osseointegrated prosthetic was presented, followed by a discussion of elevated infection risks of percutaneous devices. Second, a selection of relevant research studies and their contributions to the field of permanent percutaneous devices were highlighted. From this review, it was emphasized that previous work has focused primarily on static treatments to implants. Third, basic skin physiology and wound healing mechanisms were reviewed to better understand the dynamic, complex environment that hosts percutaneous devices. The goal of this review was to learn from what the body does so well to develop a strategy that could improve tissue integration with perctuaneous devices. It was highlighted that a very important cell in wound healing and routine skin maintenance is the mesenchymal stem cell. Because of key roles MSCs play in tissue repair and regeneration, they are highly sought after in treating several clinical conditions, in addition to improving tissue response to biomaterials. Then lastly, it was proposed that MSCs may possess the capacity to prevent epidermal downgrowth and, overall, improve tissue integration with percutaneous implants.

Based on the material presented in the previous sections, the following dissertation work was governed by two primary aims: (1) determine infection susceptibility of porous and smooth titanium percutaneous devices in an appropriate implant infection animal model, and (2) evaluate the efficacy of MSCs in improving the skin-implant seal to prevent infections of porous metal percutaneous devices.

1.11 Dissertation Chapter Overview

Each following chapter, excluding Chapter 6, is an individual published manuscript or is pending publication. An overview of the subsequent chapters are provided below, including the study question, study rationale, the hypothesis or aim that was tested, the experimental model, and the publication information.

1.11.1 Chapter 2

1.11.1.1 Study question: Can porous coatings as opposed to smooth surfaces on percutaneous implants with subcutaneous flanges create a more effective dermal barrier to infection?

1.11.1.2 Rationale: It is unclear from previous published studies if porous or smooth titanium surfaces on percutaneous and/or subcutaneous components are effective in preventing infection of percutaneous implants. This lack of clarity is due in part to the absence of strong implant infection signals in previously published small animal studies.

1.11.1.3 Hypothesis: "…*the incidence of infection of metal percutaneous devices will be lowest when both the percutaneous and the subcutaneous components have a porous coating; whereas, the incidence of infection will be highest when both the percutaneous and the subcutaneous components have a smooth surface…*" [16].

1.11.1.4 Experimental model: Four percutaneous implants with smooth and porous surfaces were implanted on the dorsum of a rabbit. The implants received weekly inoculations of *Staphylococcus aureus* creating an infectious environment to allow assessment of implant infection risk.

1.11.1.5 Publication: Isackson D, McGill LD, Bachus KN. *Percutaneous implants with porous titanium dermal barriers: an in vivo evaluation of infection risk.* Medical Engineering and Physics, 2011. 33(4): p. 418-426.

1.11.2 Chapter 3

1.11.2.1 Study question: Does the solution that is used to deliver MSCs on a porous titanium implant have an effect on cellular adherence and cytotoxicity prior to *in vivo* transplantation?

1.11.2.2 Rationale: There are a couple commonly reported solutions used to deliver MSCs for *in vivo* applications, these include serum-supplemented cell culture medium, basal culture medium (serum-free), and phosphate buffered solutions. Thus, before studying the *in vivo* contribution of MSCs in promoting tissue integration with percutaneous implants, this study sought to examine effects of these commonly reported solutions on MSCs. The end objective was to select the solution most appropriate for our future *in vivo* transplantation studies.

1.11.2.3 Study aim: The aims for this study were to determine (a) the effect the cell delivery solution had on MSC adherence to porous coated titanium surfaces, and (b) the effect the cell delivery solution had on MSC cytotoxicity when seeded on porous coated titanium surfaces over a 24-hour period.

1.11.2.4 Experimental model: *In vitro* cell culture techniques were used to quantify cellular adherence and cyotoxicity when MSCs were seeded on porous titanium surfaces in serum-supplemented cell culture medium, basal cell culture medium, and phosphate buffered saline solutions.

1.11.2.5 Publication: Isackson D, Cook KJ, Bachus KN. *In Vitro Investigation of Mesenchymal Stem Cell Cytotoxicity and Adherence to Porous Titanium Surfaces in Various Delivery Solutions for In Vivo Transplantation Studies*. Cytotechnology. Under Review.

1.11.3 Chapter 4

    1.11.3.1 Study question: Can MSCs improve the quantity, quality, and rate of tissue integration with porous metal percutaneous implants?

    1.11.3.2 Rationale: Our previous work in a rabbit model showed that porous surfaces decreased infection risk of percutaneous implants. However, in most implants there was an absence of skin integration into the percutaneous component as a result of epidermal downgrowth. Due to the contribution of MSCs in wound healing and in stimulating tissue repair, this study sought to evaluate the contribution, if any, of MSCs to stimulate epidermal and dermal ingrowth into the porous percutaneous implant such that epidermal downgrowth was eliminated. Further, this study evaluated if MSCs increased the rate of tissue integration, and if the overall quality of the tissue integration was improved.

    1.11.3.3 Hypothesis: *MSC-treated implants will have a more rapid and mature tissue integration compared to untreated implants.*

    1.11.3.4 Experimental model: An *in vivo* rat model was used to study the tissue ingrowth of MSC-treated and untreated implants placed on the rat dorsum. Histology analyses were performed at 0, 3, 7, 28, and 56 days after transplantation to assess the

quality of tissue integration and the rate of integration between the treated and untreated implants.

1.11.3.5 Publication: Isackson D, Cook KJ, McGill LD, Bachus KN. *Mesenchymal Stem Cells Increase Collagen Infiltration and Improve Wound Healing Response to Porous Titanium Percutaneous Implants.* Medical Engineering and Physics. 2011. Under Review.

1.11.4 Chapter 5

1.11.4.1 Study question: Is the infection risk decreased when percutaneous implants are treated with MSCs?

1.11.4.2 Rationale: In our original rabbit study, the primary objective was to create an infection-prone environment such that percutaneous implant infection risk could be realistically assessed. The rationale for this study was similar, though infection risk of MSC- treated porous titanium percutaneous implants was assessed in a rat model.

1.11.4.3 Hypothesis: *MSC-treated implants will present with a reduced risk of infection compared to untreated implants.*

1.11.4.4 Experimental model: Using a rat model, we tested this hypothesis by challenging MSC-treated and untreated implants with weekly bacterial inoculations two weeks after implantation to determine if the MSC-treatment prevented infection development. *Staphylococcus aureus* was used for inoculations of the implants to create an infection-prone environment. Implant infection was confirmed through clinical symptoms of infection, positive bacterial cultures, and histology evidence of tissue infection.

1.11.4.5 Publication: Isackson D, Cook KJ, McGill LD, Bachus KN.

Mesenchymal Stem Cell Therapeutics Improve Tissue Integration with Porous Metal

Percutaneous Implants and Decrease Infection Risk. Journal of Tissue Engineering and

Regenerative Medicine. 2011. Under Review.

1.11.5 Chapter 6

In Chapter 6, overall conclusions will be drawn regarding the presented research

work that sought to investigate the use of porous titanium coatings and mesenchymal

stem cell treatments to improve the tissue barrier to percutaneous implants, thus

preventing risk of infection. Research challenges and direction of future work will be

outlined with respect to percutaneous device studies and mesenchymal stem cell

therapies.

1.12 References

1.   Dillingham TR, Pezzin LE, MacKenzie EJ, Burgess AR. Use and satisfaction with prosthetic devices among persons with trauma-related amputations: a long-term outcome study. American journal of physical medicine & rehabilitation / Association of Academic Physiatrists 2001;80(8):563-571.

2.   Hoaglund FT, Jergesen HE, Wilson L, Lamoreux LW, Roberts R. Evaluation of problems and needs of veteran lower-limb amputees in the San Francisco Bay Area during the period 1977-1980. Journal of rehabilitation R&D / Veterans Administration, Department of Medicine and Surgery, Rehabilitation R&D Service 1983;20(1):57-71.

3.   Legro MW, Reiber G, del Aguila M, Ajax MJ, Boone DA, Larsen JA, et al. Issues of importance reported by persons with lower limb amputations and prostheses. J Rehabil Res Dev 1999;36(3):155-163.

4.   Lyon CC, Kulkarni J, Zimerson E, Van Ross E, Beck MH. Skin disorders in amputees. Journal of the American Academy of Dermatology 2000;42(3):501-507.

5.   Pezzin LE, Dillingham TR, Mackenzie EJ, Ephraim P, Rossbach P. Use and satisfaction with prosthetic limb devices and related services. Archives of physical medicine and rehabilitation 2004;85(5):723-729.

6.   Sherman RA. Utilization of prostheses among US veterans with traumatic amputation: a pilot survey. J Rehabil Res Dev 1999;36(2):100-108.

7.   Gailey R, Allen K, Castles J, Kucharik J, Roeder M. Review of secondary physical conditions associated with lower-limb amputation and long-term prosthesis use. J Rehabil Res Dev 2008;45(1):15-29.

8.   Bowen RE, Struble SG, Setoguchi Y, Watts HG. Outcomes of lengthening short lower-extremity amputation stumps with planar fixators. J Pediatr Orthop 2005;25(4):543-547.

9.   Branemark R, Branemark PI, Rydevik B, Myers RR. Osseointegration in skeletal reconstruction and rehabilitation: a review. J Rehabil Res Dev 2001;38(2):175-181.

10.   Pendegrass CJ, Goodship AE, Blunn GW. Development of a soft tissue seal around bone-anchored transcutaneous amputation prostheses. Biomaterials 2006;27(23):4183-4191.

11.   Hagberg K, Branemark R. One hundred patients treated with osseointegrated transfemoral amputation prostheses--rehabilitation perspective. J Rehabil Res Dev 2009;46(3):331-344.

12.   Chou TG, Petti CA, Szakacs J, Bloebaum RD. Evaluating antimicrobials and implant materials for infection prevention around transcutaneous osseointegrated implants in a rabbit model. J Biomed Mater Res A 2010;92(3):942-952.

13.   Isaacson BM, Stinstra JG, MacLeod RS, Webster JB, Beck JP, Bloebaum RD. Bioelectric analyses of an osseointegrated intelligent implant design system for amputees. J Vis Exp 2009(29):1-6.

14.   Perry EL, Beck JP, Williams DL, Bloebaum RD. Assessing peri-implant tissue infection prevention in a percutaneous model. J Biomed Mater Res B Appl Biomater 2010;92(2):397-408.

15.   Tillander J, Hagberg K, Hagberg L, Branemark R. Osseointegrated titanium implants for limb prostheses attachments: infectious complications. Clin Orthop Relat Res 2010;468(10):2781-2788.

16.   Isackson D, McGill LD, Bachus KN. Percutaneous implants with porous titanium dermal barriers: an in vivo evaluation of infection risk. Med Eng Phys 2011;33(4):418-426.

17.   Shelton TJ, Beck JP, Bloebaum RD, Bachus KN. Percutaneous osseointegrated prostheses for amputees: Limb compensation in a 12-month ovine model. J Biomech 2011;44(15):2601-2606.

18.   Carlsson L, Rostlund T, Albrektsson B, Albrektsson T, Branemark PI. Osseointegration of titanium implants. Acta Orthop Scand 1986;57(4):285-289.

19.   Albrektsson T, Branemark PI, Jacobsson M, Tjellstrom A. Present clinical applications of osseointegrated percutaneous implants. Plast Reconstr Surg 1987;79(5):721-731.

20.   Hagberg K, Branemark R, Gunterberg B, Rydevik B. Osseointegrated trans-femoral amputation prostheses: prospective results of general and condition-specific quality of life in 18 patients at 2-year follow-up. Prosthet Orthot Int 2008;32(1):29-41.

21.   Sullivan J UM, Robinson KP, et al. Rehabilitation of the trans-femoral amputee with an osseointegrated prosthesis: the United Kingdom experience. Prosthet Orthot Int 2003(27):114-120.

22.   Jacobs R, Branemark R, Olmarker K, Rydevik B, Van Steenberghe D, Branemark PI. Evaluation of the psychophysical detection threshold level for vibrotactile and pressure stimulation of prosthetic limbs using bone anchorage or soft tissue support. Prosthet Orthot Int 2000;24(2):133-142.

23.   Darouiche RO. Device-associated infections: a macroproblem that starts with microadherence. Clin Infect Dis 2001;33(9):1567-1572.

24.   Yu JL, Andersson R, Parsson H, Hallberg E, Ljungh A, Bengmark S. A bacteriologic and scanning electron microscope study after implantation of foreign bodies in the biliary tract in rats. Scand J Gastroenterol 1996;31(2):175-181.

25.   Hobson JC, Roper AJ, Andrew R, Rothera MP, Hill P, Green KM. Complications of bone-anchored hearing aid implantation. The Journal of Laryngology and Otology 2010;124(2):132-136.

26.   Badran K, Arya AK, Bunstone D, Mackinnon N. Long-term complications of bone-anchored hearing aids: a 14-year experience. The Journal of Laryngology and Otology 2009;123(2):170-176.

27.   Chu VH, Crosslin DR, Friedman JY, Reed SD, Cabell CH, Griffiths RI, et al. Staphylococcus aureus bacteremia in patients with prosthetic devices: costs and outcomes. The American Journal of Medicine 2005;118(12):1416.

28.   Darouiche RO. Treatment of infections associated with surgical implants. N Engl J Med 2004;350(14):1422-1429.

29.   Costerton W, Veeh R, Shirtliff M, Pasmore M, Post C, Ehrlich G. The application of biofilm science to the study and control of chronic bacterial infections. J Clin Invest 2003;112(10):1466-1477.

30.   Costerton JW, Stewart PS, Greenberg EP. Bacterial biofilms: a common cause of persistent infections. Science 1999;284(5418):1318-1322.

31.   Weinstein RA. Controlling antimicrobial resistance in hospitals: infection control and use of antibiotics. Emerg Infect Dis 2001;7(2):188-192.

32.   von Recum AF. Applications and failure modes of percutaneous devices: a review. J Biomed Mater Res 1984;18(4):323-336.

33.   Murphy EF. History and philosophy of attachment of prostheses to the musculo-skeletal system and of passage through the skin with inert materials. J Biomed Mater Res 1973;7(3):275-295.

34.   Winter GD. Transcutaneous implants: reactions of the skin-implant interface. J Biomed Mater Res 1974;8(3):99-113.

35.   Hall CW. Developing a permanently attached artificial limb. Bull Prosthet Res 1974:144-157.

36.   Mooney V, Schwartz SA, Roth AM, Gorniowsky MJ. Percutaneous implant devices. Ann Biomed Eng 1977;5(1):34-46.

37.   Squier CA, Collins P. The relationship between soft tissue attachment, epithelial downgrowth and surface porosity. J Periodontal Res 1981;16(4):434-440.

38.   Grosse-Siestrup C, Affeld K. Design criteria for percutaneous devices. J Biomed Mater Res 1984;18(4):357-382.

39.   Gangjee T, Colaizzo R, von Recum AF. Species-related differences in percutaneous wound healing. Ann Biomed Eng 1985;13(5):451-467.

40.   Jansen JA, van der Waerden JP, van der Lubbe HB, de Groot K. Tissue response to percutaneous implants in rabbits. J Biomed Mater Res 1990;24(3):295-307.

41.   Jansen JA, van der Waerden JP, de Groot K. Development of a new percutaneous access device for implantation in soft tissues. J Biomed Mater Res 1991;25(12):1535-1545.

42.   Paquay YC, de Ruigter J.E., van der Waerden, J.P.C.M., Jansen, J.A. Tissue reaction to Dacron velour and titanium fibre mesh used for anchorage of percutaneous devices. Biomaterials 1996;17(12):1251-1256.

43.   Paquay YC, De Ruijter AE, van der Waerden JP, Jansen JA. A one stage versus two stage surgical technique. Tissue reaction to a percutaneous device provided with titanium fiber mesh applicable for peritoneal dialysis. ASAIO J 1996;42(6):961-967.

44.   Gerritsen M, Paquay YG, Jansen JA. Evaluation of the tissue reaction to a percutaneous access device using titanium fibre mesh anchorage in goats. J Mater Sci Mater Med 1998;9(9):523-528.

45.   Gerritsen M, Lutterman JA, Jansen JA. Wound healing around bone-anchored percutaneous devices in experimental diabetes mellitus. J Biomed Mater Res 2000;53(6):702-709.

46.   Gerritsen M, Lutterman JA, Jansen JA. The influence of impaired wound healing on the tissue reaction to percutaneous devices using titanium fiber mesh anchorage. J Biomed Mater Res 2000;52(1):135-141.

47.   Walboomers XF, Jansen JA. Effect of microtextured surfaces on the performance of percutaneous devices. J Biomed Mater Res A 2005;74(3):381-387.

48.   Jansen JA, Walboomers XF. A new titanium fiber mesh-cuffed peritoneal dialysis catheter: an experimental animal study. J Mater Sci Mater Med 2001;12(10-12):1033-1037.

49.   Holgers KM, Branemark PI. Immunohistochemical study of clinical skin-penetrating titanium implants for orthopaedic prostheses compared with implants in the craniofacial area. Scand J Plast Reconstr Surg Hand Surg 2001;35(2):141-148.

50.   Holgers KM, Thomsen P, Tjellstrom A, Ericson LE. Electron microscopic observations on the soft tissue around clinical long-term percutaneous titanium implants. Biomaterials 1995;16(2):83-90.

51.	Holgers KM, Ljungh A. Cell surface characteristics of microbiological isolates from human percutaneous titanium implants in the head and neck. Biomaterials 1999;20(14):1319-1326.

52.	Holgers KM, Thomsen P, Tjellstrom A, Bjursten LM. Immunohistochemical study of the soft tissue around long-term skin-penetrating titanium implants. Biomaterials 1995;16(8):611-616.

53.	Chehroudi B, Brunette DM. Subcutaneous microfabricated surfaces inhibit epithelial recession and promote long-term survival of percutaneous implants. Biomaterials 2002;23(1):229-237.

54.	Chehroudi B, Gould TR, Brunette DM. A light and electron microscopic study of the effects of surface topography on the behavior of cells attached to titanium-coated percutaneous implants. J Biomed Mater Res 1991;25(3):387-405.

55.	Chehroudi B, Gould TR, Brunette DM. The role of connective tissue in inhibiting epithelial downgrowth on titanium-coated percutaneous implants. J Biomed Mater Res 1992;26(4):493-515.

56.	Tagusari O, Yamazaki K, Litwak P, Kojima A, Klein EC, Antaki JF, et al. Fine trabecularized carbon: ideal material and texture for percutaneous device system of permanent left ventricular assist device. Artif Organs 1998;22(6):481-487.

57.	Knabe C, Grosse-Siestrup C, Gross U. Histologic evaluation of a natural permanent percutaneous structure and clinical percutaneous devices. Biomaterials 1999;20(6):503-510.

58.	Heaney TG, Doherty PJ, Williams DF. Marsupialization of percutaneous implants in presence of deep connective tissue. J Biomed Mater Res 1996;32(4):593-601.

59.	Okada T, Ikada Y. Surface modification of silicone for percutaneous implantation. J Biomater Sci Polym Ed 1995;7(2):171-180.

60.	Smith TJ, Galm A, Chatterjee S, Wells R, Pedersen S, Parizi AM, et al. Modulation of the soft tissue reactions to percutaneous orthopaedic implants. J Orthop Res 2006;24(7):1377-1383.

61.	Chimutengwende-Gordon M, Pendegrass C, Blunn G. Enhancing the soft tissue seal around intraosseous transcutaneous amputation prostheses using silanized fibronectin titanium alloy. Biomedical Materials 2011;6(2).

62.	Gordon DJ, Bhagawati DD, Pendegrass CJ, Middleton CA, Blunn GW. Modification of titanium alloy surfaces for percutaneous implants by covalently attaching laminin. J Biomed Mater Res A 2010;94(2):586-593.

63.   Middleton CA, Pendegrass CJ, Gordon D, Jacob J, Blunn GW. Fibronectin silanized titanium alloy: a bioinductive and durable coating to enhance fibroblast attachment in vitro. J Biomed Mater Res A 2007;83(4):1032-1038.

64.   Kang NV, Pendegrass C, Marks L, Blunn G. Osseocutaneous integration of an intraosseous transcutaneous amputation prosthesis implant used for reconstruction of a transhumeral amputee: case report. J Hand Surg Am 2010;35(7):1130-1134.

65.   Fukano Y, Usui ML, Underwood RA, Isenhath S, Marshall AJ, Hauch KD, et al. Epidermal and dermal integration into sphere-templated porous poly(2-hydroxyethyl methacrylate) implants in mice. J Biomed Mater Res A 2010;94(4):1172-1186.

66.   Isenhath SN, Fukano Y, Usui ML, Underwood RA, Irvin CA, Marshall AJ, et al. A mouse model to evaluate the interface between skin and a percutaneous device. J Biomed Mater Res A 2007;83(4):915-922.

67.   Underwood RA, Usui ML, Zhao G, Hauch KD, Takeno MM, Ratner BD, et al. Quantifying the effect of pore size and surface treatment on epidermal incorporation into percutaneously implanted sphere-templated porous biomaterials in mice. J Biomed Mater Res A 2011;98(4):499-508.

68.   Williams DL, Bloebaum RD, Beck JP, Petti CA. Characterization of bacterial isolates collected from a sheep model of osseointegration. Curr Microbiol 2010;61(Copyright (C) 2011 U.S. National Library of Medicine.):574-583.

69.   Freinkel R, Woodley, DT. The Biology of the Skin. New York: The Parthenon Publishing Group Inc., 2001.

70.   Hashmi S, Marinkovich MP. Molecular organization of the basement membrane zone. Clin Dermatol 2011;29(4):398-411.

71.   Sullivan TP, Eaglstein WH, Davis SC, Mertz P. The pig as a model for human wound healing. Wound Repair Regen 2001;9(2):66-76.

72.   Dorsett-Martin WA. Rat models of skin wound healing: a review. Wound Repair Regen 2004;12(6):591-599.

73.   Rose EH, Vistnes LM, Ksander GA. The panniculus carnosus in the domestic pig. Plast Reconstr Surg 1977;59(1):94-97.

74.   Davidson JM. Animal models for wound repair. Archives of Dermatological Research 1998;290 Suppl:S1-11.

75.   Singer AJ, Clark RA. Cutaneous wound healing. N Engl J Med 1999;341(10):738-746.

76. Larjava H, Salo T, Haapasalmi K, Kramer RH, Heino J. Expression of integrins and basement membrane components by wound keratinocytes. J Clin Invest 1993;92(3):1425-1435.

77. Gurtner GC, Werner S, Barrandon Y, Longaker MT. Wound repair and regeneration. Nature 2008;453(7193):314-321.

78. Lieberman MA, Glaser L. Density-dependent regulation of cell growth: an example of a cell-cell recognition phenomenon. J Membr Biol 1981;63(1-2):1-11.

79. Eisinger M, Sadan S, Silver IA, Flick RB. Growth regulation of skin cells by epidermal cell-derived factors: implications for wound healing. Proc Natl Acad Sci U S A 1988;85(6):1937-1941.

80. Gillitzer R, Goebeler M. Chemokines in cutaneous wound healing. J Leukoc Biol 2001;69(4):513-521.

81. Klarlund JK, Block ER. Free edges in epithelia as cues for motility. Cell Adh Migr 2011;5(2):106-110.

82. Stappenbeck TS, Miyoshi H. The role of stromal stem cells in tissue regeneration and wound repair. Science 2009;324(5935):1666-1669.

83. Horbett TA. The Role of Adsorbed Proteins in Tissue Response to Biomaterials. San Diego, CA: Elsevier Academic Press, 2004.

84. Wilson CJ, Clegg RE, Leavesley DI, Pearcy MJ. Mediation of biomaterial-cell interactions by adsorbed proteins: a review. Tissue Engineering 2005;11(1-2):1-18.

85. Gretzer C, Emanuelsson L, Liljensten E, Thomsen P. The inflammatory cell influx and cytokines changes during transition from acute inflammation to fibrous repair around implanted materials. J Biomater Sci Polym Ed 2006;17(6):669-687.

86. Anderson JM, Rodriguez A, Chang DT. Foreign body reaction to biomaterials. Seminars in Immunology 2008;20(2):86-100.

87. Anderson JM. Inflammation, Wound Healing, and the Foreign-Body Response. San Diego: Elsevier Academic Press, 2004.

88. Fan K, Tang J, Escandon J, Kirsner RS. State of the art in topical wound-healing products. Plast Reconstr Surg 2011;127 Suppl 1:44S-59S.

89. Sahoo A. Stem Cells: Therapeutic Markets. Kalorama Information Market Intelligence Report 2009.

90. Hollinger JO, Hart CE, Hirsch SN, Lynch S, Friedlaender GE. Recombinant human platelet-derived growth factor: biology and clinical applications. J Bone Joint Surg Am 2008;90 Suppl 1:48-54.

91.   Hanson SE, Bentz ML, Hematti P. Mesenchymal stem cell therapy for nonhealing cutaneous wounds. Plast Reconstr Surg 2010;125(2):510-516.

92.   Badiavas EV, Falanga V. Treatment of chronic wounds with bone marrow-derived cells. Arch Dermatol 2003;139(4):510-516.

93.   Falanga V, Iwamoto S, Chartier M, Yufit T, Butmarc J, Kouttab N, et al. Autologous bone marrow-derived cultured mesenchymal stem cells delivered in a fibrin spray accelerate healing in murine and human cutaneous wounds. Tissue Engineering 2007;13(6):1299-1312.

94.   Niemeyer P, Schonberger TS, Hahn J, Kasten P, Fellenberg J, Suedkamp N, et al. Xenogenic transplantation of human mesenchymal stem cells in a critical size defect of the sheep tibia for bone regeneration. Tissue Engineering 2010;16(1):33-43.

95.   Perin EC, Silva GV. Cell-based therapy for chronic ischemic heart disease-a clinical perspective. Cardiovasc Ther 2011;29(3):211-217.

96.   Dragoo JL, Carlson G, McCormick F, Khan-Farooqi H, Zhu M, Zuk PA, et al. Healing full-thickness cartilage defects using adipose-derived stem cells. Tissue Engineering 2007;13(7):1615-1621.

97.   Niemeyer P, Szalay K, Luginbuhl R, Sudkamp NP, Kasten P. Transplantation of human mesenchymal stem cells in a non-autogenous setting for bone regeneration in a rabbit critical-size defect model. Acta Biomater 2010;6(3):900-908.

98.   Pieri F, Lucarelli E, Corinaldesi G, Aldini NN, Fini M, Parrilli A, et al. Dose-dependent effect of adipose-derived adult stem cells on vertical bone regeneration in rabbit calvarium. Biomaterials 2010;31(13):3527-3535.

99.   Gonzalez MA, Gonzalez-Rey E, Rico L, Buscher D, Delgado M. Adipose-derived mesenchymal stem cells alleviate experimental colitis by inhibiting inflammatory and autoimmune responses. Gastroenterology 2009;136(3):978-989.

100.   Togel F, Cohen A, Zhang P, Yang Y, Hu Z, Westenfelder C. Autologous and allogeneic marrow stromal cells are safe and effective for the treatment of acute kidney injury. Stem Cells Dev 2009;18(3):475-485.

101.   Fathke C, Wilson L, Hutter J, Kapoor V, Smith A, Hocking A, et al. Contribution of bone marrow-derived cells to skin: collagen deposition and wound repair. Stem Cells 2004;22(5):812-822.

102.   McFarlin K, Gao X, Liu YB, Dulchavsky DS, Kwon D, Arbab AS, et al. Bone marrow-derived mesenchymal stromal cells accelerate wound healing in the rat. Wound Repair Regen 2006;14(4):471-478.

103.   Wu Y, Chen L, Scott PG, Tredget EE. Mesenchymal stem cells enhance wound healing through differentiation and angiogenesis. Stem Cells 2007;25(10):2648-2659.

104.   Fu X, Fang L, Li X, Cheng B, Sheng Z. Enhanced wound-healing quality with bone marrow mesenchymal stem cells autografting after skin injury. Wound Repair Regen 2006;14(3):325-335.

105.   Jeon YK, Jang YH, Yoo DR, Kim SN, Lee SK, Nam MJ. Mesenchymal stem cells' interaction with skin: wound-healing effect on fibroblast cells and skin tissue. Wound Repair Regen 2010;18(6):655-661.

106.   Chen L, Tredget EE, Wu PY, Wu Y. Paracrine factors of mesenchymal stem cells recruit macrophages and endothelial lineage cells and enhance wound healing. PLoS One 2008;3(4):e1886.

107.   Kim WS, Park BS, Sung JH, Yang JM, Park SB, Kwak SJ, et al. Wound healing effect of adipose-derived stem cells: A critical role of secretory factors on human dermal fibroblasts. J Dermatol Sci 2007;48(1):15-24.

108.   Liu Y, Dulchavsky DS, Gao X, Kwon D, Chopp M, Dulchavsky S, et al. Wound repair by bone marrow stromal cells through growth factor production. J Surg Res 2006;136(2):336-341.

109.   Phinney DG, Prockop DJ. Concise review: Mesenchymal stem/multipotent stromal cells: The state of transdifferentiation and modes of tissue repair - Current views. Stem Cells 2007;25(11):2896-2902.

110.   Hocking AM, Gibran NS. Mesenchymal stem cells: paracrine signaling and differentiation during cutaneous wound repair. Exp Cell Res 2010;316(14):2213-2219.

111.   Maggini J, Mirkin G, Bognanni I, Holmberg J, Piazzon IM, Nepomnaschy I, et al. Mouse bone marrow-derived mesenchymal stromal cells turn activated macrophages into a regulatory-like profile. PLoS One 2010;5(2):e9252.

112.   Prichard HL, Reichert W, Klitzman B. IFATS collection: Adipose-derived stromal cells improve the foreign body response. Stem Cells 2008;26(10):2691-2695.

113.   Prichard HL, Reichert WM, Klitzman B. Adult adipose-derived stem cell attachment to biomaterials. Biomaterials 2007;28(6):936-946.

114.   Butt OI, Carruth R, Kutala VK, Kuppusamy P, Moldovan NI. Stimulation of peri-implant vascularization with bone marrow-derived progenitor cells: monitoring by in vivo EPR oximetry. Tissue Eng ineering 2007;13(8):2053-2061.

115.   Hall CW, Cox PA, McFarland SR, Ghidoni JJ. Some factors that influence prolonged interfacial continuity. J Biomed Mater Res 1984;18(4):383-393.

116.   Harrison RG. On the stereotropism of embryonic cells. Science 1911;34(870):279-281.

117.   Gottrup F, Agren MS, Karlsmark T. Models for use in wound healing research: a survey focusing on in vitro and in vivo adult soft tissue. Wound Repair Regen 2000;8(2):83-96.

118.   Godin B, Touitou E. Transdermal skin delivery: predictions for humans from in vivo, ex vivo and animal models. Advanced Drug Delivery Reviews 2007;59(11):1152-1161.

119.   Scott RC, Corrigan MA, Smith F, Mason H. The influence of skin structure on permeability: an intersite and interspecies comparison with hydrophilic penetrants. J Invest Dermatol 1991;96(6):921-925.

120.   Stahl J, Niedorf F, Kietzmann M. Characterisation of epidermal lipid composition and skin morphology of animal skin ex vivo. Eur J Pharm Biopharm 2009;72(2):310-316.

121.   Baker DG. Natural pathogens of laboratory mice, rats, and rabbits and their effects on research. Clin Microbiol Rev 1998;11(2):231-266.

122.   Beydon D, Payan JP, Grandclaude MC. Comparison of percutaneous absorption and metabolism of di-n-butylphthalate in various species. Toxicol In Vitro 2010;24(1):71-78.

Table 1.1. Comparisons in vertebrate skin physiology. *Staphylococcus aureus* (S. aureus); *Staphylococcus epidermidis* (S. epidermidis). *Discrepancy in literature.

	Human [69, 74, 75, 117-119]	Miniature Pig [71, 74, 117, 118, 120]	Rat [72, 74, 117-121]	Rabbit [74, 117, 121, 122]	Mouse [118, 121]
Epidermis	Yes (50-120 µm)	Yes (30-140 µm)	Yes (~ 32 µm)	Yes	Yes (~ 29 µm)
Basement Membrane	Yes	Yes	Yes	Yes	Yes
Dermis	Yes	Yes	Yes	Yes	Yes
Hypodermis	Yes	Yes	Yes	Yes	Yes
Whole skin thickness (mm)	~2.97	~2	~2.09	~1.3	~0.70
Transit Time (days)	14	28-30	--	--	--
Hair density (follicles per cm^2)	0.63-32*	~20-50*	~793-6400*	Unknown	Unknown
Panniculus carnosus	No	Yes and no (location dependent)	Yes	Yes	Yes
Skin closure: contraction or epithelialization	Epithelialization	Epithelialization	Contraction	Contraction	Contraction
Skin layers attached to underlying muscle and fascia?	Yes	Yes	No	No	No
Immune Cell Population (different from humans)		--	--	Heterophil instead of neutrophil	--
Primary commensal microorganisms	S. aureus, S. epidermidis	S. aureus	S. aureus	S. aureus	S. aureus
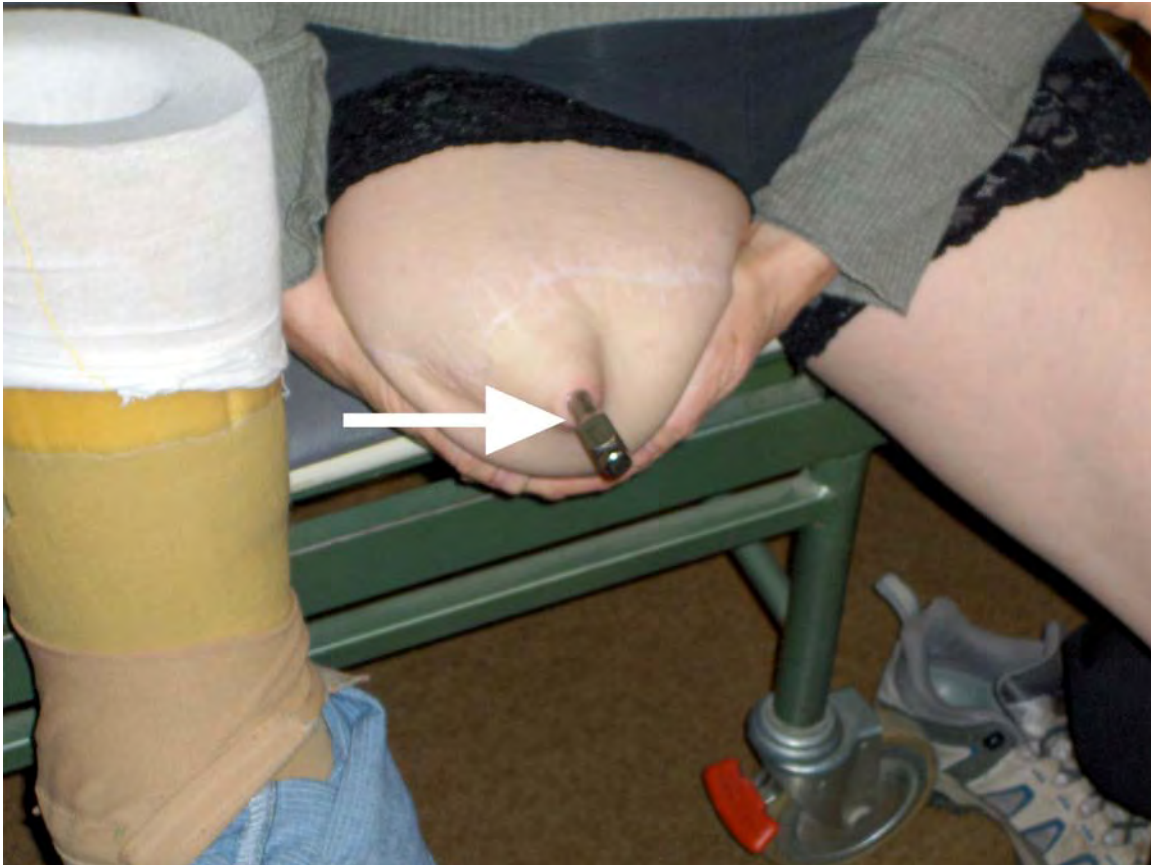
Figure 1.1. Amputee with percutaneous osseointegrated prosthetic. An artificial limb can be attached to the metal component that is exiting the skin. It is critical that a seal is developed at the skin-implant interface (arrow).
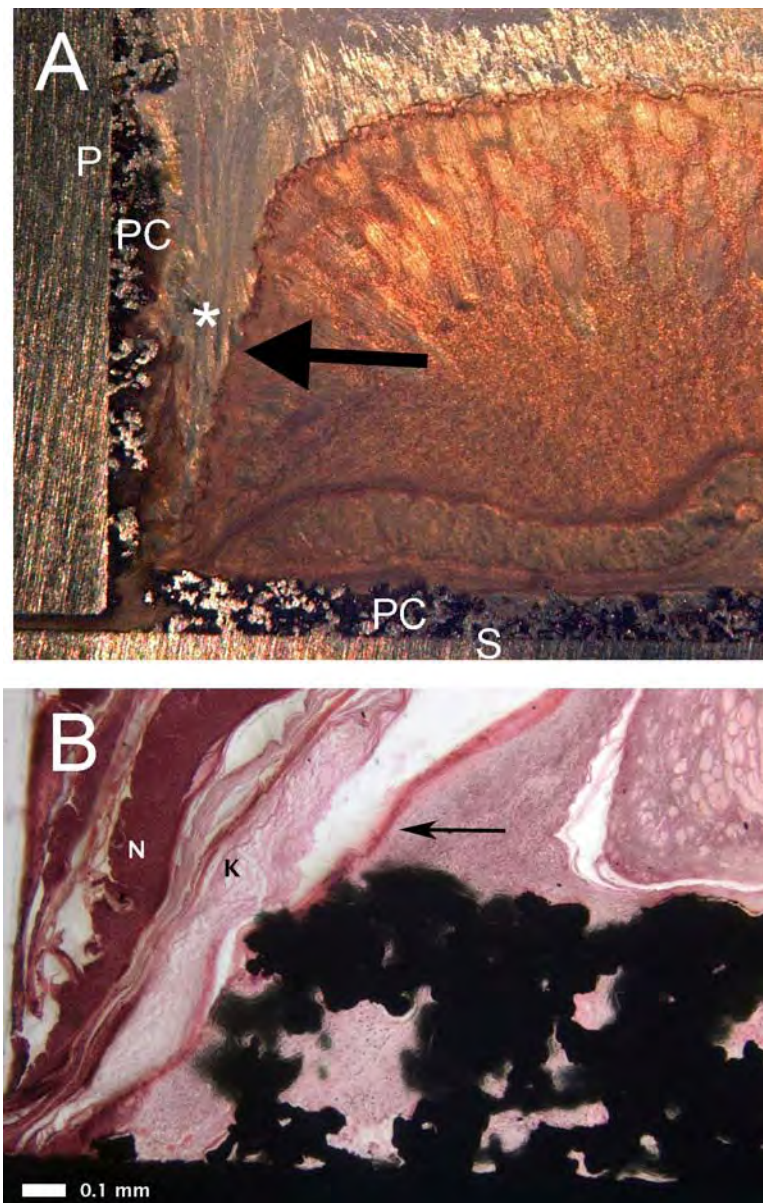
Figure 1.2. Epidermal dowgnrowth and marsupialization. (A) Arrow points to epidermis that has migrated downward creating a sinus tract (asterisk) between the skin and the percutaneous post (P). There is an absence of skin integration into the porous coating (PC) on the percutaneous post, but there is tissue integration into porous coating of subcutaneous flange (S) (macroscope 2x magnification). (B) Histology photo demonstrating epidermal downgrowth (arrow) resulting in marsupialization. Degenerative neutrophils (N) and keratin (K) fill the sinus tract (H&E; 4x magnification).

CHAPTER 2

PERCUTANEOUS IMPLANTS WITH POROUS TITANIUM DERMAL

BARRIERS: AN *IN VIVO* EVALUATION OF INFECTION RISK

Dorthyann Isackson, Lawrence D. McGill, Kent N. Bachus

Percutaneous implants with porous titanium dermal barriers: An *in vivo* evaluation of infection risk

Dorthyann Isackson [a,b,c], Lawrence D. McGill [d], Kent N. Bachus [a,b,c,*]

[a] Orthopaedic Research Laboratory, University of Utah Orthopaedic Center, Salt Lake City, UT 84108, USA
[b] Department of Bioengineering, University of Utah, Salt Lake City, UT 84112, USA
[c] Bone and Joint Research Laboratory, Department of Veterans Affairs, Salt Lake City, UT 84148, USA
[d] ARUP Laboratories, Animal Reference Pathology, Salt Lake City, UT 84108, USA

A B S T R A C T

Osseointegrated percutaneous implants are a promising prosthetic alternative for a subset of amputees. However, as with all percutaneous implants, they have an increased risk of infection since they breach the skin barrier. Theoretically, host tissues could attach to the metal implant creating a barrier to infection. When compared with smooth surfaces, it is hypothesized that porous surfaces improve the attachment of the host tissues to the implant, and decrease the infection risk. In this study, four titanium implants, manufactured with a percutaneous post and a subcutaneous disk, were placed subcutaneously on the dorsum of eight New Zealand White rabbits. Beginning at four weeks post-op, the implants were inoculated weekly with 10^8 CFU *Staphylococcus aureus* until signs of clinical infection presented. While we were unable to detect a difference in the incidence of infection of the porous metal implants, smooth surface (no porous coating) percutaneous and subcutaneous components had a 7-fold increased risk of infection compared to the implants with a porous coating on one or both components. The porous coated implants displayed excellent tissue ingrowth into the porous structures; whereas, the smooth implants were surrounded with a thick, organized fibrotic capsule that was separated from the implant surface. This study suggests that porous coated metal percutaneous implants are at a significantly lower risk of infection when compared to smooth metal implants. The smooth surface percutaneous implants were inadequate in allowing a long-term seal to develop with the soft tissue, thus increasing vulnerability to the migration of infecting microorganisms.

Published by Elsevier Ltd on behalf of IPEM.

1. Introduction

Currently, most amputees use a socket-type device to connect their prosthetic limbs to their bodies. These socket prostheses are designed to fit snugly around the residual limbs and are held in place mechanically through the use of belts, cuffs, or suction. Over the years, technological advancements with socket prostheses have greatly improved the lives of amputees, allowing them to be more mobile and to better engage in an active lifestyle. However, socket prostheses are not without limitations, including: overload and irritation of the adjacent soft tissues [1–6], disuse osteoporosis in the residual limb [7], difficulty in ongoing socket fit due to weight fluctuations and muscular atrophy [2,5,6], and difficulty in fitting individuals with short residual limbs [8].

To overcome these limitations, osseointegrated percutaneous implants are being developed as an alternative to socket-type devices [9–15]. As with dental implants, osseointegrated percutaneous implants are anchored to the bone and pass through the skin, resulting in an abutment to which an artificial prosthetic attaches [9,11,14,16,17]. In Europe, patients receiving these implants report improvements in mobility [18,19] activity levels [18,19], gait performance [18,19], and "osseoperception," a sensory feedback in the amputated limb from the surrounding environment [9,19,20]. While osseointegrated percutaneous prostheses show great promise for the amputee population, they permanently disrupt the skin barrier and are at constant risk of infection [14,19].

At a reported 18% infection rate, osseointegrated percutaneous prosthetics are similar to other clinically used percutaneous implants (i.e. bone-anchored hearing aids, catheters, and ventricular assist devices) with respect to increased infection rates [14,19]. Infection vulnerability in all percutaneous and subcutaneous implants relies upon, among other factors, the attachment and integration between the skin and the implant [15,21,22]. It is assumed that poor skin integration with the percutaneous component is evident by a sinus tract formation between the skin and

* Corresponding author at: Orthopaedic Research Laboratory, University of Utah, Department of Orthopaedics, 590 Wakara Way, Room A100, Salt Lake City, UT 84108, USA. Tel.: +1 801 587 5200; fax: +1 801 587 5211.
E-mail address: Kent.Bachus@hsc.utah.edu (K.N. Bachus).

the implant. This creates opportunity for commensal and non-commensal bacteria to migrate into the sinus tract and colonize, resulting in infection, tissue morbidity, implant removal, and even mortality. The sinus tract formation can result from epidermal downgrowth, which is marked by the epithelial layer migrating down alongside the implant as an attempt to remove the implant with the ultimate goal of restoring the skin as the definitive barrier [21,23].

There are many strategies targeted at improving the integration between the host soft tissue and the percutaneous device, including biological approaches (i.e. protein-coated devices [24,25], drug-releasing devices [26], antimicrobial strategies [13], etc.) and engineering approaches (i.e. changes in device structure [27,28], application of different materials [13,28–30], surface topography alterations [10,31–33], etc.). Previous work demonstrated that designing the percutaneous implant to have a subcutaneous disk increases the surface area for host tissue integration, thus improving implant-tissue attachment [10,27,34,35]. Likewise, altering the surface topography of the percutaneous device by creating micro-machined grooves [10,33], pits [33], or porous surfaces [36,37] increases the surface area on the implant allowing for increased cell attachment. While previous studies report skin attachment improvements at the skin/implant interface [10,13,33,36,38–40], it is not well understood if altering the surface topography on the percutaneous and/or the subcutaneous component of a percutaneous device is most important in the development of a barrier to infection when the implants are challenged with bacteria. Previous studies [10,32,36,37] aimed at preventing infection of percutaneous devices lack a strong infection signal, thus making it difficult to interpret the implant infection vulnerability.

This study aimed at improving the skin/implant interface of percutaneous implants with subcutaneous flanges while studying their infection vulnerability. Specifically, it was evaluated whether adding a porous coating to the percutaneous component, to the subcutaneous component, or to both components decreased the infection risk of the percutaneous implants. For the purposes of this study, the implants were not osseointegrated as our efforts were aimed at investigating infection risk of the percutaneous implants, and evaluating the interface integrity between the implant and the soft tissues. Our research objective was to study the infection susceptibility of metal percutaneous implants with smooth and porous coatings, investigating the hypothesis that *the incidence of infection of metal percutaneous devices will be lowest when both the percutaneous and the subcutaneous components have a porous coating; whereas, the incidence of infection will be highest when both the percutaneous and the subcutaneous components have a smooth surface.*

2. Materials and methods

2.1. Implants

For this study, Ti6Al4V implants were fabricated at the School of Medicine Machine Shop (University of Utah, Salt Lake City, UT, USA). They consisted of two components – a cylindrical percutaneous post, measuring 10 mm in diameter × 15 mm in height, and a subcutaneous disk, measuring 30 mm in diameter × 10 mm in height (Fig. 1). The percutaneous post was attached to the subcutaneous disk by a 1/4″–20 threaded hole centrally located in the subcutaneous disk. The implant components had either a smooth polished surface or a porous surface coating (P^2 Thortex, Inc. Portland, OR). Scanning electron microscopy images (SEM 6100, JEOL, USA, Peabody, MA) of the porous coating on the implants determined the average pore size and porosity to be ~400 μm and ~60%, respectively [41–43]. A surface profilometer (Zygo NewView 5032, Natsume Optical Corp, Japan) was used
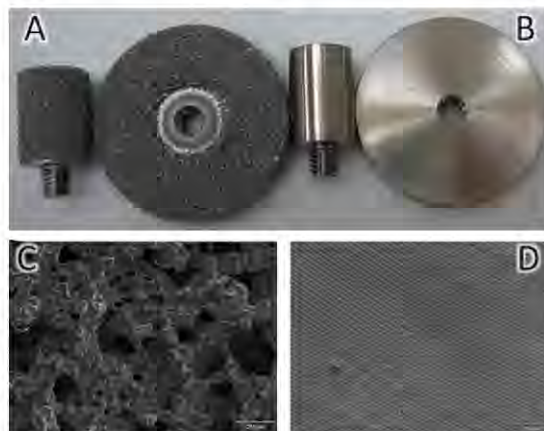

Fig. 1. Porous coated and smooth surface percutaneous implants. (A and B) Percutaneous implants consisted of two components – a subcutaneous disk and a percutaneous post – that had a porous coating (A) or a smooth surface (B). The percutaneous post was attached to the subcutaneous disk through the central threaded hole. (C) Scanning electron microscope (SEM) image of the porous coating demonstrating the porosity to be ~60% and the pore size to be ~400 μm (accelerating voltage: 20.0 kV; magnification: 65). (D) SEM image of smooth surface titanium (voltage: 20.0 kV; magnification: 65).

to determine the surface microtopography of the smooth surface, with Ra (arithmetical mean roughness) and Rq (root-mean square roughness) values determined to be 0.64 μm and 0.76 μm, respectively.

Therefore, the following four implant combinations were investigated *in vivo*: (1) a smooth percutaneous post with a smooth subcutaneous disk (S/S), (2) smooth percutaneous post with a porous subcutaneous disk (S/P), (3) porous percutaneous post with a smooth subcutaneous disk (P/S), and (4) porous percutaneous post with a porous subcutaneous disk (P/P).

2.2. Passivation, sterilization, and endotoxin testing

The titanium metal implants were passivated according to the ASTM F86 standard. Briefly, the implants were sonicated in distilled water for one hour, sonicated in acetone for one hour, sonicated in distilled water for one hour, and allowed to air dry. The implants were then autoclaved as routinely performed prior to surgical procedures for sterilization purposes. Following sterilization, a sampling of implants was tested using the LAL QCL-1000® Assay (Lonza, Walkersville, MD), according to manufacturer's directions, confirming endotoxin levels were below detection level (<0.05 EU/ml).

2.3. Overview of study design

The study was conducted with an approved animal protocol from the Institutional Animal Care and Use Committee at the University of Utah. A total of eight New Zealand White Rabbits (age 5–30 months, sex indiscriminate, weight 6–9 kg) were randomly assigned to two groups. Each animal received the four implant combinations discussed above and these were surgically implanted on the animal's dorsum. The animals were allowed to heal and recover over a four-week period. Group 1 animals ($n = 6$) then received weekly bacterial inoculations directly to the skin/implant interface of the four implants. Group 2 ($n = 2$) animals did not receive bacterial inoculations throughout the experiment, serving as a baseline control. The duration of bacterial inoculations was dependent on

when signs of clinical infection were observed at any of the implant locations. When clinical infection was observed in one or more of the implants, the animal was euthanized and infection analysis was performed.

2.4. Animal surgery

The day prior to surgery, a 25 µg Duragesic (fentanyl) patch was placed on the animal dorsum. Pre-operatively on the day of surgery, animals were administered antibiotics (20 mg/kg Cefazolin) to prevent development of infection due to the surgical procedures. The animals were then sedated (Xylazine 2 mg/kg), and their backs were close-shaved. Animals were placed in ventral recumbence on a warm water blanket and secured. Anesthesia (Ketamine 20 mg/kg) was administered, and throughout surgery animals received 1–5% Isoflurane in oxygen via facemask. The central portion of the dorsum was routinely scrubbed and draped for surgical procedures. Two 4-cm long incisions were made along the spine, the first, dorsal near the scapulae; the second incision was made more caudally near the iliac crest. For each incision, using blunt dissection, two subcutaneous pockets were created each lateral to the spine. The anatomical location of the implants on the animal's dorsum was randomized among animals. One subcutaneous disk was placed in each pocket. The incisions were then sutured closed (Ethicon vicryl 3–0). A small incision was made over the centrally located threaded hole in each subcutaneous disk. The percutaneous posts were then seated into the subcutaneous disks through the small incision. Animals were allowed to recover and freely mobilize following surgery. Post-operative antibiotics (20 mg/kg Cefazolin) were administered twice a day for three days to prevent infection development due to the surgical procedures. No additional antibiotics were administered to the animals for the remainder of the study.

Overall animal health, implant condition, inflammation, and infection were inspected daily. Clinical infection was determined according to signs of Grade II clinical infection per Checketts and Otterburn [44]. Symptoms of Grade II clinical infection included: redness of skin, swelling, discharge from implant site, pain and tenderness, temperature increase, and loss of animal appetite [13,44,45]. When an implant was determined clinically infected, the animal was euthanized by initial administration of Xylazine (2 mg/kg) followed by Beuthanasia (1 ml/4.5 kg s).

2.5. Staphylococcus aureus inoculation

Producing a reliable infection signal of percutaneous implants can be difficult in laboratory animals due to their controlled environment and their superior ability to wound heal and fight infection [10,33,40,46–48]. Thus, an inoculation of bacteria was necessary to accurately study infection of these implants. Bacterial inoculations began after a four-week period following surgery to provide sufficient time for tissue integration and attachment to the implant. Therefore, the integrity of the dermal tissue barrier to infection could be challenged in each implant combination. Following four weeks post-op, Group 1 animals were started on a weekly inoculation of 10^8 colony forming units (CFU) of Staphylococcus aureus (S. aureus) (ATCC# 49230, ATCC, Manassas, VA). The S. aureus was grown on Columbia Blood agar plates (Hardy Diagnostics, Santa Maria, CA) from a frozen stock with at least two passages prior to application [45]. From colonies on the plate, a 0.5 McFarland standard was made in brain heart infusion broth with ~10% glycerol. Using a sterile pipette, a vile of the bacterial solution was applied to each implant site on each animal in Group 1 once per week. The weekly bacterial inoculations were given until signs of Grade II clinical infection manifested in any implant, at which point the animal was euthanized. The duration of the experimental period

came to completion when the last animal of Group 1 presented with infection.

2.6. Microbiology analysis

Prior to bacterial inoculation, skin culture swabs (BBL™ CultureSwab™, Becton Dickinson, Sparks, MD) taken at each implant site recorded the baseline microbial flora on the skin. At sacrifice, skin culture swabs and soft tissue biopsies were obtained from each implant. The swabs from the skin cultures were then streaked onto Columbia blood agar plates (Hardy Diagnostics, Santa Maria, CA). For the soft tissue biopsy, a 2 cm × 2 cm area at the skin/post interface was scrubbed, as performed routinely prior to surgery, with alternating Povidone-iodine and 70% Ethanol scrubs. A 7-mm biopsy punch (Acu-Punch®, Acuderm Inc., Ft. Lauderdale, FL) of soft tissue was obtained from this scrubbed region. Using sterile forceps and a sterile scalpel, the specimen was placed in fastidious broth (Hardy Diagnostics, Santa Maria, CA). The specimens were sent for microbiological analysis (ARUP Laboratories, Salt Lake City, UT).

2.7. Histology

Each implant with attached soft tissue was carefully harvested from the animal after being euthanized. The specimens were fixed in 10% neutral buffered formalin, dehydrated (Tissue Tek Vacuum Infiltration Process, Miles Scientific), and embedded in methyl methacrylate according to routine laboratory procedures [49]. Once polymerized, a ~4-mm thick transverse section, encompassing the entire implant with surrounding soft tissue was cut with a custom, water-cooled, high-speed, cut-off saw with a diamond-edged blade [49]. These sections were then ground using a variable-speed grinding wheel (Buehler Incorporated, Lake Bluff, IL) to 50–70 µm thick sections and polished to an optical finish [49].

The sections were stained with H&E. Briefly, the slides were deplasticized in xylene, then rehydrated in 100% ethanol, 95% ethanol, 80% ethanol, and distilled water. They were then placed in Mayer's Hematoxylin (Richard Allan Scientific) at 50–55 °C for 10 min, in running distilled water for 10 min, and blotted dry with a KimWipe. The sections were soaked in a solution of Eosin Y-Phloxine (Richard Allan Scientific) with Glacial Acetic Acid (Fisher Scientific) Solution (3:1) for 45 s, and then soaked in 100% ethanol for 45 s. The sections were evaluated under a light macroscope (Nikon Macroscope, SMZ800 1–50×, Nikon, Japan) and under a light microscope (Nikon Eclipse E600, Nikon, Japan). Digital photographs were taken (Optronics, Goleta, CA) and analyzed with commercially available imaging software (Optronics MagnaFire™ SP vs. 1.0 × 5, Optronics, Goleta, CA and Image-Pro® PLUS, Media Cybernetics, Inc., Bethesda, MD).

2.8. Histology analysis

The following parameters were analyzed of the implant histological preparations: (a) extent of epidermal downgrowth as determined by the percentage of percutaneous post in contact with host tissue; (b) quantitative analysis of inflammatory cells – polymorphonuclear leukocytes (PMNs), lymphocytes, plasma cells, macrophages, foreign body giant cells (FBGCs); and (c) quantitative analysis of neovasculature (i.e. vessels measuring <100 µm in diameter).

To determine the degree of epidermal downgrowth, the length of post that was in contact with host tissue was measured and converted to a percentage based on the total length of the percutaneous post. The right and left side values were averaged and analyses were conducted.

Table 1

Histopathologic criteria with corresponding grades for implant histology analysis. Polymorphonuclear leukocytes (PMNs), lymphocytes, plasma cells, macrophages, foreign body giant cells (FBGCs), percentage of adipose tissue coverage, and vasculature were counted per area on each histology section. The percentage of adipose tissue coverage refers to the percentage of area on the subcutaneous disk that was infiltrated with adipose tissue. Vasculature included blood vessels <100 μm in diameter.

Histopathologic Grade	PMNs	Lymphocytes	Plasma Cells	Macrophages	FBGCs	Adipose tissue coverage (%)	Vasculature
0	0	0	0	0	0	0	0
1	1–10	1–30	1–10	1–10	1–3	1–20	1–20
2	11–20	31–99	11–30	11–30	4–9	21–50	21–60
3	21–40	91–270	31–90	31–90	10–27	51–80	61–180
4	>40	>270	>90	>90	>27	81–100	>180

Raw inflammatory cell count numbers were determined on both the right and left sides of the implant in the tissue adjacent to the post, tissue within the porous coating of the percutaneous post, tissue adjacent to the subcutaneous disk, and tissue within the porous coating of the subcutaneous disk. The left and right side raw cell count numbers were averaged for each section of analysis. To determine the amount of vasculature present, the blood vessels measuring less than 100 μm in diameter were counted and raw numbers were generated as described with the cell count numbers. The raw numbers for both the inflammatory cells and the blood vessels were assigned a grade from a histopathologic grading scale (Table 1), developed in accordance with a veterinary histopathologist and coauthor [Associated and Regional University Pathologists (ARUP) Laboratories, Animal Reference Pathology, Salt Lake City, UT]. The maximum grade of the four sections was used as the representative implant histopathologic grade, with which statistical analyses were performed.

2.9. Statistics

Infection data on the four implant types were graphically displayed with a Kaplan–Meier survival plot, and the infection risks of the four implant types were analyzed using the Cox Regression test (two-tailed, $p < 0.05$) (Stata/IC vs.10.1, Statacorp, College Station, TX). The histological data were analyzed with the Mann–Whitney U-test (two-tailed, $p < 0.05$) (Stata/IC vs.10.1, Statacorp, College Station, TX).

3. Results

3.1. Implant infection time course

During the four-week post-operative period, no clinical signs of infection of the percutaneous implants were observed in either Group 1, or Group 2 animals. Additionally, throughout the experimental period of 14 weeks, no clinical signs of infection were observed in the Group 2 animals. After 5 weeks of bacterial inoculations, Group 1 animals began to present with Grade II clinical signs of infection (Table 2). The first two infections were seen in the

S/S implants, as confirmed by positive bacterial growth in the skin culture swabs, positive bacterial growth in the soft tissue biopsies, and histological evidence of granulation tissue and cellular debris. After 6 weeks of bacterial inoculations, the third infection was of a P/P implant. Following 9 weeks of bacterial inoculations, two more infections presented – one P/S implant and the other a S/S implant. The last implant infection in the treated group developed in a S/S implant after 10 weeks of bacterial inoculations. There was no correlation found between site of implant placement and infection. Further, it was found that the wide age range and the animal gender did not have any role on infection vulnerability.

3.2. Infection risk of the four percutaneous implants with S. aureus inoculations

The P/P implants had an 80% reduced risk of infection relative to the S/S implants (hazard ratio 0.19, 95% confidence, $p = 0.145$) (Fig. 2). The P/S implants had a 77% reduced risk of infection relative to the S/S implants (hazard ratio 0.23, 95% confidence, $p = 0.192$). The S/P implants could not be statistically analyzed with the Cox Regression test as there were no failures or infections of these implants.

Evaluating the Kaplan–Meier plot, it was noted that the implants with a porous coating – the P/S, S/P, and P/P implants – seemed to have similar Kaplan–Meier curves with respect to the curve representing the S/S implants. A Kaplan–Meier Plot and a Cox Regression analysis was performed on the S/S implants and the implants with a porous coating (S/P, P/S, and P/P), demonstrating the S/S implants to have a significant, 7-fold increase in the risk of infection ($p = 0.022$) compared to the porous coated implants (Fig. 2).

3.3. Implant histology

Epidermal downgrowth and sinus tract formation was a common observation among all implants. Of the 26 implants histologically evaluated, 11 of the implants displayed epidermal downgrowth to the attachment point of the percutaneous post to the subcutaneous disk (Fig. 3). The average percentage of post that was in contact with the tissue and the actual length of post that was

Table 2

Summary of percutaneous implant infections. Treated and untreated animals are represented in rows with corresponding implants in columns. The number of weeks is the number of bacterial inoculation weeks until clinical infection presented. CNS – Coagulase negative *Staphylococcus aureus*.

	S/S	S/P	P/S	P/P	Biopsy bacterium of infected implant
Treated_A	5 weeks				S. aureus/SCN
Treated_B	5 weeks		NA		S. aureus/SCN
Treated_C			NA	6 weeks	S. aureus
Treated_D	9 weeks				S. aureus
Treated_E	NA		9 weeks		S. aureus
Treated_F	10 weeks				S. aureus
Total # of Infections of Treated Implants	4 of 5	0 of 6	1 of 4	1 of 6	
Untreated_G					No infections
Untreated_H					No infections
Total # of Infections of Untreated Implants	0 of 2	0 of 2	0 of 2	0 of 2	

NA – implant removed from study due to percutaneous post missing during study duration.
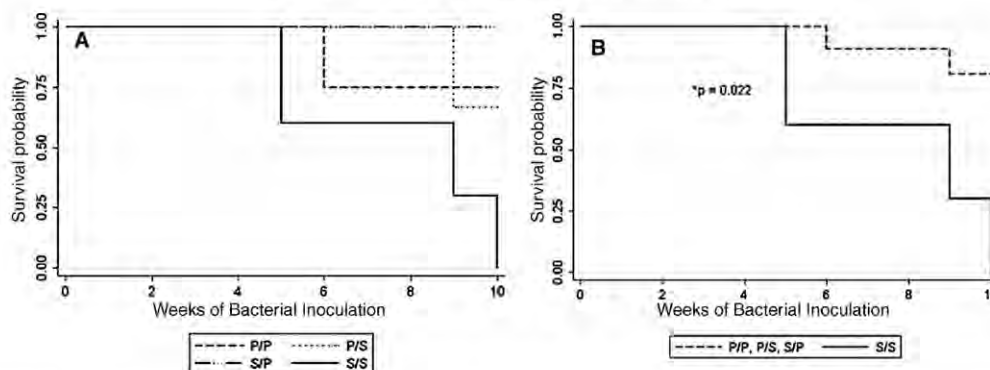
Fig. 2. Kaplan–Meier survival estimates of the percutaneous implants over time. (A) Implants plotted independently to each other ($p > 0.05$). (B) S/S implants compared to implants with a porous coating (P/P, P/S, and S/P) ($^*p = 0.022$).

in contact with the tissue was as follows for each implant: 5.81% (S/S; 0.87 mm, SD 1.10), 5.06% (S/P; 0.76 mm, SD 0.41), 5.56% (P/S; 0.83 mm, SD 1.19), and 5.76% (P/P; 0.86 mm, SD 1.00). In some cases among the S/S implants, the epidermis would migrate along and towards the perimeter of the subcutaneous disk (Fig. 3). No statistical differences were found regarding epidermal downgrowth and implant type (i.e. S/S, S/P, P/S, or P/P). Accompanying the epidermal downgrowth, sinus tracts formed between the epidermis and the implant, being filled with keratin and degenerative neutrophils (Fig. 3).

The porous coating on the subcutaneous disks was infiltrated with a fibrovascular tissue (Fig. 4). The porous coated percutaneous posts did not display tissue infiltration to the extent of the subcutaneous disks. Rather the epidermis migrated downward yielding little to no infiltration of soft tissue into the pores of the post (Fig. 4). The porous structures were filled with a mild to moderate presence of inflammatory cells, including polymorphonuclear leukocytes (histopathologic grade 2), lymphocytes (histopathologic grade 3), plasma cells (histopathologic grade 2), and macrophages (histopathologic grade 2). Multinucleated macrophages and foreign body giant cells were also observed to be present to a mild degree, corresponding to a histopathologic grade of 2 (Fig. 5). Neovasculature was present to a moderate degree (histopathologic grade 3) in the pores and above the pores in the newly formed granulation tissue. Adipose tissue infiltrated the pores (histopathologic grade 3), above and below the thin fibrous capsule, and was significantly more abundant in the P/P and S/P implants than the S/S and P/S implants ($p < 0.05$) (Fig. 6).

There was a fibrovascular tissue capsule surrounding the smooth subcutaneous disks with little attachment to the implant surface (Fig. 7). This fibrous encapsulation was composed of organized extracellular matrix fibers that were aligned parallel to the implant surface, representative of an immature tissue that is commonly seen surrounding implanted materials [50]. Similarly to the porous coated percutaneous posts, the epidermis migrated downward, and as a result, there was little epidermal and subcutaneous tissue attachment to the post (Fig. 3). Evaluation of the cellular infiltrates surrounding the non-infected smooth surface implants was mainly composed of fibroblasts, lymphocytes, and PMNs. At the interface of the host tissue and the implant, there was a layer of inflammatory cells with a mild to moderate presence, including macrophages (histopathologic grade 3), FBGCs (histopathologic grade 2), PMNs (histopathologic grade 3), plasma cells (histopathologic grade 3), and lymphocytes (histopathologic grade 3). Adipose tissue infiltration or encapsulation of the smooth surface implants

was minimal with a histopathologic grade of 1. Neovascularization was present to a mild degree (histopathologic grade 2).

Implants that were infected had cellular debris between the tissue and the implant, with granulation tissue surrounding the cellular debris (Fig. 7).

4. Discussion

Preventing infection of osseointegrated percutaneous prostheses is absolutely necessary for clinical success. Our work investigated the infection susceptibility of metal percutaneous implants when a porous coating was added to the surface, testing the hypothesis that the *incidence of infection of metal percutaneous devices will be lowest when both the percutaneous and the subcutaneous components are porous coated on the implant; whereas, incidence of infection will be highest when both the percutaneous and the subcutaneous components have a smooth surface*. Our aim was to determine whether or not the location of the porous coating on the percutaneous and/or subcutaneous components contributed to the incidence of infection. Our results show that when both the percutaneous and the subcutaneous components have a smooth surface they have a 7-fold increase in risk of infection compared to implants with a porous coating on one or both components. Incidence of infection is significantly reduced when the implant has a porous surface, and our results suggest that, at the least, a porous subcutaneous component is essential to decreasing this risk of infection, notably as the S/P implants did not develop infection during the study period.

Limitations to this study are 2-fold. First, due to the study design, we were not able to follow the infection risk of the remaining implants in an animal at the time one implant presented with infection. To do so would have required an antibiotic treatment, which would detract from the goals of the study. However, this study design allowed us to minimize any animal variation between the four implants. Ultimately, the presented results address the hypothesis regarding which implant was most vulnerable to infection and that was determined to be the S/S implants. Second, evaluations in a small animal model have inherent translational limitations as a result of skin physiological and anatomical differences between rabbits and humans. Most notably, rabbits have a panniculous carnosus, a muscle in the subcutaneous tissues, which humans do not possess. The presence of this underlying muscle in rabbits causes skin wound healing to occur more rapidly by contraction rather than by epithelialization, which is a slower healing
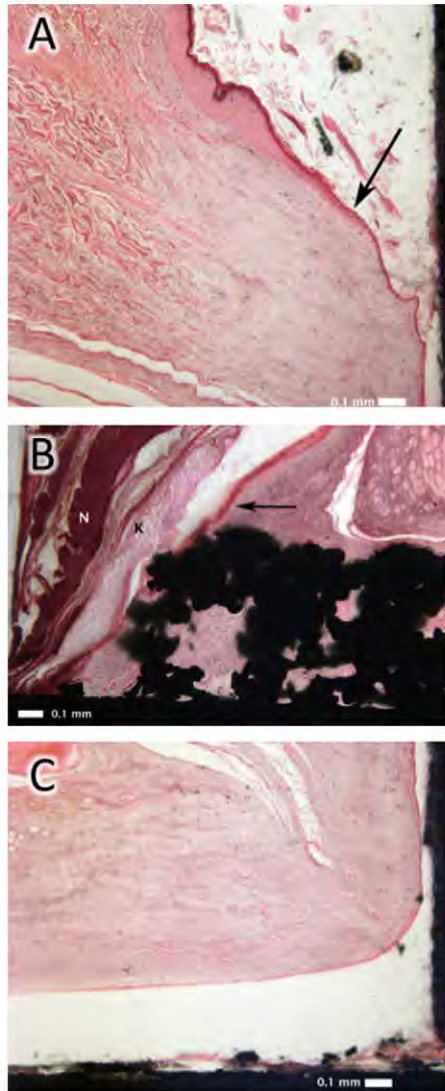
Fig. 3. Epidermal downgrowth with a sinus tract at the implant interface was observed in the majority of implant specimens. (A) Epidermis (black arrow) migrated down along the post (right black strip). (B) Epidermal downgrowth (black arrow) that continued to the point where the post (left side of photo) attached to the subcutaneous disk (black portion in bottom of photo). The sinus tract was filled with degenerative neutrophils (N) and keratin (K). (C) The epidermis migrated down the percutaneous post (black strip on right of photo) and continued to migrate adjacent to subcutaneous disk (black strip on bottom of photo). Note the absence of soft tissue attachment to smooth surface of implant. All 4× original magnification.

Fig. 4. Tissue reaction to porous coated implants. (A) Vasculature, fibroblasts, and scattered inflammatory cells were observed within the porous structures and found lining the metal surface. 10× original magnification. (B) A macroscopic view of the implant demonstrates the downward migration of the epidermis (black arrow). The percutaneous post (P) with a porous coating (PC) is on the left and the subcutaneous disk (D) with a porous coating (PC) is at the bottom of the photo. 2× original magnification.

process [51,52]. Despite this inherent limitation, this rabbit model provides important findings that can be applied to future studies when studying infections of percutaneous implants in animal models with skin more similar to humans.

We propose that the increased risk of infection with the smooth surface implants is due to the lack of attachment of the host tissue to the smooth surface. The result is an incomplete barrier to preventing microbial migration and subsequent infection.
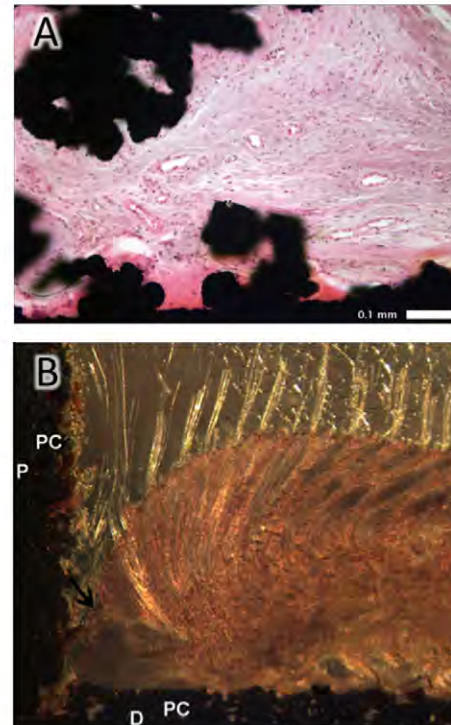
Smooth surface implants have less surface area for tissue attachment, and the fibrous capsule which develops around the surface allows the implants to move within the soft tissue making it difficult for any soft tissue seal to form [53]. It is generally believed that any "mechanical irritation" produced by stress and movement at an implant interface yields a thicker fibrous capsule formation [31,53], which was observed in this study. The absence of soft tissue attachment to the smooth surfaces was seen during the histological processing as the tissue would separate from the implant; whereas, this was not observed with the porous implants. It should be noted that the histological processing with PMMA embedment can cause the tissue to separate from the implant surface. However, this detachment was much less obvious, or not observed with the porous coated implants. The separation between the soft tissue and the smooth surface implants can be attributed to an absence of an initial attachment or integration formed *in vivo*.

The surface topography of implants greatly influences the tissue response and subsequent attachment to the implant, which in turn affects the implant's vulnerability to infection. As seen in previous studies, tissue attachment to subcutaneous implants is increased when the implant is roughened or porous coated [10,31,53–55]. In a study performed by Kim and colleagues, surfaces with varying roughness or grooves resulted in greater tissue attachment and less fibrous capsule formation compared to the smooth surfaces, which had a thick fibrous capsule formation, similar to the presented results. Tissue integration with a rough or porous surface is
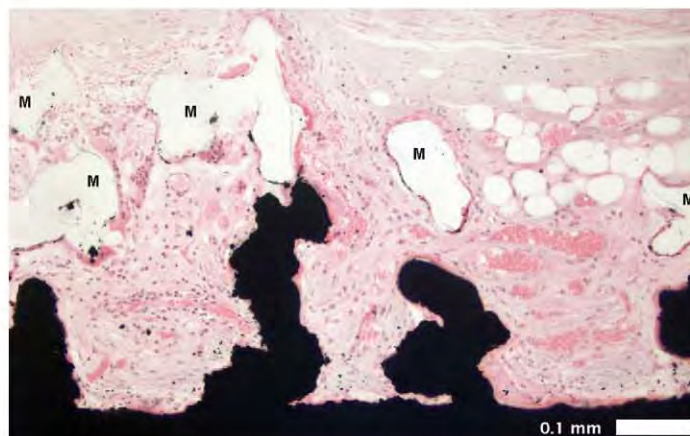
Fig. 5. Cellular infiltrates and vascularity within and around the porous structures. Macrophages and foreign body giant cells lined the implant surface (black). During histological processing, some of the porous coating was removed (M), allowing a clear view of the cells lining the implant surface. 10× original magnification.
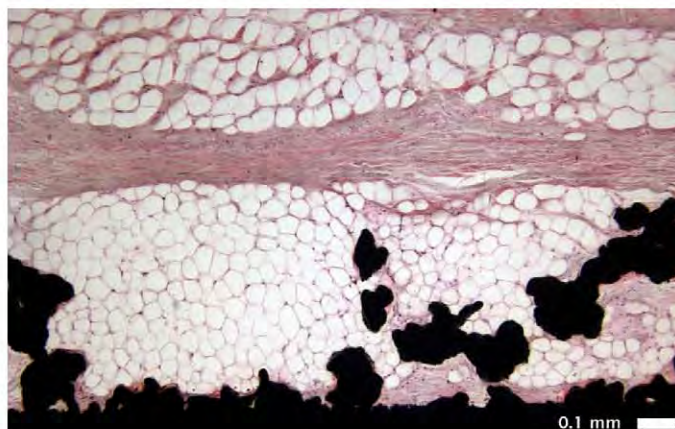
Fig. 6. Adipose tissue infiltration into porous structures. Note the adipose tissue above and below the thin fibrous capsule. 4× original magnification.

a barrier to infecting microorganisms. This has been shown in work by Merritt et al. [22], who demonstrated that once subcutaneous porous implants were invaded with tissue, they were less susceptible to infection than an implant with a smooth surface [22]. Unlike the implants we investigated, the implants in the work performed by Merritt et al. [22] were subcutaneous with no percutaneous components. Our work found that, after four weeks post-op, infection vulnerability of porous implants was significantly decreased
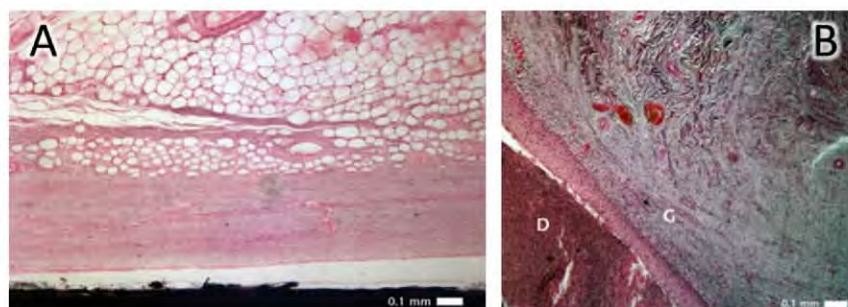
Fig. 7. Tissue reaction to smooth surface implants. (A) Fibrous capsule surrounding a smooth surface. (B) Cellular debris (D) and granulation tissue (G) in a clinically infected implant. All 4× original magnification.

compared to smooth surface implants. This supports the results of Merritt et al. [22] in that smooth surface implants are more vulnerable to infection at later time points (i.e. at least 4 weeks post-op). The porous coated surfaces allow for tissue integration and attachment, providing a barrier to migrating microorganisms and a mechanical "lock" of the tissue with the device, thus limiting any movement or micromotion of the implant in the tissue that would weaken the attachment.

This study demonstrates that percutaneous implants with a smooth surface are at a significantly increased risk of infection compared to percutaneous implants with a porous coated surface. These results highlight the importance of soft tissue integration with the porous implant as being a barrier to invading microorganisms, and demonstrate the ineffectiveness of a smooth polished surface to allow for soft tissue attachment. Though the porous coating was effective in reducing the risk of infection, it was not completely effective in altogether eliminating the risk of infection. In light of the timing of clinical infections of percutaneous osseointegrated prosthetics, it is reported that these prosthetics present with infection on average three years after surgical implantation [14]. It is difficult to translate the timing of onset of infection with our results and with what is seen in the clinic as our study is an example of a more extreme bacteria-challenged environment, with the average of seven weeks before infection was observed. Thus our results further demonstrate that S/S implants in an excessive bacterial environment will develop infection more frequently than an implant with a porous coating. Further strategies evaluating implant designs and incorporating biologics into the implants and in the adjacent tissues will be necessary to initiate and successfully produce a healthy, permanent integration between the implant and the host tissue.

Acknowledgements

Conflict of interest statement

All authors confirm that there is no potential conflict of interest including employment, stock ownership, consultancies, honoraria, paid expert testimony, and patent applications/registrations influencing this work.

References

[1] Dillingham TR, Pezzin LE, MacKenzie EJ, Burgess AR. Use and satisfaction with prosthetic devices among persons with trauma-related amputations: a long-term outcome study. Am J Phys Med Rehabil 2001;80(August (8)):563–71.
[2] Hoaglund FT, Jergesen HE, Wilson L, Lamoreux LW, Roberts R. Evaluation of problems and needs of veteran lower-limb amputees in the San Francisco Bay Area during the period 1977–1980. J Rehabil Res Dev (Veterans Administration, Department of Medicine and Surgery, Rehabilitation R&D Service) 1983;20(July (1)):57–71.
[3] Legro MW, Reiber G, del Aguila M, Ajax MJ, Boone DA, Larsen JA, et al. Issues of importance reported by persons with lower limb amputations and prostheses. J Rehabil Res Dev 1999;36(July (3)):155–63.
[4] Lyon CC, Kulkarni J, Zimerson E, Van Ross E, Beck MH. Skin disorders in amputees. J Am Acad Dermatol 2000;42(March (3)):501–7.
[5] Pezzin LE, Dillingham TR, Mackenzie EJ, Ephraim P, Rossbach P. Use and satisfaction with prosthetic limb devices and related services. Arch Phys Med Rehabil 2004;85(May (5)):723–9.
[6] Sherman RA. Utilization of prostheses among US veterans with traumatic amputation: a pilot survey. J Rehabil Res Dev 1999;36(April (2)):100–8.
[7] Gailey R, Allen K, Castles J, Kucharik J, Roeder M. Review of secondary physical conditions associated with lower-limb amputation and long-term prosthesis use. J Rehabil Res Dev 2008;45(1):15–29.
[8] Bowen RE, Struble SG, Setoguchi Y, Watts HG. Outcomes of lengthening short lower-extremity amputation stumps with planar fixators. J Pediatr Orthop 2005;25(July–August (4)):543–7.
[9] Branemark R, Branemark PI, Rydevik B, Myers RR. Osseointegration in skeletal reconstruction and rehabilitation: a review. J Rehabil Res Dev 2001;38(March–April (2)):175–81.
[10] Pendegrass CJ, Goodship AE, Blunn GW. Development of a soft tissue seal around bone-anchored transcutaneous amputation prostheses. Biomaterials 2006;27(August (23)):4183–91.
[11] Hagberg K, Branemark R. One hundred patients treated with osseointegrated transfemoral amputation prostheses – rehabilitation perspective. J Rehabil Res Dev 2009;46(3):331–44.
[12] Isaacson BM, Stinstra JG, MacLeod RS, Webster JB, Beck JP, Bloebaum RD. Bioelectric analyses of an osseointegrated intelligent implant design system for amputees. J Vis Exp 2009;29:1–6.
[13] Chou TG, Petti CA, Szakacs J, Bloebaum RD. Evaluating antimicrobials and implant materials for infection prevention around transcutaneous osseointegrated implants in a rabbit model. J Biomed Mater Res A 2010;92(March 1 (3)):942–52.
[14] Tillander J, Hagberg K, Hagberg L, Branemark R. Osseointegrated titanium implants for limb prostheses attachments: infectious complications. Clin Orthop Relat Res 2010;(May 15).
[15] Perry EL, Beck JP, Williams DL, Bloebaum RD. Assessing peri-implant tissue infection prevention in a percutaneous model. J Biomed Mater Res B Appl Biomater 2010;92(February (2)):397–408.
[16] Carlsson L, Rostlund T, Albrektsson B, Albrektsson T, Branemark PI. Osseointegration of titanium implants. Acta Orthop Scand 1986;57(August (4)):285–9.
[17] Albrektsson T, Branemark PI, Jacobsson M, Tjellstrom A. Present clinical applications of osseointegrated percutaneous implants. Plast Reconstr Surg 1987;79(May (5)):721–31.
[18] Hagberg K, Branemark R, Gunterberg B, Rydevik B. Osseointegrated trans-femoral amputation prostheses: prospective results of general and condition-specific quality of life in 18 patients at 2-year follow-up. Prosthet Orthot Int 2008;32(March (1)):29–41.
[19] Sullivan JUM, Uden M, Robinson KP, Sooriakumaran S. Rehabilitation of the trans-femoral amputee with an osseointegrated prosthesis: the United Kingdom experience. Prosthet Orthot Int 2003;27:114–20.
[20] Jacobs R, Branemark R, Olmarker K, Rydevik B, Van Steenberghe D, Branemark PI. Evaluation of the psychophysical detection threshold level for vibrotactile and pressure stimulation of prosthetic limbs using bone anchorage or soft tissue support. Prosthet Orthot Int 2000;24(August (2)):133–42.
[21] von Recum AF. Applications and failure modes of percutaneous devices: a review. J Biomed Mater Res 1984;18(April (4)):323–36.
[22] Merritt K, Shafer JW, Brown SA. Implant site infection rates with porous and dense materials. J Biomed Mater Res 1979;13(January (1)):101–8.
[23] Winter GD. Transcutaneous implants: reactions of the skin-implant interface. J Biomed Mater Res 1974;8(3):99–113.
[24] Middleton CA, Pendegrass CJ, Gordon D, Jacob J, Blunn GW. Fibronectin silanized titanium alloy: a bioinductive and durable coating to enhance fibroblast attachment in vitro. J Biomed Mater Res A 2007;(June 21).
[25] Okada T, Ikada Y. Surface modification of silicone for percutaneous implantation. J Biomater Sci Polym Ed 1995;7(2):171–80.
[26] Jarrell JD, Dolly B, Morgan JR. Rapid screening, in vitro study of metal oxide and polymer hybrids as delivery coatings for improved soft-tissue integration of implants. J Biomed Mater Res A 2010;92(March 1 (3)):1094–104.
[27] Grosse-Siestrup C, Affeld K. Design criteria for percutaneous devices. J Biomed Mater Res 1984;18(April (4)):357–82.
[28] Mooney V, Schwartz SA, Roth AM, Gorniowsky MJ. Percutaneous implant devices. Ann Biomed Eng 1977;5(March (1)):34–46.
[29] Heaney TG, Doherty PJ, Williams DF. Marsupialization of percutaneous implants in presence of deep connective tissue. J Biomed Mater Res 1996;32(December (4)):593–601.
[30] Paquay YC, de Ruijter JE, van der Waerden JPCM, Jansen JA. Tissue reaction to Dacron velour and titanium fibre mesh used for anchorage of percutaneous devices. Biomaterials 1996;17(12):1251–6.
[31] Kim H, Murakami H, Chehroudi B, Textor M, Brunette DM. Effects of surface topography on the connective tissue attachment to subcutaneous implants. Int J Oral Maxillofac Implants 2006;21(May–June (3)):354–65.
[32] Walboomers XF, Jansen JA. Effect of microtextured surfaces on the performance of percutaneous devices. J Biomed Mater Res A 2005;74(September 1 (3)):381–7.
[33] Chehroudi B, Brunette DM. Subcutaneous microfabricated surfaces inhibit epithelial recession and promote long-term survival of percutaneous implants. Biomaterials 2002;23(January (1)):229–37.
[34] Jansen JA, van der Waerden JP, de Groot K. Development of a new percutaneous access device for implantation in soft tissues. J Biomed Mater Res 1991;25(December (12)):1535–45.

[35] Paquay YC, De Ruijter AE, van der Waerden JP, Jansen JA. A one stage versus two stage surgical technique tissue reaction to a percutaneous device provided with titanium fiber mesh applicable for peritoneal dialysis. ASAIO J 1996;42(November–December (6)):961–7.

[36] Isenhath SN, Fukano Y, Usui ML, Underwood RA, Irvin CA, Marshall AJ, et al. A mouse model to evaluate the interface between skin and a percutaneous device. J Biomed Mater Res A 2007;(June 13).

[37] Pitkin M, Raykhtsaum G, Pilling J, Galibin OV, Protasov MV, Chihovskaya JV, et al. Porous composite prosthetic pylon for integration with skin and bone. J Rehabil Res Dev 2007;44(5):723–38.

[38] LaBerge M, Bobyn JD, Rivard CH, Drouin G, Duval P. Study of soft tissue ingrowth into canine porous coated femoral implants designed for osteosarcomas management. J Biomed Mater Res 1990;24(July (7)):959–71.

[39] Rosengren A, Wallman L, Danielsen N, Laurell T, Bjursten LM. Tissue reactions evoked by porous and plane surfaces made out of silicon and titanium. IEEE Trans Biomed Eng 2002;49(April (4)):392–9.

[40] Gerritsen M, Paquay YG, Jansen JA. Evaluation of the tissue reaction to a percutaneous access device using titanium fibre mesh anchorage in goats. J Mater Sci Mater Med 1998;9(September (9)):523–8.

[41] Bobyn JD, Pilliar RM, Cameron HU, Weatherly GC. The optimum pore size for the fixation of porous-surfaced metal implants by the ingrowth of bone. Clin Orthop Relat Res 1980;150(July–August):263–70.

[42] Mastrogiacomo M, Scaglione S, Martinetti R, Dolcini L, Beltrame F, Cancedda R, et al. Role of scaffold internal structure on in vivo bone formation in macroporous calcium phosphate bioceramics. Biomaterials 2006;27(June (17)):3230–7.

[43] van Lenthe GH, Hagenmuller H, Bohner M, Hollister SJ, Meinel L, Muller R. Nondestructive micro-computed tomography for biological imaging and quantification of scaffold-bone interaction in vivo. Biomaterials 2007;28(May (15)):2479–90.

[44] Checketts RGMA, Otterburn M. Pin track infection and the principles of pint site care. Orthofix External Fixation Trauma Orthop 2000:97–103.

[45] Williams D, Bloebaum R, Petti CA. Characterization of Staphylococcus aureus strains in a rabbit model of osseointegrated pin infections. J Biomed Mater Res A 2008;85(May (2)):366–70.

[46] Gangjee T, Colaizzo R, von Recum AF. Species-related differences in percutaneous wound healing. Ann Biomed Eng 1985;13(5):451–67.

[47] Jansen JA, Paquay YG, van der Waerden JP. Tissue reaction to soft-tissue anchored percutaneous implants in rabbits. J Biomed Mater Res 1994;28(September (9)):1047–54.

[48] Smith TJ, Galm A, Chatterjee S, Wells R, Pedersen S, Parizi AM, et al. Modulation of the soft tissue reactions to percutaneous orthopaedic implants. J Orthop Res 2006;24(July (7)):1377–83.

[49] Emmanual J, Hornbeck C, Bloebaum RD. A polymethyl methacrylate method for large specimens of mineralized bone with implants. Stain Technol 1987;62(November (6)):401–10.

[50] Anderson JM, Rodriguez A, Chang DT. Foreign body reaction to biomaterials. Semin Immunol 2008;20(April (2)):86–100.

[51] Singer AJ, Clark RA. Cutaneous wound healing. N Engl J Med 1999;341(September 2 (10)):738–46.

[52] Davidson JM. Animal models for wound repair. Arch Dermatol Res 1998;290(July (Suppl.)):S1–11.

[53] Picha GJ, Drake RF. Pillared-surface microstructure and soft-tissue implants: effect of implant site and fixation. J Biomed Mater Res 1996;30(March (3)):305–12.

[54] Recum AF, Shannon CE, Cannon CE, Long KJ, Kooten TG, Meyle J. Surface roughness, porosity, and texture as modifiers of cellular adhesion. Tissue Eng 1996;2(Winter (4)):241–53.

[55] Ungersbock A, Pohler O, Perren SM. Evaluation of the soft tissue interface at titanium implants with different surface treatments: experimental study on rabbits. Biomed Mater Eng 1994;4(4):317–25.

CHAPTER 3

IN VITRO INVESTIGATION OF MESENCHYMAL STEM CELL

CYTOTOXICITY AND ADHERENCE TO POROUS TITANIUM

SURFACES IN VARIOUS DELIVERY SOLUTIONS FOR

IN VIVO TRANSPLANTATION STUDIES

3.1 Abstract

Percutaneous medical devices often fail in the host tissue due to poor skin and soft tissue attachment. To improve tissue integration with porous titanium percutaneous implants, it is suggested that delivering mesenchymal stem cells (MSC) could be effective due to their proven tissue repair and regenerative capacities. Prior to *in vivo* delivery, we sought to determine the effect the cell delivery solution had on cellular viability and adherence to porous titanium surfaces over 24 hours. MSCs were seeded on porous titanium surfaces in the following delivery solutions: complete cell culture medium, basal cell culture medium without serum, and phosphate-buffered saline (PBS). Cellular adherence and cytotoxicity levels were analyzed in each solution over 24 hours. Cellular adherence slowly increased over time in all delivery solutions, with significant differences between basal cell culture medium and PBS at 8 hours after cell seeding. Furthermore, cytotoxicity slowly increased within the first 12 hours for all solutions, but increased significantly for PBS between 12 and 24 hours. MSC adherence and viability

on the porous titanium surfaces was similar between basal culture medium and serum-supplemented medium; however, significance in cell adherence and cytotoxicity was seen with PBS solutions following 8-12 hours after cell seeding. To avoid an immunogenic response often associated with serum-supplemented media, while still providing sufficient nutrients for cellular adherence and viability, our results suggest one can use a basal culture medium if delivery is performed within 24 hours following cell seeding.

3.2 Introduction

Direct skeletal attachment of an artificial limb replacement, also referred to as an osseointegrated percutaneous prosthetic, is an alternative solution for a subset of amputees [1, 2]. Though promising in many ways, these percutaneous devices are vulnerable to infection at the interface between the skin and the implant [3]. Thus, current research endeavors are focused on improving integration of the skin with the percutaneous component to create a long-term seal from invading pathogens.

Our previous work has shown that a commercially pure porous coated titanium surface when compared to a smooth polished surface was effective in decreasing infection susceptibility of percutaneous implants in a bacterial challenged animal model [4]. However, a porous coating was not sufficient in completely preventing epidermal downgrowth, a phenomenon suggested to provide an avenue for microbial invasion and subsequent infection [5, 6]. To address the epidermal downgrowth phenomenon, we believe that if a sufficiently vascularized soft tissue bed and appropriate wound healing cues are provided, the downward migration of the epidermis could be prevented and tissue integration improved. An area of research that can address this need to improve

vascularization and provide wound healing cues for the migrating epidermis is that of regenerative medicine and the delivery of adult mesenchymal stem cells (MSCs) [7].

Mesenchymal stem cells serve a very important role in wound healing and repair [7-11], and are being evaluated for several clinical conditions, including damaged articular cartilage [12], bone defects [13, 14], soft tissue augmentation [15, 16], and chronic ischemic heart disease [17]. Many of these conditions present a need to seed the MSCs onto a scaffold and to deliver the cell-seeded scaffold at an appropriate time to the diseased or damaged tissue. Whether MSCs are seeded on scaffolds to repair cartilage injury, or whether MSCs are seeded on scaffolds to repair a soft tissue defect, it is important to know if (a) the delivery solution and (b) the time frame for delivery have any deleterious effect on the cells being delivered.

Cell delivery solutions can range from simple saline solutions [18, 19], to cell culture media containing animal serum [20], to basal cell culture media without animal serum [21], to more complex delivery platforms such as collagen or fibrin gels [22, 23]. Saline or phosphate-buffered saline solutions do not have the necessary nutrients for cellular activity, which could be a problem if cell delivery is not performed immediately. It is widely acknowledged that cell culture media containing animal-derived serum carry potential to elicit an immune response within the body, thus having potential negating effects on the desired stem cell treatment. Thus, it is preferable to seed and deliver cells in a medium that can provide enough nutrients to retain cellular activity, while not eliciting an immunogenic or inflammatory response *in vivo*.

Cell delivery time frames after cell seeding can range from delivering minutes to hours to days. An appropriate delivery time frame is often dependent on a specific

condition being treated, for example, if the clinical procedure to prepare the tissue site requires many hours, or if the state of the cells needs to be differentiated or undifferentiated. In any case, the most desired time frame will be one that, at the very least, allows for maximal cell adherence and cell viability on the implant/scaffold.

For the purpose of this study and upcoming transplantation studies using our previously established percutaneous implant model [4], we sought to determine: (a) the effect the cell delivery solution had on MSC adherence to porous coated titanium surfaces; and (b) the effect the cell delivery solution had on MSC cytotoxicity when seeded on porous coated titanium surfaces over a 24-hour period. Porous titanium surfaces are of interest to our study goals as titanium is a material that would likely be used in fabricating osseointegrated percutaneous prosthetics. To the best of our knowledge, there are no published studies to date evaluating MSC adherence and cytotoxicity in various delivery solutions on porous titanium surfaces.

3.3 Materials and Methods

3.3.1 Preparation and surface characterization of titanium surfaces

The porous titanium surfaces (pTi) consisted of a solid substrate fabricated from Ti6Al4V at the School of Medicine Machine Shop (University of Utah, Salt Lake City, UT, USA), and had a 1mm thick porous coating fabricated from commercially pure titanium (P^2 Thortex, Inc., Portland, OR, USA). Scanning electron microscopy (Hitachi S3000-N) was used to determine the average pore size of the porous coating, and microCT (Xradia MicroXCT system) analysis was performed to determine the relative porosity of the porous coating.

Both smooth titanium surfaces (sTi) and roughened titanium surfaces (rTi) were fabricated from Ti6Al4V at the School of Medicine Machine Shop (University of Utah, Salt Lake City, UT, USA). A roughened surface texture was created by sandblasting the smooth surface. Optical profilometry (Zygo NewView 5032, Natsume Optical Corp, Japan) was used to determine the average Ra values of the surfaces.

All titanium surfaces were cut to fit in a 12-well cell culture plate (Falcon, BD Biosciences, Bedford, MA, USA).

3.3.2 Endotoxin testing, passivation, and sterilization

All titanium surfaces were passivated according to ASTM F86 standards. Briefly, the titanium pieces were sonicated in distilled water, then in acetone (Sigma-Aldrich, St. Louis, MO, USA), followed by another distilled water wash before being washed in a 49% nitric acid (Macron Chemicals, Center Valley, PA, USA) solution for 2 hours. They were then sonicated in distilled water and allowed to air dry overnight.

Prior to each experiment, all titanium surfaces were sterilized as routinely performed using an autoclave (NAPCO 8000-DSE, Winchester, VA, USA).

All titanium surfaces were tested for endotoxin using the LAL QCL-1000® Assay (Lonza, Walkersville, MD, USA), according to manufacturer's directions. Endotoxin levels were found to be below detection level (< 0.05 EU/ml).

3.3.3 ASC isolation and culture

The adipose-derived mesenchymal stem cell (ASC) population was isolated from the inguinal and epididymal regions of a male Sprague Dawley rat following modified

previously published protocols [24-26]. Briefly, upon harvest, the adipose tissue was

minced and washed extensively in sterile Dulbecco's phosphate buffered saline (Hyclone,

Logan, UT, USA). The adipose tissue was digested in 0.075% Collagenase Type I

(Gibco-Invitrogen, Carlsbad, CA, USA) at 37°C in a shaking water bath. The digest was

neutralized with complete media, consisting of DMEM/F-12 (Hyclone, Logan, UT,

USA), 10% MSC Qualified FBS (Gibco-Invitrogen, Carlsbad, CA, USA), and 1%

antibiotic/antimycotic (Gibco-Invitrogen, Carlsbad, CA, USA). The tissue was

centrifuged at 1200g for 10 minutes, and then incubated in a red blood cell lysis buffer

(160 mM ammonium chloride) at 37°C in a shaking water bath. The tissue homogenate

was centrifuged at 1200g for 10 minutes and the pellet was resuspended in complete cell

culture medium and plated in a T-75 tissue culture flask (Falcon, BD Biosciences,

Bedford, MA, USA). Following 24 hours, the flask was washed to remove any non-

adherent cell population. Thereafter, the cell culture media was changed every 2-3 days.

The cells were passaged at 80% confluency with 0.25% Trypsin/EDTA (Gibco-

Invitrogen, Carlsbad, CA, USA). Passages 4-6 were used for the adherence and

cytotoxicity studies.

3.3.4 BMMSC culture

The bone marrow-derived mesenchymal stem cell population (BMMSC) was

purchased from the Texas A&M University System Health Science Center and was

derived from a 4-month old male Lewis rat. The BMMSCs were cultured in complete

medium, consisting of MEM α with L-glutamine (Gibco-Invitrogen, Carlsbad, CA,

USA), 20% FBS (Premium select, Atlanta Biologicals, Lawrenceville, GA, USA), 2% L-

glutamine (200 mM, Gibco-Invitrogen, Carlsbad, CA, USA), and 1%

antibiotic/antimycotic (Gibco-Invitrogen, Carlsbad, CA, USA). The cells were cultured

in T-75 tissue culture flasks (Falcon, BD Biosciences, Bedford, MA, USA) and passaged

at 80% confluency with 0.25% Trypsin/EDTA (Gibco-Invitrogen, Carlsbad, CA, USA).

Passage 8 BMMSCs were used for the cytotoxicity studies.

3.3.5 Characterization of MSCs

To verify the multilineage differentiation potential, passages 2-9 of the ASCs and

BMMSCs were differentiated into adipogenic and osteogenic lineages over a 3-week

period using a commercial kit according to manufacturer's directions (Hyclone, Logan,

UT, USA). To confirm differentiation, Oil Red O (Sigma-Aldrich, St. Louis, MO, USA)

was used to stain the lipid droplets of the adipogenic cultures, and Alizarin Red S

(Sigma-Aldrich, St. Louis, MO, USA) was used to stain the calcium deposits of the

osteogenic cultures. Dermal fibroblasts (CRL-1414, ATCC, Manassas, VA, USA) and

epidermal cells (CCL-68, ATCC, Manassas, VA, USA) were used as controls.

To confirm the immunophenotype of the MSCs, the cells were stained for a panel

of cell surface markers, according to Harting et al [27] and Dominici et al [28]. Both

ASCs and BMMSCs (passages 2-9) were stained for the following: CD90-PerCP/Cy5.5

(BioLegend, San Diego, CA, USA), CD29-FITC (LifeSpan BioSciences, Seattle, WA,

USA), CD45-APC/Cy7 (BioLegend, San Diego, CA, USA), CD34-PE/Cy7 (Santa Cruz

Biotechnology, Santa Cruz, CA, USA), CD79α-PE (Santa Cruz Biotechnology, Santa

Cruz, CA, USA), and CD11b-AF647 (AbD Serotec, Raleigh, NC, USA). Isotype

controls included the following: APC Mouse IgG1, κ (BioLegend, San Diego, CA, USA),

FITC Armenian Hamster IgG (BioLegend, San Diego, CA, USA), FITC Mouse IgG2a, κ (BioLegend, San Diego, CA, USA), and PE Mouse IgG (Santa Cruz Biotechnology, Santa Cruz, CA, USA). Flow cytometry was performed on a FACSCanto-II Analyzer (Becton-Dickinson, San Jose, CA, USA) with appropriate compensation using BD CompBead Plus Particles (BD Biosciences, San Diego, CA, USA), and data were analyzed using FACSDiva software (Becton-Dickinson, San Jose, CA, USA). Results are expressed as a percent of the total cells gated, which are calculated by subtracting the % gated of non-labeled cells from the % gated of labeled cells.

3.3.6 Adherence of ASCs on porous titanium surfaces in various cell delivery solutions

The ASCs (passages 4-6) were seeded on the porous titanium surfaces in four different cell delivery solutions: (1) complete culture medium (see above for ASCs), (2) basal cell culture media (DMEM/F-12, Hyclone, Logan, UT, USA), (3) phosphate buffered saline with calcium and magnesium (PBS +/+, Hyclone, Logan, UT, USA), and (4) PBS without calcium and magnesium (PBS -/-, Hyclone, Logan, UT, USA). Each porous titanium surface was placed in a 12-well tissue culture plate (Falcon, BD Biosciences, Bedford, MA, USA), then carefully seeded with 500,000 cells in 50 µl of appropriate cell delivery solution and incubated at 37°C with 5-10% CO_2. Cell adherence analyses were performed at 4, 8, and 24 hours after seeding. To determine the number of cells adhered, the porous titanium surfaces were gently rinsed with complete media in each well, removing any unbound cells, after which the titanium pieces were removed from the well. Adherent cells on the well surface were disassociated using

0.25% Trypsin/EDTA (Gibco-Invitrogen, Carlsbad, CA, USA).   Cells adhered to the

well surface and cells in the supernatant were counted using a hemocytometer, and

viability was assessed using 0.4% Trypan Blue (Gibco-Invitrogen, Carlsbad, CA, USA).

The number of cells adhered to the titanium surface ($Cells_{pTi}$) was determined by

subtracting the total number of cells counted in the well ($Cells_{TCP}$) and supernatant

($Cells_{SUP}$) from the total number of cells initially seeded on the implant ($Cells_I$).

$$Cells_{pTi} = Cells_I - (Cells_{TCP} + Cell_{SUP})$$

To visualize adhered cells on the porous titanium surface, the removed titanium

pieces with adherent cells were fixed in 10% neutral buffered formalin (Fisher Scientific,

Pittsburgh, PA, USA), rinsed, and then imaged using low-vacuum scanning electron

microscopy with electron backscattered diffraction (SEM/EBSD, FEI™ Quanta™ 600

FEG, Hillsboro, OR, USA). All cellular adherence experiments were independently

performed three times.

3.3.7 Cytotoxicity on titanium surfaces in various cell delivery

solutions

The ASCs and the BMMSCs (passage 8) were separately seeded on the porous

titanium surfaces in three different cell delivery solutions. For the ASCs, the delivery

solutions included: (1) complete culture medium (see above for ASCs), (2) basal cell

culture medium (DMEM/F-12, Hyclone, Logan, UT, USA), and (3) PBS with calcium &

magnesium (Hyclone, Logan, UT, USA). For the BMMSCs, the solutions included: (1)

complete culture medium (see above for BMMSCs), (2) basal cell culture medium (MEM

α, Gibco-Invitrogen, Carlsbad, CA, USA), and (3) PBS with calcium and magnesium

(Hyclone, Logan, UT, USA). To serve as controls, cells were seeded on smooth polished titanium surfaces, roughened titanium surfaces, and on tissue culture plastic of a 12-well plate (Falcon, BD Biosciences, Bedford, MA, USA). Each titanium piece was carefully seeded with 500,000 cells in 50 µl of delivery solution in a 12-well plate (Falcon, BD Biosciences, Bedford, MA, USA) to ensure cells were cultured on the titanium pieces without overflowing into the wells. Following seeding, 1.5 ml of delivery solution was carefully added to each well. The 12-well culture plates were then incubated at 37˚C with 5-10% CO_2 until analysis time point. To analyze cytotoxicity of the ASCS and BMMSCs, the Vybrant Cytotoxicity Assay Kit (V-23111, Molecular Probes, Eugene, OR, USA) was used and followed according to manufacturer's directions. Cytotoxicity was assessed at 0, 4, 12, and 24 hours following cell seeding. All cytotoxicity experiments were independently performed three times.

3.3.8 Statistical analysis

Data are represented as mean values ± standard error (SE) or ± standard deviation (SD) as specified. For the ASC adherence studies, statistical significance was determined ($p < 0.05$, two-tailed, 95% confidence interval) using a paired t-test (SPSS vs.11.5, Armonk, NY, USA) for comparisons between cell delivery groups within each time point. With the paired t-test, using data that are matched on time point, this test statistic correctly controls for cell passage number. For the BMMSC cytotoxicity studies, statistical significance was determined ($p < 0.05$, two-tailed, 95% confidence interval) using an independent sample student t-test (SPSS vs.11.5, Armonk, NY, USA) for comparisons between cell delivery groups which was performed separately for each time

point. The Benjamini-Hochberg test was used for multiple comparison tests between

groups across the time points (Stata/IC 10.1, College Station, TX, USA). We report

Benjamini-Hochberg adjusted *p* values, which maintains the false discovery rate (FDR) at

the nominal alpha 0.05 level [29]. Controlling for multiplicity in the standard fashion,

such as with the Bonferroni procedure which controls the family-wise error rate (FWER),

is not justified, while control for the FDR provides the correct control for multiplicity

[29-31].

3.4 Results

3.4.1 Preparation and surface characterization of titanium surfaces

The porosity of the porous titanium surfaces was determined to be ~55% using

microCT analysis. The average pore size as determined by SEM analysis was found to

be ~360um (Figure 3.1). The average Ra values of the smooth and roughened titanium

surfaces were 0.53um (SD=0.13) and 1.41um (SD=0.21), respectively.

3.4.2 Characterization of MSCs

Both ASCs and BMMSCs were successfully differentiated into adipogenic and

osteogenic lineages, as seen by the formation and staining of lipid droplets and calcified

extracellular matrix deposits (Figure 3.2). Differentiation was not observed in the control

ASCs and BMMSCs that did not receive differentiation medium. Further, differentiation

was not observed in the dermal fibroblast and epidermal cell cultures that were cultured

in differentiation media (data not shown). The cell surface markers were detected in

consistent proportions on the ASC and BMMSC populations, showing greater than 90%

positive for CD90 and CD29, and less than or around 10% positive for CD45, CD34,

CD11b, and CD79α (Table 3.1).

3.4.3 Adherence of ASCs on porous titanium surfaces in various

cell delivery solutions

The adherence of ASCs on the porous titanium surfaces in the four cell delivery

solutions was analyzed over a 24-hour period. Due to limitations of the porous coated

surface, it was determined the most appropriate method to determine cellular adherence

was through quantitation of the adherent cells to the wells and the floating cells in

supernatant using trypan blue staining and counting with a hemacytometer. These

numbers provided an indirect quantitation of cells adhered on the porous coating.

Significantly ($p < 0.05$) more cells were adhered to the porous titanium in the

basal cell culture medium at 8 hours (433,500 cells) compared to the PBS without

calcium and magnesium (364,750 cells). Throughout the entire 24-hour time period, it

was found that cell adherence minimally increased over time in all four delivery solutions

(Figure 3.3). At 4 hours, approximately 80% of originally seeded ASCs were adherent to

the porous surface when seeded in the complete media (430,278 cells) and in the basal

culture media (408,875 cells). At 24 hours, 89.5% of ASCs (447,500 cells) were

adherent on the porous titanium in complete culture medium and 86.7% of ASCs

(433,500 cells) were adherent in basal culture medium. Overall, no significant differences

were found between complete media and the basal culture medium. Cells seeded in both

PBS solutions were about 70% adherent (375,875 cells in PBS+/+ and 357,875 cells in

PBS-/-) at 4 hours and reached just under 80% (410,250 cells in PBS+/+ and 399,000

cells in PBS-/-) at 24 hours. No significant differences were found among each solution

over the three time points using the multiple comparison procedure.

To visualize the adherent cells, SEM/EBSD images were captured of the porous

surfaces in each solution at each time point. Imaging confirmed the cell count numbers

in that no large differences were observed among the four delivery solutions over the 24-

hour period (Figure 3.4).

3.4.4 Cytotoxicity on titanium surfaces in various cell delivery

solutions

The cytotoxicity of the ASCs and the BMMSCs were evaluated in the delivery

solutions over a 24-hour period using a commercially available Vybrant™ Cytotoxicity

assay, which measures the levels of the cytosolic enzyme glucose 6-phosphate

dehydrogenase (G6PD) that is released into the surrounding medium from damaged cells.

The cells were seeded on the porous titanium surfaces as was performed to examine

cellular adherence. In addition, the cells were also seeded on smooth polished titanium

surfaces, roughened titanium surfaces, and tissue culture plastic to serve as controls

assessing for any potential cytotoxic effect the titanium produced on the adherent cell

population. All data were normalized to wells in which the cells were fully lysed,

creating 100% cytotoxicity, thus the data are represented as relative percent cytotoxicity.

Cytotoxicity levels and trends were similar between both the ASCs and the

BMMSCs, and as such, data are shown only for the BMMSCs. It was found that

cytotoxicity levels remained fairly consistent within 4 hours after seeding, but was

significantly increased at the 12-hour time point between PBS and complete medium ($p <$

0.05), and almost significantly different at the 24-hour time point between PBS and basal

culture medium ($p = 0.054$) (Figure 3.5). Cytotoxicity levels of cells seeded on the

porous titanium pieces in PBS increased 43% between 12 and 24 hours (Figure 3.6a).

When seeded in PBS on tissue culture plastic, a similar increase was observed, with 22%

cytotoxicity at 12 hours increasing to 79% cytotoxicity at 24 hours, a 57% increase

(Figure 3.6b). Cytotoxicity increased from 8% to 11% on the porous titanium surface in

the basal culture medium between the 12- and 24-hour time points. The cells on the

porous titanium pieces in complete medium had overall lower cytotoxicity levels, with

~1% cytotoxicity at 12 hours and 4% cytotoxicity at 24 hours. Both basal culture

medium and complete medium exhibited a 3% increase in cytotoxicity. Overall trends in

cytotoxicity levels were similar whether or not cells were seeded on the porous titanium

pieces (Figure 3.6).

3.5 Discussion

Successful outcomes of stem cell therapies are dependent on, among other factors,

cell viability and cellular adherence on the delivery platform, which could be a

manufactured implant surface, a tissue engineered scaffold, or a cell delivery suspension.

Our work evaluated whether or not commonly used and reported cell delivery solutions

would have an effect over a 24-hour period on cellular adherence and cytotoxicity when

cells were seeded on porous titanium surfaces. Specifically, we were interested in using a

solution that provided nutrients for cellular activity during a 24-hour period while at the

same time did not cause a concern for an immunogenic response when transplanted *in

vivo*.

We found that cellular adherence over twenty-four hours was not significantly different between basal cell culture medium and complete cell culture medium (i.e. serum supplemented). At 8 hours after seeding, statistical significance was seen between basal cell culture medium and PBS without calcium and magnesium. Overall, as expected, the common trend was that cellular adherence minimally increased over time in all solutions, with complete medium > basal cell culture medium > PBS with calcium and magnesium > PBS without calcium and magnesium. As cellular adherence was not significantly different between complete medium and basal cell culture medium over time, we can conclude that basal cell culture medium is sufficient for allowing cellular adherence in a 24-hour time period.

Similar to the cellular adherence results, cytotoxicity was not significantly different over twenty-four hours between basal cell culture medium and complete cell culture medium. Significant differences in cytotoxicity levels began to appear 12 hours after seeding between complete medium and PBS, and close to significantly different between basal culture medium and PBS at 24 hours. As cytotoxicity differences between the solutions began to dramatically differentiate between 4 and 12 hours from seeding, this reflects the effect basic nutrients and more complex nutrients provided in basal cell culture media and complete media, respectively, have on cell viability when compared to simple saline solutions. Regarding the loss of viability of cells when in PBS, similar results have shown that viability of cells stored in PBS begin to dramatically decrease between 6 and 8 hours [32, 33]. Lane et al. showed further that cells stored in PBS after 24 hours not only had greatly reduced viability, but their growth rate was even more markedly reduced [34]. Though these studies were investigating cells stored in

suspension versus cells adhered to a surface, the trends are similar and the central theme is consistent in that a nutrient-deprived solution should not be a primary cell storage solution for periods longer than 12 hours.

Interestingly, the cytotoxicity levels were consistently lower on the porous surfaces compared to cytotoxicity levels of cells seeded on tissue culture plastic in all three solutions. On the other hand, the cytotoxicity levels were noticeably higher on the smooth and roughened titanium surfaces compared to the tissue culture plastic. We speculate that the contoured and tortuous porous coating limited complete availability of G6PD in the supernatant to be accessible for analysis. Though great care was taken to triturate the wells so that G6PD was homogenously suspended in the supernatant, we suspect that the porous coating limited those efforts. Given that the smooth and rough titanium surfaces had slightly increased cytotoxicity levels, this suggests that the titanium did affect cellular activity to a certain extent. Similar results were shown previously regarding cell growth rates in that BMMSCs and ASCs have slightly increased proliferation rates on tissue culture plastic compared to Ti6Al4V, though differences were not statistically significant [35].

A few limitations are present within this study. Due to the porous titanium surfaces, it was difficult to accurately quantitate the exact number of cells adhered. The methods we used to determine the number of cells adhered were adequate to provide a semi-quantitative analysis. Another concern is that the porous, smooth, and roughened titanium pieces were each a different size (i.e., triangular piece compared to circular pieces). This was due to limited availability of porous surfaces that would fit a 12-well culture plate. Though they were a different size, the same number of cells was seeded on

all surfaces, and since the porous surface did provide an increased surface area, this accommodated to a certain extent for the difference in sizes. Additional concerns might arise regarding the stem cell multilineage differentiation capacity and the immunophenotypic characteristic of the cells after culture on the titanium pieces in the different solutions over 24 hours. Previous groups have characterized the functionality and immunophenotype of MSCs when suspended in PBS over a 24-hour period and have confirmed they retain their capacity for multilineage differentiation and immunophenotypic expression [32, 33]. Studies evaluating stem cell characteristics when cultured on titanium alloy showed similar results when compared to routinely cultured MSCs on tissue culture plastic [35]. Though MSC characteristics have not been fully characterized when grown on titanium in a PBS solution for 24 hours, this may not be as critical for our future *in vivo* studies since we have shown the level of cytotoxicity to reach 55%, which is considerable and not desirable when the end goal is transplanting cells *in vivo*. With that said, future studies should confirm the functional and phenotypic stem cell characteristics of the cells after being adhered to titanium in PBS.

Our investigations show that between 8 and 12 hours after seeding, the lack of nutrients in a delivery solution begins to significantly decrease cellular adherence on porous titanium surfaces. Further, solutions lacking necessary components for cellular metabolism begin to dramatically induce cellular damage as evidenced by increased cytotoxicity levels at 12 hours after seeding. For future *in vivo* studies in which cells will be seeded and delivered on a porous titanium substrate, we have shown that using a basal cell culture medium is equivalent to serum-supplemented cell culture medium when

transplanting within a 24-hour period. This will allow for maximal cellular adherence and viability while diminishing concerns of eliciting an immunogenic response.

3.7 References

1.   Hagberg K, Branemark R. One hundred patients treated with osseointegrated transfemoral amputation prostheses--rehabilitation perspective. J Rehabil Res Dev 2009;46(3):331-344.

2.   Branemark R, Branemark PI, Rydevik B, Myers RR. Osseointegration in skeletal reconstruction and rehabilitation: a review. J Rehabil Res Dev 2001;38(2):175-181.

3.   Tillander J, Hagberg K, Hagberg L, Branemark R. Osseointegrated titanium implants for limb prostheses attachments: infectious complications. Clin Orthop Relat Res 2010;468(10):2781-2788.

4.   Isackson D, McGill LD, Bachus KN. Percutaneous implants with porous titanium dermal barriers: an in vivo evaluation of infection risk. Med Eng Phys 2011;33(4):418-426.

5.   von Recum AF. Applications and failure modes of percutaneous devices: a review. J Biomed Mater Res 1984;18(4):323-336.

6.   Winter GD. Transcutaneous implants: reactions of the skin-implant interface. J Biomed Mater Res 1974;8(3):99-113.

7.   Stappenbeck TS, Miyoshi H. The role of stromal stem cells in tissue regeneration and wound repair. Science 2009;324(5935):1666-1669.

8.   Jeon YK, Jang YH, Yoo DR, Kim SN, Lee SK, Nam MJ. Mesenchymal stem cells' interaction with skin: wound-healing effect on fibroblast cells and skin tissue. Wound Repair Regen 2010;18(6):655-661.

9.   Phinney DG, Prockop DJ. Concise review: Mesenchymal stem/multipotent stromal cells: The state of transdifferentiation and modes of tissue repair - Current views. Stem Cells 2007;25(11):2896-2902.

10.   Wu Y, Chen L, Scott PG, Tredget EE. Mesenchymal stem cells enhance wound healing through differentiation and angiogenesis. Stem Cells 2007;25(10):2648-2659.

11.   Fathke C, Wilson L, Hutter J, Kapoor V, Smith A, Hocking A, et al. Contribution of bone marrow-derived cells to skin: collagen deposition and wound repair. Stem Cells 2004;22(5):812-822.

12.   Wakitani S, Goto T, Pineda SJ, Young RG, Mansour JM, Caplan AI, et al. Mesenchymal cell-based repair of large, full-thickness defects of articular cartilage. Journal of Bone and Joint Surgery - Series A 1994;76(4):579-592.

13.   Lendeckel S, Jodicke A, Christophis P, Heidinger K, Wolff J, Fraser JK, et al. Autologous stem cells (adipose) and fibrin glue used to treat widespread traumatic calvarial defects: case report. J Craniomaxillofac Surg 2004;32(6):370-373.

14.   Kretlow JD, Spicer PP, Jansen JA, Vacanti CA, Kasper FK, Mikos AG. Uncultured marrow mononuclear cells delivered within fibrin glue hydrogels to porous scaffolds enhance bone regeneration within critical-sized rat cranial defects. Tissue Engineering 2010;16(12):3555-3568.

15.   Choi JS, Yang HJ, Kim BS, Kim JD, Kim JY, Yoo B, et al. Human extracellular matrix (ECM) powders for injectable cell delivery and adipose tissue engineering. J Control Release 2009.

16.   Moseley TA, Zhu M, Hedrick MH. Adipose-derived stem and progenitor cells as fillers in plastic and reconstructive surgery. Plast Reconstr Surg 2006;118(3 Suppl):121S-128S.

17.   Perin EC, Silva GV. Cell-based therapy for chronic ischemic heart disease-a clinical perspective. Cardiovasc Ther 2011;29(3):211-217.

18.   Fu X, Fang L, Li X, Cheng B, Sheng Z. Enhanced wound-healing quality with bone marrow mesenchymal stem cells autografting after skin injury. Wound Repair Regen 2006;14(3):325-335.

19.   Pieri F, Lucarelli E, Corinaldesi G, Aldini NN, Fini M, Parrilli A, et al. Dose-dependent effect of adipose-derived adult stem cells on vertical bone regeneration in rabbit calvarium. Biomaterials 2010;31(13):3527-3535.

20.   Sikavitsas VI, van den Dolder J, Bancroft GN, Jansen JA, Mikos AG. Influence of the in vitro culture period on the in vivo performance of cell/titanium bone tissue-engineered constructs using a rat cranial critical size defect model. J Biomed Mater Res A 2003;67(3):944-951.

21.   Meretoja VV, Tirri T, Aaritalo V, Walboomers XF, Jansen JA, Narhi TO. Titania and titania-silica coatings for titanium: comparison of ectopic bone formation within cell-seeded scaffolds. Tissue Engineering 2007;13(4):855-863.

22.   Bensaid W, Triffitt JT, Blanchat C, Oudina K, Sedel L, Petite H. A biodegradable fibrin scaffold for mesenchymal stem cell transplantation. Biomaterials 2003;24(14):2497-2502.

23.   Lee HJ, Yu C, Chansakul T, Hwang NS, Varghese S, Yu SM, et al. Enhanced chondrogenesis of mesenchymal stem cells in collagen mimetic peptide-mediated microenvironment. Tissue Engineering 2008;14(11):1843-1851.

24.   Bjorntorp P, Karlsson M, Pertoft H, Pettersson P, Sjostrom L, Smith U. Isolation and characterization of cells from rat adipose tissue developing into adipocytes. Journal of Lipid Research 1978;19(3):316-324.

25.   Bunnell BA, Flaat M, Gagliardi C, Patel B, Ripoll C. Adipose-derived stem cells: isolation, expansion and differentiation. Methods 2008;45(2):115-120.

26.   Zuk PA, Zhu M, Mizuno H, Huang J, Futrell JW, Katz AJ, et al. Multilineage cells from human adipose tissue: implications for cell-based therapies. Tissue Engineering 2001;7(2):211-228.

27.   Harting M, Jimenez F, Pati S, Baumgartner J, Cox C, Jr. Immunophenotype characterization of rat mesenchymal stromal cells. Cytotherapy 2008;10(3):243-253.

28.   Dominici M, Le Blanc K, Mueller I, Slaper-Cortenbach I, Marini F, Krause D, et al. Minimal criteria for defining multipotent mesenchymal stromal cells. The International Society for Cellular Therapy position statement. Cytotherapy 2006;8(4):315-317.

29.   Benjamini Y, Hochberg, Y. Controlling the false discovery rate: a practical and powerful approach to multiple testing. J R Statist Soc, Series B (Methodological) 1995;57(1):289-300.

30.   Rosner B. Fundamentals of Biostatistics. 6 ed. Belmont, CA: Brooks/Cole Cengage Learning, 2006.

31.   Moye L. Handbook of Statistics 27: Epidemiology and Medical Statistics. New York: Elsevier, 2008.

32.   Muraki K, Hirose M, Kotobuki N, Kato Y, Machida H, Takakura Y, et al. Assessment of viability and osteogenic ability of human mesenchymal stem cells after being stored in suspension for clinical transplantation. Tissue Engineering 2006;12(6):1711-1719.

33.   Pal R, Hanwate M, Totey SM. Effect of holding time, temperature and different parenteral solutions on viability and functionality of adult bone marrow-derived mesenchymal stem cells before transplantation. J Tissue Eng Regen Med 2008;2(7):436-444.

34.   Lane TA, Garls D, Mackintosh E, Kohli S, Cramer SC. Liquid storage of marrow stromal cells. Transfusion 2009;49(7):1471-1481.

35.   Tognarini I, Sorace S, Zonefrati R, Galli G, Gozzini A, Carbonell Sala S, et al. In vitro differentiation of human mesenchymal stem cells on Ti6Al4V surfaces. Biomaterials 2008;29(7):809-824.

Table 3.1. BMMSC phenotypic characterization. Cell surface marker expression determined by flow cytometry on P.6 – P.8 BMMSCs. Data are represented as means ± SD.

Cell Surface Marker	Percent Positive	Percent Negative
CD29	100 ± 0	0 ± 0
CD90	100 ± 0	0 ± 0
CD34	4.7 ± 2.2	95.3 ± 2.2
CD45	0.3 ± 0.1	99.7 ± 0.1
CD11b	11.6 ± 17.3	88.2 ± 17.7
CD79a	9.1 ± 7.5	91.3 ± 7.1
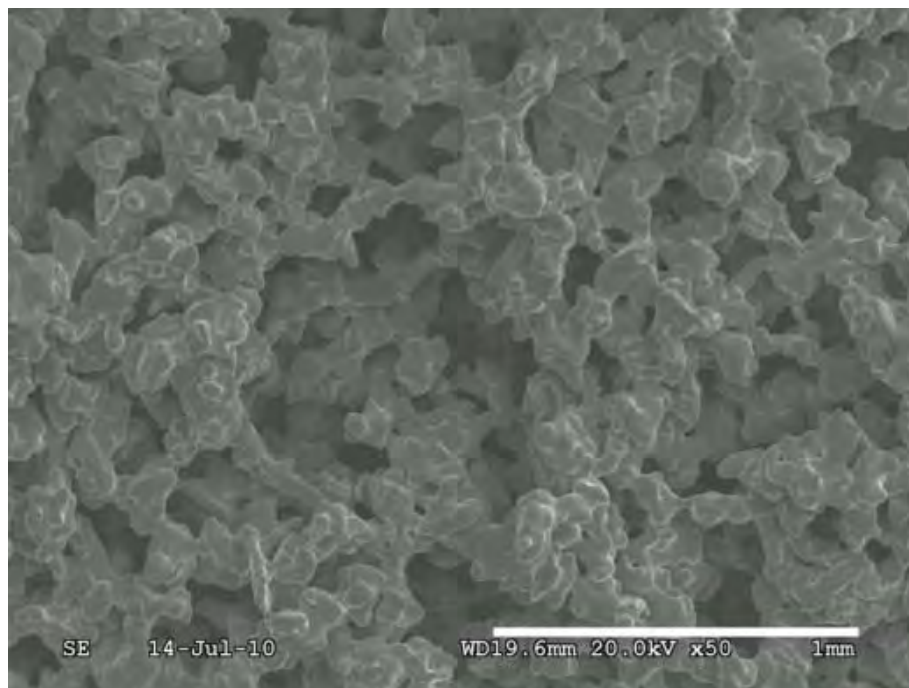
Figure 3.1. Commercially pure titanium porous coating. Scanning electron microscopy image (SEM) of the titanium porous coating having ~360μm pore size and ~55% porosity (magnification: 50x; accelerating voltage: 20.0kV). Scale bar is 1mm in length.
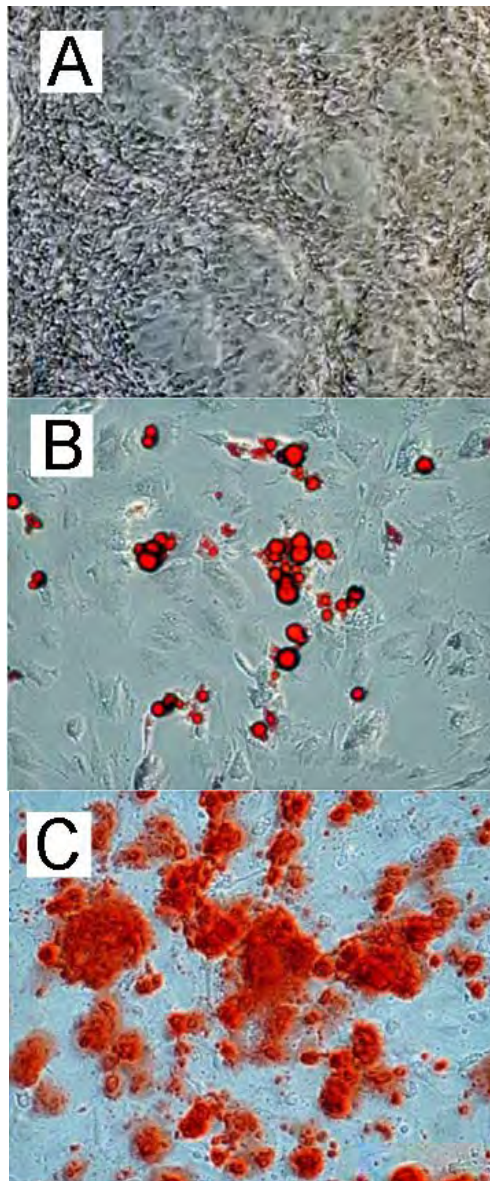
Figure 3.2 Differentiation of P.8 BMMSCs. (A) Control cells in complete growth medium (4x magnification). (B) Adipogenic differentiation and Oil Red O staining of lipid droplets (10x magnification). (C) Osteogenic differentiation and Alizarin Red S staining of calcium deposits (10x magnification).
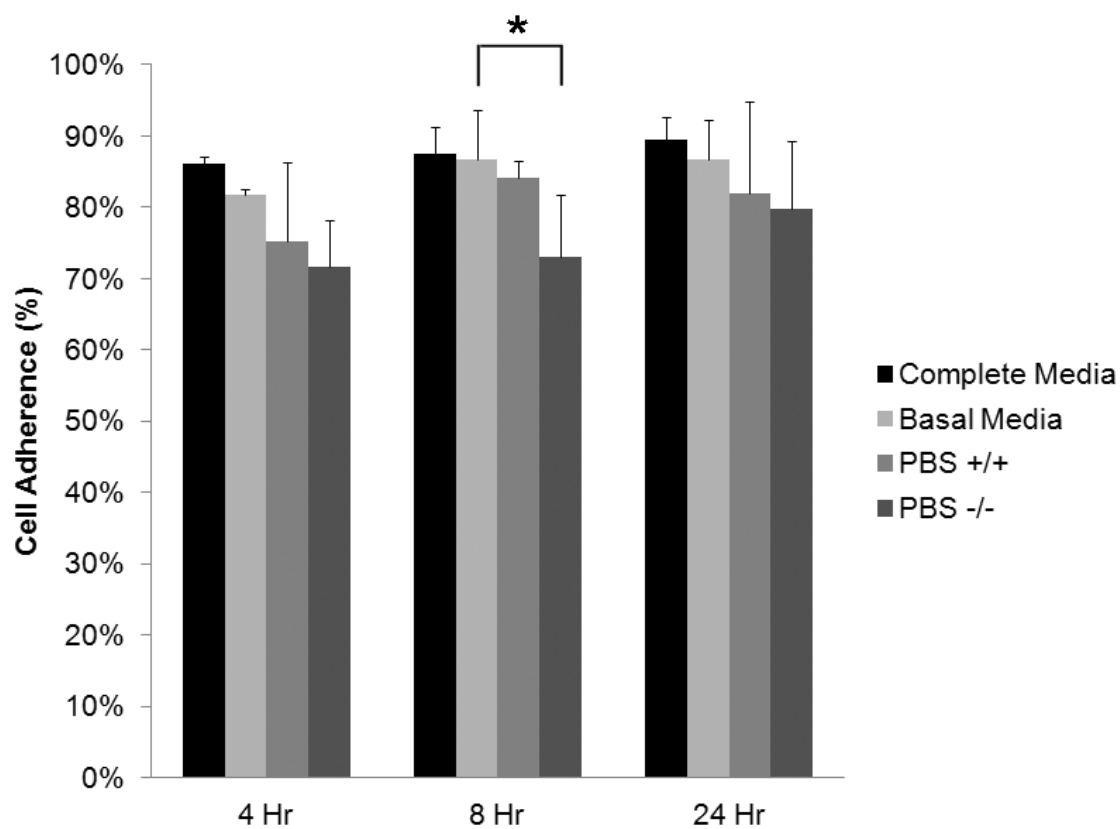
Figure 3.3 Effect of delivery solution on adherence of ASCs over a 24-hour period when seeded on pTi. *Significance ($p < 0.05$) between basal cell culture medium and PBS -/- at 8 hours after seeding. The data are represented as mean +SEM, n=3.
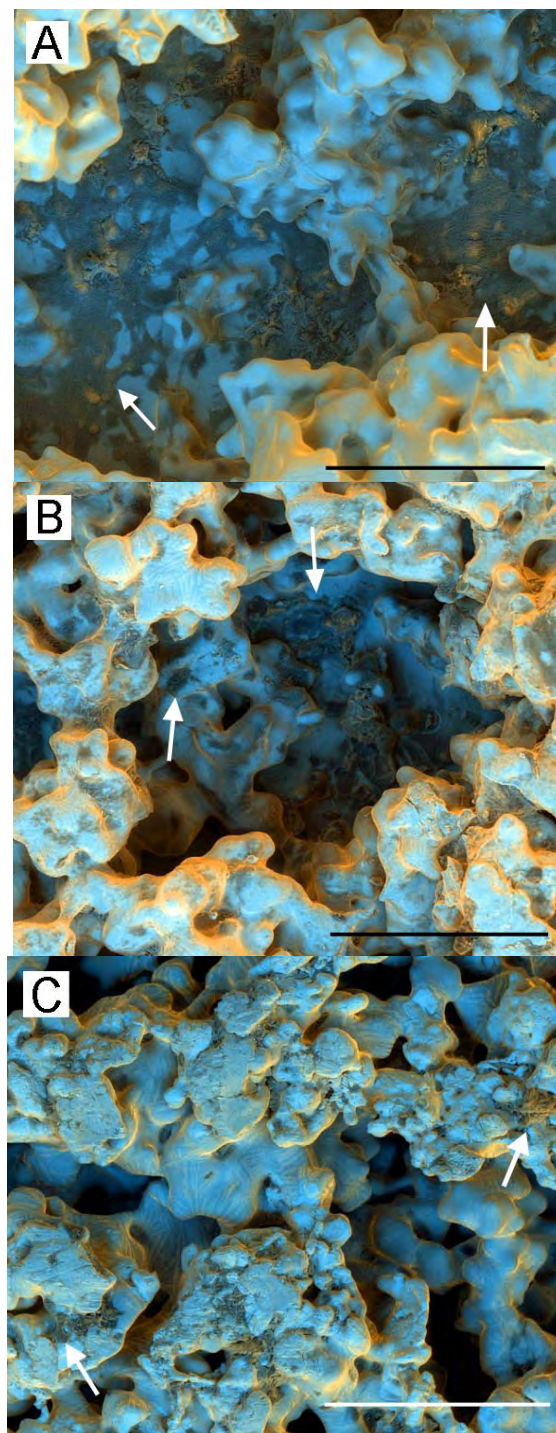
Figure 3.4. SEM/EBSD of MSC adherence on pTi (white arrows) at 8 hours. (A) complete culture medium, (B) basal cell culture medium, and (C) PBS-/- (accelerating voltage: 15.0 kV). Scale bar is 300 µm in length.
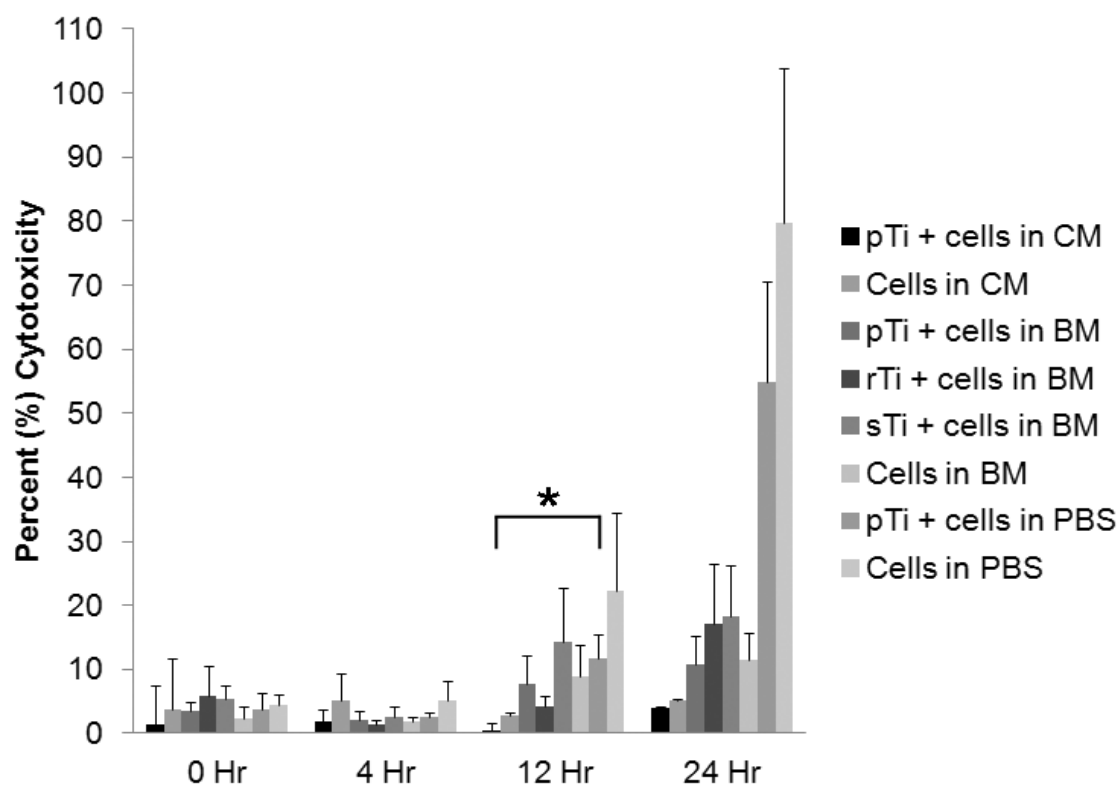
Figure 3.5 Percent cytotoxicity on titanium surfaces. Effect of delivery solution on cytotoxicity levels over a 24-hour period when MSCs are seeded on pTi, sTi, rTi, and tissue culture plastic. *Significance ($p < 0.05$) between pTi + cells in CM and pTi + cells in PBS at 12 hours. Data are represented as mean +SEM, n=3.
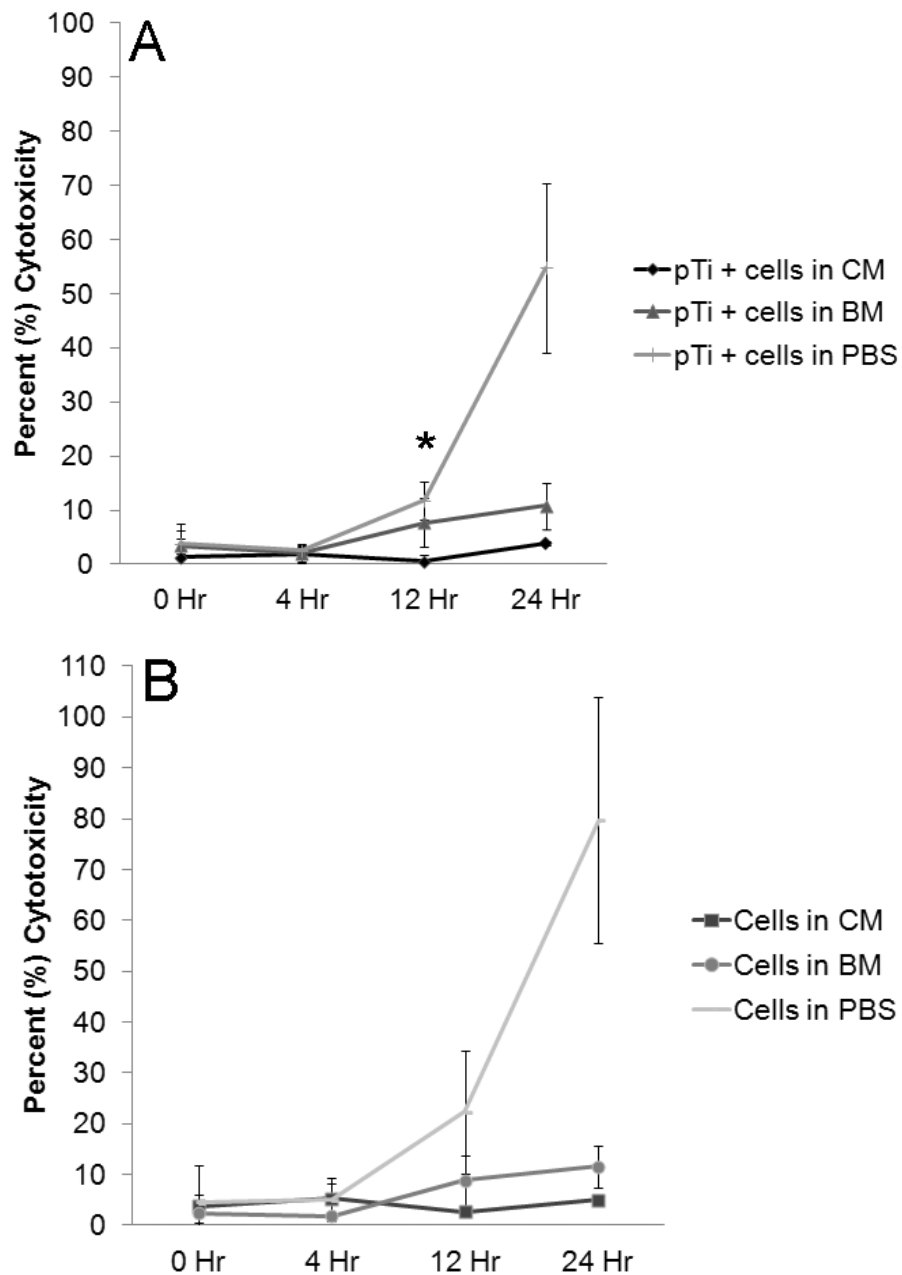
Figure 3.6 Cytotoxicity comparison between pTi and tissue culture plastic. Cytotoxicity begins to dramatically increase 12 hours after seeding whether or not the MSCs are seeded on a porous titanium piece. (A) MSCs seeded on pTi. (B) MSCs seeded on tissue culture plastic. *Significance ($p < 0.05$) between pTi + cells in CM and pTi + cells in PBS at 12 hours. Data are represented as mean ± SEM, n=3.

CHAPTER 4

MESENCHYMAL STEM CELLS INCREASE COLLAGEN

INFILTRATION AND IMPROVE WOUND HEALING

RESPONSE TO POROUS TITANIUM

PERCUTANEOUS IMPLANTS

4.1 Abstract

Epidermal downgrowth, commonly associated with long-term percutaneous

implants, weakens the skin-implant seal and greatly increases the vulnerability of the site

to infection. To improve the skin attachment and early tissue integration with porous

metal percutaneous implants, we evaluated the effect of bone marrow-derived

mesenchymal stem cells (BMMSCs) to provide wound healing cues and vascularization

to the dermal and epidermal tissues in establishing a barrier with the implant. Two

porous metal percutaneous implants, one treated with BMMSCs and one untreated, were

placed on the dorsum of a Lewis rat. Implants were evaluated at 0, 3, 7, 28, and 56 days

after transplantation. Histological analysis evaluated cellular infiltrates, vascularization,

quantity and quality of tissue ingrowth, epidermal downgrowth, and fibrous

encapsulation. The amount of collagen infiltrating the porous coating was significantly

greater for the BMMSC-treated implants at 3 and 28 days following transplantation

compared to untreated implants. There was an early influx and resolution of cellular inflammatory infiltrates in the treated implants compared to the untreated. Vascularization increased over time in both treated and untreated implants, with no statistical significance. Epidermal downgrowth was minimally observed in all implants with no correlation to MSC treatment. Our results suggest that BMMSCs can influence an early and rapid resolution of acute and chronic inflammation in wound healing, and can stimulate early collagen deposition and granulation tissue associated with later stages of wound repair. These findings provide evidence that BMMSCs can stimulate a more rapid and improved barrier between the skin and porous metal percutaneous implant.

4.2 Introduction

Bone-anchored hearing aids, dental implants, and osseointegrated percutaneous prosthetics are clinically used metal percutaneous devices that are implanted for the lifetime of the individual, and they all require an impassable attachment between the skin and device. When the skin and soft tissue attachment to the implant breaks down or weakens, the susceptibility to infection substantially increases and places the entire device at risk of failure, leading to potential tissue morbidity and device removal.

Previously, we demonstrated with a rabbit model that percutaneous implants with a commercially pure titanium porous coating have a 7-fold decreased risk of infection compared to percutaneous implants with smooth polished titanium surfaces [1]. We observed that in a majority of the implants, the epidermis had migrated internally along the percutaneous component, creating a sinus tract that was filled with keratin and degenerative neutrophils. In fact, several other groups have demonstrated this same

result, which is commonly referred to as epidermal downgrowth, and when accompanied by a sinus tract, marsupialization [2-5]. It is thought that epidermal downgrowth/marsupialization is one of the leading factors attributed to the implant site's risk of infection [2-4, 6-8].

The explanations for this phenomenon are not entirely clear, though possible explanations could include insufficient wound healing signaling cues and cell contact inhibition in the epidermal and dermal tissues [9-11], along with insufficient vascularization of the dermal tissues in providing nutrients for the restoration of the epidermal and dermal barrier [2, 3, 12]. It is also thought that implant motion in the subcutaneous tissue space creates an unstable environment for epidermal attachment to the implant [3, 4, 13]. To address these and other potential mechanisms, there is a need to investigate biological strategies that can interact with the dynamic nature of the dermal and epidermal tissues such that epidermal downgrowth is prevented, and tissue attachment to the percutaneous implant is maximized.

One such strategy is that of mesenchymal stem cell therapy, which is currently being exploited for treatment of several clinical conditions due to their pivotal role in tissue repair and regeneration. Adult mesenchymal stem cells (MSCs) reside in several niches within the body, though for most clinical applications are commonly derived from bone marrow and adipose tissue [14]. Several wound healing studies through the years have published very promising results regarding the ability of MSCs to accelerate wound healing [15-18], increase vascularization [16-18], increase cellularity [16-18], and increase collagen content and wound strength [15, 18, 19]. It is suggested that MSCs produce these effects through two suggested mechanisms: (1) through paracrine signaling

mechanisms, releasing soluble signaling factors, including epidermal growth factor (EGF), keratinocyte growth factor (KGF), insulin-like growth factor-1 (IGF-1), vascular endothelial growth factor-α (VEGF-α), angiopoietin-1 (Ang-1), macrophage inflammatory protein (MIP-1a and MIP-1b), platelet-derived growth factor (PDGF-BB), fibroblast growth factor (FGF), among others [20-22]; and/or (2) through differentiation into resident cells [16, 23].

With regards to the ability of MSCs to influence healing around biomaterials, Prichard et al showed that when adipose-derived mesenchymal stem cells (ASCs) are attached to a biomaterial and implanted in subcutaneous tissue, the ASCs are able to attenuate the foreign body response (FBR) and increase the microvascular density adjacent to the implant surface [24]. Additional studies evaluating scaffolds or implants seeded with MSCs have also reported similar effects of increased vasculature and increased rates of healing within the MSC-treated scaffolds [25, 26].

Using this established work with MSCs, the goal of this study was to evaluate the ability of the MSCs to stimulate and influence an improved skin and soft tissue integration with porous titanium percutaneous implants, hypothesizing that *MSC treated implants will have a more rapid and robust tissue integration compared to untreated implants.* We tested our hypothesis by evaluating five outcomes important in assessing successful wound healing and tissue response to percutaneous implants: (1) inflammatory cellular infiltrates, (2) neovascularization, (3) quality and quantity of tissue integration, (4) epidermal downgrowth, and (5) fibrous encapsulation. Through histological evaluations of these five outcomes, we were able to assess the influence the MSC

treatment had on *stimulating a more rapid and robust tissue integration* with the percutaneous implant.

4.3 Materials and Methods

4.3.1 Ethical statement

      All animal studies were performed according to the *Guide for the Care and Use of Laboratory Animals[27]* and all protocols were approved by the University of Utah Institutional Animal Care and Use Committee (IACUC).

4.3.2 Study design

      The study consisted of 25 animals that were randomly assigned to five groups based on the experimental time point: day 0 (n=3), 3 days (n=6), 7 days (n=6), 28 days (n=5), and 56 days (n=5). Each animal received two implants: (1) treated with 6×10^{6} MSCs and (2) untreated (control). The two implants were randomly assigned placement on the rat dorsum to accommodate for placement-specific biases. Randomization was performed using simple computerized randomization procedures. The Lewis rat served as our animal model and BMMSC source. Lewis rats are commonly used for wound healing studies, and since they are a syngeneic species, this allowed transfer of BMMSCs from one rat to another rat without concern for an immunogenic response [28].

4.3.3 Implant fabrication

      The percutaneous implant consisted of a Ti6Al4V substrate fabricated by the School of Medicine Machine Shop (University of Utah, Salt Lake City, UT, USA).

These substrates then received a commercially pure titanium porous coating (P^2 Thortex, Inc., Portland, OR, USA) that was 1mm thick on the substrate. The porous coating had a ~55% porosity that was previously determined using microCT (Xradia MicroXCT system), and had an average pore size of ~360um that was previously determined using scanning electron microscopy (SEM, Hitachi S3000-N). The percutaneous portion of the implant was cylindrical with a 5mm diameter. At 3mm from the implant top, the implant surface gradually sloped outward to a final subcutaneous base diameter of 17mm. The implant height was 12mm (Figure 4.1).

4.3.4 Endotoxin testing, passivation, and sterilization

All porous titanium percutaneous implants were passivated according to ASTM F86 standards. Briefly, the implants were sonicated in distilled water, then in acetone (Sigma-Aldrich, St. Louis, MO, USA), followed by another distilled water wash before being soaked in 49% nitric acid (Macron Chemicals, Center Valley, PA, USA) for 2 hours. They were then sonicated in distilled water and allowed to air dry overnight.

Prior to each experiment all implants were sterilized as routinely performed using an autoclave (NAPCO 8000-DSE, Winchester, VA, USA).

All implants were tested for endotoxin before and after sterilization using the LAL QCL-1000® Assay (Lonza, Walkersville, MD, USA), according to manufacturer's directions. Endotoxin levels were found to be below detection level (< 0.05 EU/ml).

4.3.5 Bone marrow-derived mesenchymal stem cell culture and scale-up

The bone marrow-derived mesenchymal stem cells (BMMSCs) were derived

from a 4-month old male Lewis rat and were purchased from Texas A&M University

System Health Science Center. The BMMSCs were cultured in complete growth

medium, consisting of MEM α with L-glutamine (Gibco-Invitrogen, Carlsbad, CA,

USA), 20% FBS (Premium select, Atlanta Biologicals, Lawrenceville, GA, USA), 2% L-

glutamine (200 mM, Gibco-Invitrogen, Carlsbad, CA, USA), and 1%

antibiotic/antimycotic (Gibco-Invitrogen, Carlsbad, CA, USA). The cells were seeded at

100 cells/cm^2 density, cultured in T-75 tissue culture flasks (Falcon, BD Biosciences,

Bedford, MA, USA), and passaged at 80% confluency with 0.25% Trypsin/EDTA

(Gibco-Invitrogen, Carlsbad, CA, USA).

To scale-up the number of BMMSCs needed for the *in vivo* transplantations, the

BMMSCs were seeded at a density of 1000 cells/cm^2 and cultured in HYPER*Flask*™

Cell Culture Vessels (Corning Inc., Lowell, MA, USA). Passage 8 BMMSCs were then

cryopreserved in aliquots of 9x10^6 cells until *in vivo* transplantation. All implants were

treated with one lot of P.8 BMMSCs.

4.3.6 Characterization of BMMSCs

To verify a consistent multilineage differentiation potential, passages 6-9 of

BMMSCs were differentiated into adipogenic and osteogenic lineages over a 3-week

period using a commercial kit according to manufacturer's directions (StemPro®,

Invitrogen, Carlsbad, CA, USA). To confirm differentiation, Oil Red O (Sigma-Aldrich,

St. Louis, MO, USA) was used to stain the lipid droplets of the adipogenic cultures, and

Alizarin Red S (Sigma-Aldrich, St. Louis, MO, USA) was used to stain the calcium deposits of the osteogenic cultures. Dermal fibroblasts (CRL-1414, ATCC, Manassas, VA, USA) and epidermal cells (CCL-68, ATCC, Manassas, VA, USA) were used as controls.

To confirm the immunophenotype of the BMMSCs, the cells were stained for a panel of cell surface markers, according to Harting et al [29] and Dominici et al [30]. The BMMSCs (passages 6-8) were stained with the following fluorescent-conjugated antibodies: CD90-PerCP/Cy5.5 (BioLegend, San Diego, CA, USA), CD29-FITC (LifeSpan BioSciences, Seattle, WA, USA), CD45-APC/Cy7 (BioLegend, San Diego, CA, USA), CD34-PE/Cy7 (Santa Cruz Biotechnology, Santa Cruz, CA, USA), CD79α-PE (Santa Cruz Biotechnology, Santa Cruz, CA, USA), and CD11b-AF647 (AbD Serotec, Raleigh, NC, USA). Isotype controls included the following: APC Mouse IgG1, κ (BioLegend, San Diego, CA, USA), FITC Armenian Hamster IgG (BioLegend, San Diego, CA, USA), FITC Mouse IgG2a, κ (BioLegend, San Diego, CA, USA), and PE Mouse IgG (Santa Cruz Biotechnology, Santa Cruz, CA, USA). Flow cytometry was performed on a FACSCanto-II Analyzer (Becton-Dickinson, San Jose, CA, USA) with appropriate compensation using BD CompBead Plus Particles (BD Biosciences, San Diego, CA, USA), and data were analyzed using FACSDiva software (Becton-Dickinson, San Jose, CA, USA). Results are expressed as a percent of the total cells gated, which are calculated by subtracting the percent gated of non-labeled cells from the percent gated of labeled cells.

4.3.7 Seeding of BMMSCs on porous coated percutaneous implants

The day prior to surgery, an aliquot of cells was thawed and recovered in complete growth medium. Before surgery, the cells were detached with 0.25% Trypsin/EDTA (Gibco-Invitrogen, Carlsbad, CA, USA), and $6x10^6$ cells were suspended in 100µl of MEM α (Gibco-Invitrogen, Carlsbad, CA, USA). The BMMSC suspension was carefully added in 10µl droplets onto the porous coated implant. The treated implant was incubated at 37°C with 5-10% CO_2 for 1-2 hours, then carefully transported to the surgery suite, where transplantation occurred within 4-6 hours after cell seeding. Our prior *in vitro* validation studies showed that maximal cell adherence and maximal cell viability can be achieved if cells were seeded in MEM α and delivered within a 4-12 hour time frame after cell seeding.

4.3.8 Animal surgeries

Male Lewis rats (n=25, ~170g and ~6 weeks old), were obtained (Harlan Laboratories, Livermore, CA, USA), and their health was monitored for a week after arrival to ensure fitness of use for surgical procedures. Prior to surgery, animals were housed in groups of three, and after surgery, animals were individually housed (Thoren Caging Systems, Inc., Hazleton, PA, USA). The average room temperature was 71°C with 33% relative humidity, and a 12 hour on/12 hour off light cycle. Animals were fed a standard laboratory diet and water *ad libitum*.

All surgeries were performed under sterile conditions with aseptic technique. Animals were induced with 3-5% Isoflurane (VetOne, Meridian, ID, USA) via inhalation and maintained at 1-3% during operation. Animals were monitored throughout surgical

procedures, specifically heart rate, respiratory rate, blink reflex, skin color, temperature, and % Isoflurane setting. The dorsum of the rat was close-shaved, then animal was positioned on the surgical table. A routine surgical scrub was performed on the dorsum, consisting of alternating scrubs of Povidone-Iodine Solution (Purdue Products L.P., Stamford, CT, USA) and 70% ethyl alcohol, finished with a final scrub of chlorhexidine (CareFusion, San Diego, CA, USA) [31]. A 4-cm incision was made diagonally across the dorsum. Two subcutaneous pockets were created with blunt dissection. The anterior subcutaneous pocket was 2.5cm lateral to the spine on the right side of the animal, just posterior to the scapula. The posterior subcutaneous pocket was 2.5cm lateral to the spine on the left side of the animal, just anterior to the ilium. Using a 4.0mm biopsy punch (Robbins Instruments, Chatham, NJ, USA), a hole was placed through each subcutaneous pocket, being 2.5cm from the central incision. The porous titanium percutaneous implants were then carefully inserted into the subcutaneous pockets and the percutaneous components were inserted through the holes in the skin. This location provided a 5-cm distance between the two implants. The implants that were untreated (control) were submersed in sterile MEM α (Gibco-Invitrogen, Carlsbad, CA, USA) prior to being inserted in the tissue. Once both implants were placed, the central incision was closed with an interrupted vertical mattress suture using 4-0 Vicryl (Ethicon®, Johnson & Johnson, Somerville, NJ, USA). Upon anesthesia recovery and physical mobility, animals were returned to their cages and administered Buprenorphine (Hospira, Lake Forest, IL, USA), 0.05mg/kg, subcutaneous, for analgesia, and as necessary twice per day following 72 hours from surgery. Animals were given Rimadyl wafers (Rodent MD's™, Bio-Serv®, Frenchtown, NJ, USA) for continued pain-relief and water *ad libitum* for 24-

72 hours following surgical procedure. Once animals were no longer showing signs of pain, they were returned to their standard laboratory diet. Animals were observed daily during the first week after surgery, and every other day thereafter until sacrifice. Signs of clinical infection of the implant, any changes to the implant, and overall animal health and well being were assessed.

4.3.9 Implant harvest and histology processing

The animals were euthanized via CO_2 asphyxiation. The implant specimens with generous tissue margins were carefully excised from the dorsum and fixed in 10% neutral buffered formalin (Fisher Scientific, Pittsburgh, PA, USA). The specimens were then dehydrated through ascending grades of ethyl alcohol (Tissue Tek Vacuum Infiltration Process, Miles, Scientific, USA), and embedded in methyl methacrylate (MMA) according to routine laboratory procedures [32]. Upon polymerization, transverse sections (~1mm thick) were cut using a water-cooled, high-speed, lapidary slab saw with a diamond-edged cutting blade (Lortone, Inc., Mukilteo, WA, USA; MK Diamond Products, Inc., Torrence, CA, USA). These sections were ground to 150μm thickness and polished to an optical finish using a variable-speed grinding wheel (Buehler Inc., Lake Bluff, IL, USA).

The sections were stained with hematoxylin and eosin (H&E) or Multiple Stain Solution (MSS, Polysciences, Inc., Warrington, PA, USA). For H&E staining, the slides were placed in Mayer's Hematoxylin (Electron Microscopy Sciences, Hatfield, PA, USA) at 50-55°C for 2-3 hours, then washed in running tap water for 10 minutes. Slides were placed in Eosin Y-Phloxine (Richard Allan Scientific, Kalamazoo, MI, USA) with

Glacial Acetic Acid (Fisher Scientific, Pittsburgh, PA, USA) Solution (3:1) for 10-30

minutes, then rinsed in 100% ethyl alcohol (Fisher Scientific, Pittsburgh, PA, USA). The

slides stained with MSS were placed in acid-alcohol (1% hydrochloric acid; 70% ethyl

alcohol) for 5-10 minutes, then rinsed in distilled water. The MSS was added drop-wise

on the slide to completely cover the section, incubated at 50-55°C on a slide warmer for

8-10 minutes, then gently rinsed in running tap water.

4.3.10 Histology analyses

Slides were interpreted using a light microscope (Optiphot-2, Nikon, Japan;

BX41, Olympus, Center Valley, PA, USA). Images were captured (Retiga 1300,

QImaging, Surrey, BC, Canada) and measurements were made using Bioquant Nova

Prime software (version 6.9.10MR, Bioquant Image Analysis, Nashville, TN, USA).

All histology slides were de-identified by one author (KJC), and blindly

interpreted and analyzed by two authors (DI and LDM). As seen in Figure 4.2, thirteen

$1mm^2$ boxes were analyzed around the implant. A Mertz Graticle was used to

standardize the location and the $1mm^2$ box area for cell counting, tissue volume fill, and

overall interpretation and analysis. As described in Table 4.1, the following five

outcomes were analyzed: cellular infiltrates, neovascularization, quality and rate of tissue

ingrowth, epidermal downgrowth, and fibrous encapsulation.

4.3.11 Statistical analysis

All data are presented as means ± mean standard error (SEM) or means ± standard

deviation (SD). The data obtained within each group were analyzed using a Paired t-Test

($p \le 0.05$, two-tailed, 95% CI) (SPSS vs.11.5, Armonk, NY, USA), meaning implants within each animal were paired. To test for significance across time between the measured outcomes, a multiple comparison procedure was performed using the Benjamini-Hochberg test ($p \le 0.05$, two-tailed, 95% CI) (Stata/IC 10.1, College Station, TX, USA). We report Benjamini-Hochberg adjusted *p* values, which maintains the false discovery rate (FDR) at the nominal alpha 0.05 level [33]. Controlling for multiplicity in the standard fashion, such as with the Bonferroni procedure which controls the family-wise error rate (FWER), is not justified, while control for the FDR provides the correct control for multiplicity [33-35].

4.4 Results

4.4.1 Characterization of BMMSCs

The BMMSCs were successfully differentiated into the adipogenic and osteogenic lineages, as seen by the formation and staining of lipid droplets and calcified extracellular matrix deposits (Figure 4.3). Differentiation was not observed in the control BMMSCs that did not receive the differentiation medium. Further, differentiation was not observed in the dermal fibroblasts and epidermal cells that were cultured in the differentiation media (data not shown). The cell surface markers were detected in consistent proportions on the BMMSC populations, showing greater than 90% positive for CD90 and CD29, and less than or around 10% positive for CD45, CD34, CD11b, and CD79α (Table 4.2).

4.4.2 Clinical observations

There were no surgical infections or complications. All animals healed

uneventfully and successfully made it to the experimental end point. There were no

symptoms of clinical infection and no implants were lost in the study.

4.4.3 Histological observations and histopathology interpretations

4.4.3.1 Day 0 animals (n=3/3)

The implants within the "day 0" animals were *in situ* approximately 30 minutes

before being harvested and fixed. Tissue surrounding the implant was healthy and was

observed to not be integrating with the porous surface. The only cells observed in the

porous coating were macrophages and red blood cells, both on the ventral and caudal side

of the implant (Figure 4.4). Interestingly, all of the treated implants demonstrated a

macrophage infiltration in the porous coating, while only one of the three untreated

implants displayed this infiltration. Further, there was an absence of polymorphonuclear

leukocytes within the porous surface of all implants.

4.4.3.2 Day 3 animals (n=6/6)

At time of sacrifice, most "day 3" implants, including treated and untreated, still

had a fibrin clot formation at the skin/implant interface (Figure 4.5). The treated implants

had a significantly increased infiltration of collagen matrix ($p = 0.05$) and a significantly

decreased presence of fibrin/serum ($p < 0.05$) in porous coating compared to the

untreated implants (Figure 4.6). The treated implants had higher macrophage and

lymphocyte counts, while the untreated implants had higher PMN counts (Figures 4.7 and

4.8). There was very little vasculature seen within the pores of both implants (Figure 4.7). The epidermis of both treated and untreated implants appeared to be attaching to the porous surface. As the fibrous capsule was poorly defined at this early time point, no measurements are reported.

4.4.3.3 Day 7 animals (n=6/6)

By one week, the fibrin clot had resolved at the skin/implant interface for both treated and untreated implants. For the treated implants, the epidermis was integrating and the dermal tissue was beginning to fill pores, with majority of tissue being an immature collagenous infiltration with little fibrin/serum. Granulomatous inflammation was present, with an increased fibroblast infiltration and collagen deposition compared to the untreated implants (Figure 4.7). The overall tissue response reflected a chronic inflammation phase of wound healing. Vasculature in the treated implants was still minimal. Scattered red blood cells and remnants of hemorrhage were present, indicative of implant motion within the tissue space.

As for the untreated implants, there was no epidermal downgrowth and the epidermis was integrating into porous coating in most implants. Dermal tissue was beginning to integrate in some implants, though not all, and was commonly a fibrin/serum stromal tissue, with occasional immature collagen infiltration (Figure 4.7). The untreated implants presented with fewer inflammatory cells compared to the treated implants, though no statistical significance was found ($p = 0.09$) (Figure 4.8). Vasculature was minimally present, and mostly seen outside the pores. A few implants had remnants of a hemorrhage, suggesting motion in the tissue space.

Fibrous capsule measurements are not reported for treated and untreated implants as there was an absence of a structured and continuous encapsulation.

4.4.3.4 Day 28 animals (n=5/5)

At four weeks, the skin attachment had stabilized at the skin/implant interface for treated and untreated implants (Figure 4.5). For the treated implants, the epidermis had thoroughly migrated into the porous coating, with vascularized tissue observed in the higher pores above where epidermis was integrating (Figure 4.9). A fibrovascular tissue was integrating into pores with significantly more collagen compared to the untreated ($p < 0.05$) (Figure 4.6). Cellular infiltrates had decreased since 7 days, with granulation tissue present in and around pores (Figure 4.8). Hemosiderin was seen in the tissue of some implants which is indicative of bruising that probably resulted from implant movement.

For the untreated implants, most of the tissue integrating was a granulomatous inflammatory tissue with little fibrovascular tissue, evident of later chronic inflammatory response to early granulation tissue formation. Epithelium was integrating with all implants, though slight downgrowth was observed in two implants; however, similar to the treated implants, there was vascularized tissue in pores above the epidermal integration (Figure 4.9). Cellular infiltrates increased from the 7-day time point, demonstrating higher inflammatory cell counts, with fewer fibroblast infiltrates in contrast to the treated implants (Figure 4.8).

Fibrous capsule thickness was similar between the treated and untreated implants (50.7 ± SD 10.5 µm and 58.7 ± SD 11.5 µm, respectively), with vascularization observed in capsule.

4.4.3.5 Day 56 animals (n=5/5)

At 8 weeks, the skin was very settled around the implant for both treated and untreated. For the treated implants, epidermal and dermal integration was consistent in all implants, including vascularized tissue in pores of post above where epidermis was integrating, similar to that seen at 28 days though with more mature tissue. A minimal inflammatory response was observed, with granulation tissue present and evidence of tissue reorganization. A mature collagen filled the pores, with a slight decrease in cellular infiltrates compared to 28-day implants, and a slight increase in vascularization (Figures 4.6 and 4.8). The metal surface was lined with flat macrophages, indicating a foreign body reaction.

For the untreated implants, there was good epithelial integration with the pores. A mild inflammatory response was observed along with a fibrovascular tissue. Foreign body response was beginning as evidenced by the metal surface lined with macrophages and foreign body giant cells (Figure 4.10). The untreated implants did have higher counts of foreign body giant cells compared to the treated implants, though no statistical significance was found ($p = 0.56$) (Figure 4.8). There was a higher influx of cellular infiltrates compared to the treated implants and the 28-day untreated implants, though not statistically significant ($p = 0.08$) (Figure 4.8).

The fibrous capsule thickness was slightly higher for the untreated implants compared to the treated implants, being 69.6 µm (±SD 21.0 µm), and 61.6 µm (±SD 21.0 µm), respectively. No statistical significance was determined ($p = 0.53$).

4.5 Discussion

Preventing epidermal downgrowth and improving the epidermal and dermal integration with porous metal percutaneous implants is of paramount importance for long-term functionality and sustainability. This long-term seal is critical for eliminating the risk of infection development at the skin-implant interface.

We have shown that implants treated with MSCs have an accelerated production of a collagen matrix into the porous coating compared to untreated implants. Further, this was mirrored by the fact that fibrin/serum was significantly decreased over time in the treated implants compared to the untreated. We have also shown that MSCs stimulated an accelerated and short-lived acute inflammatory wound healing response that transitioned into a chronic wound healing response, as evidenced by the early influx and resolution of inflammatory cellular infiltrates, much earlier than that observed with the untreated implants. Our data suggest that the foreign body response was also slightly decreased by evidence of fewer FBGCs and a thinner fibrous encapsulation; however, the differences between treated and untreated were not large enough to produce statistical significance. Unlike many previous studies, we did not see a significant difference in neovascularization between the treated and untreated implants. We also were not able to show significant differences or any trends regarding the epidermal downgrowth

phenomenon between the treated and untreated implants as there was minimal downgrowth overall in both groups.

It is known that in normal wound healing conditions, BMMSCs play a fundamental role in collage type I and III production [36]. Previous studies confirm our results in that cutaneous wounds treated with MSCs resulted in an increased rate of collagen synthesis and greater formation of granulation tissue compared to untreated wounds [15, 18, 19]. These studies have further demonstrated that with an increase in collagen synthesis this results in an increase in wound strength [15]. Though we didn't measure the tissue pull-out force, it is possible that when MSCs are seeded on porous coated percutaneous implants, a stronger integration potentially could result between the biomaterial surface and the tissue. Future studies investigating the pull-out force and other parameters measuring the strength of attachment are warranted to positively confirm this MSC-effect.

With regards to the increase in cellular infiltrates, it has been shown that BMMSC conditioned medium recruits CD4/80+ and CD68 macrophages to the wound site at 7 and 14 days after application [20]. Similarly, others have shown BMMSCs to increase the cumulative cellular infiltrates in treated wounds at 7 days and 14 days post-transplantation [16, 17]. These previous studies confirm our results, and together they reflect that BMMSCs play a fundamental role in recruiting macrophages and other inflammatory cellular infiltrates to the wound site to begin tissue repair. The macrophage infiltration in the "day 0" implants was an interesting finding. In light of the above results, possible explanations regarding the early and more prominent recruitment of macrophages is through a response to the presence of the transplanted cells, or a

migratory response to the chemokine release from the BMMSCs. Chen et al. demonstrated both *in vitro* and *in vivo* that BMMSCs secrete high levels of MIP-1 and monocyte chemoattractant protein (MCP-5), both of which are important in the recruitment of macrophages [20]. Additionally, they also showed increased secretion of RANTES from BMMSCs compared to the secretion profile from dermal fibroblasts [20].

In addition to the early recruitment of inflammatory cells, it has also been demonstrated that MSCs attenuate the foreign body response [24, 37]. Our results weakly corroborate these previous data in that the fibrous capsule thickness was decreased with treated implants and FBGCs were not as prevalent. Differences in results could be attributed to the materials being investigated in that the previous work evaluated polyurethane materials, whereby we were investigating titanium, and studies have shown the FBR to vary depending on the material properties [38]. In addition, the FBR varies with respect to surface texturing [39], and since we were investigating a porous surface compared to the smooth surface in the Prichard et al. study, this is yet another factor that may have influenced different results. Possible mechanisms involved in the MSC-attenuated FBR may be due to the early resolution of inflammation, specifically macrophages, since macrophages are crucial in development of fibrosis and formation of FBGCs. Given that there are few studies showing interplay between MSCs and FBR progression, further work is needed to provide more convincing results elucidating possible cellular and signaling mechanisms.

One main impetus of this study was to prevent epidermal downgrowth with MSC treatments, by influence of increased vascularization and/or increased wound healing cues. With regards to vascularization, our results did not coincide with previous evidence

that MSCs increase neovascularization in wounds [16, 17] and around implanted

biomaterials [24]. Similar to our results, McFarlin and colleagues demonstrated an

absence of significant differences in neovascularization between MSC treated and

untreated wounds [15]. It is not entirely clear why the MSC treatment did not

significantly increase neovascularization. One possible suggestion is that with the early

resolution of the acute inflammatory stage of wound healing and the accelerated

infiltration of granulation tissue, it is possible there was an early resolution of

angiogenesis and thus early disintegration of blood vessels [40]. Though we did not see

an overall decrease in numbers of blood vessel formation, we did see the production rate

of neovascularization decrease over the eight week period.

Another explanation to the limited epidermal downgrowth, between both treated

and untreated implants, could be related to the implant geometry, specifically the gradual

sloping surface. This sloping surface may have provided a slight tension to the skin,

specifically to the underlying dermal tissue, which potentially could have stimulated

keratinocyte, fibroblast, and myofibroblast proliferation and migration [41, 42]. We

eliminated right angles in our implant design as to our knowledge, there are no biological

right angles that native tissue must integrate with, and it has been shown that when a

device with a right angle is implanted, a dead space is typically formed and filled with

inflammatory cells, as can be seen in both subcutaneous [13, 43] and percutaneous

applications [3, 4, 44-46]. The effect of the implant geometry should be looked into

further, especially since our previous results, which used a percutaneous implant with

right perpendicular angles, demonstrated epidermal downgrowth in nearly all of the

porous metal percutaneous implants [1].

To address the theory that motion or movement of the percutaneous implant can inhibit epidermal attachment, thus contributing to the downward migration [3, 4, 13], we observed histological signs of movement in the subcutaneous space (e.g. remnants of hemorrhage and hemosiderin). However, these histological observations were not accompanied by epidermal downgrowth. Further work evaluating implant geometry, as stated above, and wound healing signaling cues important in epidermal migration might provide more insight as to possible reasons why the epidermis may or may not form a stable attachment with the implant.

Though we have demonstrated some encouraging results in this study, there are some limitations to be kept in mind. First, an inability to accurately know the number of viable MSCs delivered to the tissue. During the cell seeding process, the cells were seeded with equal distribution throughout the entire porous coating on the dorsal portion of the implant. When the implant-cell construct was placed in the animal, all the cells that were in the uppermost portion of the post most likely died. Thus, the total cell number that was delivered was most likely less than what was estimated. Second, and related to the first, is that any shearing force between the tissue and implant during *in situ* implantation may have pulled off some of the cells on the implant surface. This could possibly be accommodated for by modifying the titanium surface with adhesion proteins such as collagen, fibronectin, or laminin that may ultimately increase the strength of attachment between the MSCs and the implant surface. Third, though we placed the implants as far apart as possible (5 cm), we cannot confirm that the cells did not migrate to the untreated implant; however, this implant arrangement allowed us to eliminate animal variability in directly comparing treated and untreated implants. Lastly, the

sample size of our study may have limited our ability in further achieving statistical significance with some of the results. In future studies, this can be addressed by increasing sample size with respect to a power analysis of the data presented in this study.

We have demonstrated that porous titanium percutaneous implants treated with MSCs accelerate tissue integration into the implant and accelerate the wound healing response and tissue reorganization in the pores. While MSCs are known to increase the rate of healing in cutaneous wounds, we have now presented results that suggest that MSCs can increase rates of healing and tissue integration to porous metal percutaneous implants. With the current use of long-term percutaneous implants in the clinic and the various problems associated with skin integration, this study presents encouraging data that could further be explored to improve the functionality and longevity of these clinically used percutaneous devices.

4.6 Acknowledgements

4.7 References

1.   Isackson D, McGill LD, Bachus KN. Percutaneous implants with porous titanium dermal barriers: an in vivo evaluation of infection risk. Med Eng Phys 2011;33(4):418-426.

2.   Winter GD. Transcutaneous implants: reactions of the skin-implant interface. J Biomed Mater Res 1974;8(3):99-113.

3.   von Recum AF. Applications and failure modes of percutaneous devices: a review. J Biomed Mater Res 1984;18(4):323-336.

4.   Pendegrass CJ, Goodship AE, Blunn GW. Development of a soft tissue seal around bone-anchored transcutaneous amputation prostheses. Biomaterials 2006;27(23):4183-4191.

5.   Grosse-Siestrup C, Affeld K. Design criteria for percutaneous devices. J Biomed Mater Res 1984;18(4):357-382.

6.   Hall CW, Cox PA, McFarland SR, Ghidoni JJ. Some factors that influence prolonged interfacial continuity. J Biomed Mater Res 1984;18(4):383-393.

7.   Jansen JA, Walboomers XF. A new titanium fiber mesh-cuffed peritoneal dialysis catheter: an experimental animal study. J Mater Sci Mater Med 2001;12(10-12):1033-1037.

8.   Knabe C, Grosse-Siestrup C, Gross U. Histologic evaluation of a natural permanent percutaneous structure and clinical percutaneous devices. Biomaterials 1999;20(6):503-510.

9.   Gillitzer R, Goebeler M. Chemokines in cutaneous wound healing. J Leukoc Biol 2001;69(4):513-521.

10.   Lieberman MA, Glaser L. Density-dependent regulation of cell growth: an example of a cell-cell recognition phenomenon. J Membr Biol 1981;63(1-2):1-11.

11.   Harrison RG. On the Stereotropism of Embryonic Cells. Science 1911;34(870):279-281.

12.   Freinkel R, Woodley, DT. The Biology of the Skin. New York: The Parthenon Publishing Group Inc., 2001.

13.   Kim H, Murakami H, Chehroudi B, Textor M, Brunette DM. Effects of surface topography on the connective tissue attachment to subcutaneous implants. Int J Oral Maxillofac Implants 2006;21(3):354-365.

14.   Pachon-Pena G, Yu G, Tucker A, Wu X, Vendrell J, Bunnell BA, et al. Stromal stem cells from adipose tissue and bone marrow of age-matched female donors display distinct immunophenotypic profiles. J Cell Physiol 2011;226(3):843-851.

15.   McFarlin K, Gao X, Liu YB, Dulchavsky DS, Kwon D, Arbab AS, et al. Bone marrow-derived mesenchymal stromal cells accelerate wound healing in the rat. Wound Repair Regen 2006;14(4):471-478.

16.   Wu Y, Chen L, Scott PG, Tredget EE. Mesenchymal stem cells enhance wound healing through differentiation and angiogenesis. Stem Cells 2007;25(10):2648-2659.

17.   Badiavas EV, Falanga V. Treatment of chronic wounds with bone marrow-derived cells. Arch Dermatol 2003;139(4):510-516.

18.   Fu X, Fang L, Li X, Cheng B, Sheng Z. Enhanced wound-healing quality with bone marrow mesenchymal stem cells autografting after skin injury. Wound Repair Regen 2006;14(3):325-335.

19.   Jeon YK, Jang YH, Yoo DR, Kim SN, Lee SK, Nam MJ. Mesenchymal stem cells' interaction with skin: wound-healing effect on fibroblast cells and skin tissue. Wound Repair Regen 2010;18(6):655-661.

20.   Chen L, Tredget EE, Wu PY, Wu Y. Paracrine factors of mesenchymal stem cells recruit macrophages and endothelial lineage cells and enhance wound healing. PLoS One 2008;3(4):e1886.

21.   Kim WS, Park BS, Sung JH, Yang JM, Park SB, Kwak SJ, et al. Wound healing effect of adipose-derived stem cells: A critical role of secretory factors on human dermal fibroblasts. J Dermatol Sci 2007;48(1):15-24.

22.   Liu Y, Dulchavsky DS, Gao X, Kwon D, Chopp M, Dulchavsky S, et al. Wound repair by bone marrow stromal cells through growth factor production. J Surg Res 2006;136(2):336-341.

23.   Phinney DG, Prockop DJ. Concise review: Mesenchymal stem/multipotent stromal cells: The state of transdifferentiation and modes of tissue repair - Current views. Stem Cells 2007;25(11):2896-2902.

24.   Prichard HL, Reichert W, Klitzman B. IFATS collection: Adipose-derived stromal cells improve the foreign body response. Stem Cells 2008;26(10):2691-2695.

25.   Pieri F, Lucarelli E, Corinaldesi G, Aldini NN, Fini M, Parrilli A, et al. Dose-dependent effect of adipose-derived adult stem cells on vertical bone regeneration in rabbit calvarium. Biomaterials 2010;31(13):3527-3535.

26.   Altman AM, Matthias N, Yan Y, Song YH, Bai X, Chiu ES, et al. Dermal matrix as a carrier for in vivo delivery of human adipose-derived stem cells. Biomaterials 2008;29(10):1431-1442.

27.   Institute of Laboratory Animal Research CoLS, National Research Council. Guide for the Care and Use of Laboratory Animals. Washington, D.C.: National Academy Press, 1996.

28.   Dorsett-Martin WA. Rat models of skin wound healing: a review. Wound Repair Regen 2004;12(6):591-599.

29.   Harting M, Jimenez F, Pati S, Baumgartner J, Cox C, Jr. Immunophenotype characterization of rat mesenchymal stromal cells. Cytotherapy 2008;10(3):243-253.

30.   Dominici M, Le Blanc K, Mueller I, Slaper-Cortenbach I, Marini F, Krause D, et al. Minimal criteria for defining multipotent mesenchymal stromal cells. The International Society for Cellular Therapy position statement. Cytotherapy 2006;8(4):315-317.

31.   Darouiche RO, Wall MJ, Jr., Itani KM, Otterson MF, Webb AL, Carrick MM, et al. Chlorhexidine-Alcohol versus Povidone-Iodine for Surgical-Site Antisepsis. N Engl J Med 2010;362(1):18-26.

32.   Emmanual J, Hornbeck C, Bloebaum RD. A polymethyl methacrylate method for large specimens of mineralized bone with implants. Stain Technology 1987;62(6):401-410.

33.   Benjamini Y, Hochberg, Y. Controlling the false discovery rate: a practical and powerful approach to multiple testing. J R Statist Soc, Series B (Methodological) 1995;57(1):289-300.

34.   Rosner B. Fundamentals of Biostatistics. 6 ed. Belmont, CA: Brooks/Cole Cengage Learning, 2006.

35.   Moye L. Handbook of Statistics 27: Epidemiology and Medical Statistics. New York: Elsevier, 2008.

36.   Fathke C, Wilson L, Hutter J, Kapoor V, Smith A, Hocking A, et al. Contribution of bone marrow-derived cells to skin: collagen deposition and wound repair. Stem Cells 2004;22(5):812-822.

37.   Prichard HL, Reichert WM, Klitzman B. Adult adipose-derived stem cell attachment to biomaterials. Biomaterials 2007;28(6):936-946.

38.   Gretzer C, Emanuelsson L, Liljensten E, Thomsen P. The inflammatory cell influx and cytokines changes during transition from acute inflammation to fibrous repair around implanted materials. J Biomater Sci Polym Ed 2006;17(6):669-687.

39.   Rosengren A, Wallman L, Danielsen N, Laurell T, Bjursten LM. Tissue reactions evoked by porous and plane surfaces made out of silicon and titanium. IEEE Transactions on Bio-medical Engineering 2002;49(4):392-399.

40.   Ilan N, Mahooti S, Madri JA. Distinct signal transduction pathways are utilized during the tube formation and survival phases of in vitro angiogenesis. J Cell Sci 1998;111 (Pt 24):3621-3631.

41.   Agha R, Ogawa R, Pietramaggiori G, Orgill DP. A review of the role of mechanical forces in cutaneous wound healing. J Surg Res 2011;171(2):700-708.

42.   Silver FH, Siperko LM, Seehra GP. Mechanobiology of force transduction in dermal tissue. Skin Res Technol 2003;9(1):3-23.

43.   Sanders JE, Rochefort JR. Fibrous encapsulation of single polymer microfibers depends on their vertical dimension in subcutaneous tissue. J Biomed Mater Res A 2003;67(4):1181-1187.

44.   Smith TJ, Galm A, Chatterjee S, Wells R, Pedersen S, Parizi AM, et al. Modulation of the soft tissue reactions to percutaneous orthopaedic implants. J Orthop Res 2006;24(7):1377-1383.

45.   Heaney TG, Doherty PJ, Williams DF. Marsupialization of percutaneous implants in presence of deep connective tissue. J Biomed Mater Res 1996;32(4):593-601.

46.   Gerritsen M, Lutterman JA, Jansen JA. The influence of impaired wound healing on the tissue reaction to percutaneous devices using titanium fiber mesh anchorage. J Biomed Mater Res 2000;52(1):135-141.

Table 4.1. Histology outcomes and procedures for analysis and interpretations. Refer to Figure 4.2 for implant locations. Each box was 1mm^2 and covered porous coating. Polymorphonuclear leukocytes (PMNs); foreign body giant cells (FBGCs).

Outcomes	Locations	Analysis
Cellular Infiltrates (PMNs, Lymphocytes, Plasma Cells, Macrophages, FBGCs)	Boxes 1-13	Each cell type was counted at 200x magnification
Neovascularization	Boxes 1-13	Number of blood vessels ($\geq 7\mu m$) were counted at 200x magnification
Tissue Ingrowth	Boxes 1-13	Determined % fill of collagen and % fill of fibrin/serum using 100x magnification
Epidermal Downgrowth	~Boxes 1 and 13; 3 measurements taken per side	Measured distance (μm) between leading edge of epidermis and starting location of downgrowth at 200x magnification
Fibrous Capsule	Boxes 2-12; 3 measurements taken per box	Measured distance (μm) of fibrous capsule thickness at 200x magnification

Table 4.2. Cell surface marker expression determined by flow cytometry on P.8 BMMSCs. Data is represented as percent of the gated population.

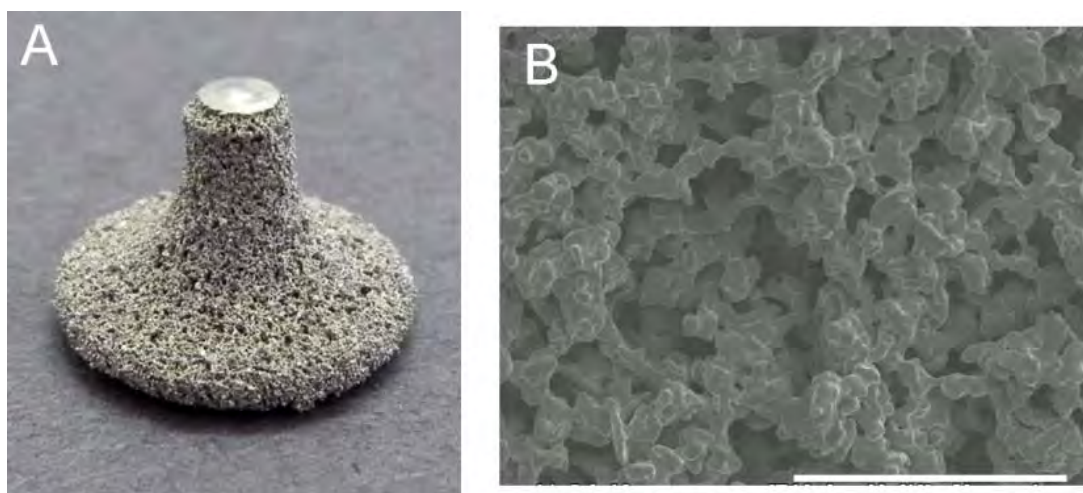| Cell Surface Marker	Percent Positive	Percent Negative
CD29	100	0
CD90	100	0
CD34	3.3	96.7
CD45	0.2	99.8
CD11b	1.1	98.9
CD79a	13.8	86.9

Figure 4.1. Porous metal percutaneous implant. (A) Porous metal percutaneous implant used in study. (B) Scanning electron microscopy image (SEM) of titanium porous coating having ~360 µm pore size and ~55% porosity (magnification: 50x; accelerating voltage: 20.0kV). Scale bar is 1mm in length.
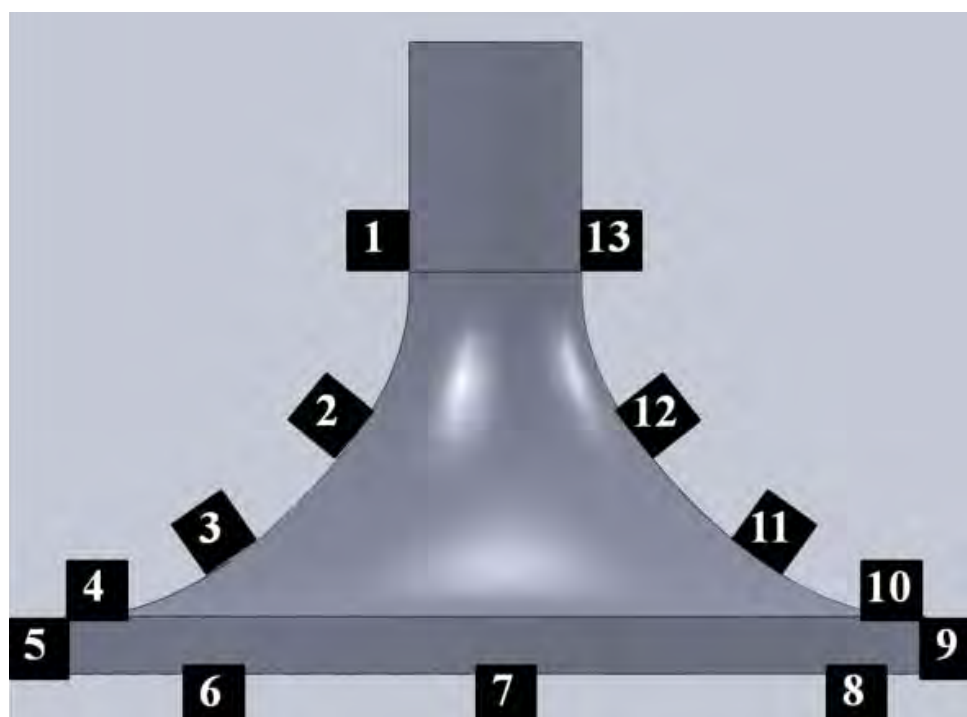
Figure 4.2. Histology analysis template. Analysis was performed in the 13, 1mm^2 boxes around the implant surface. This is a cartoon graphic of the titanium substrate, thus the boxes are positioned over the 1mm porous coating.
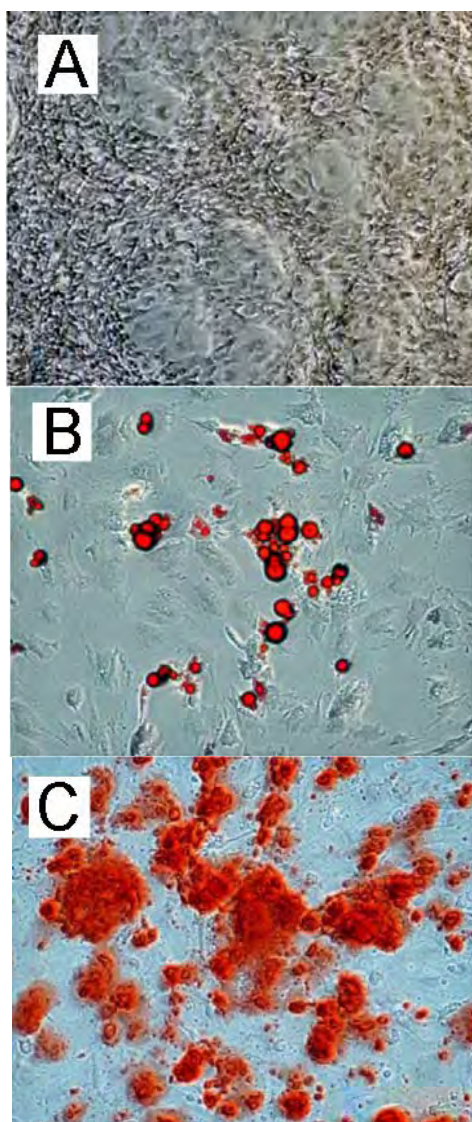
Figure 4.3. Differentiation of P.8 BMMSCs. (A) Control cells in complete growth medium (4x magnification). (B) Adipogenic differentiation and Oil Red O staining of lipid droplets (10x magnification). (C) Osteogenic differentiation and Alizarin Red S staining of calcium deposits (10x magnification).
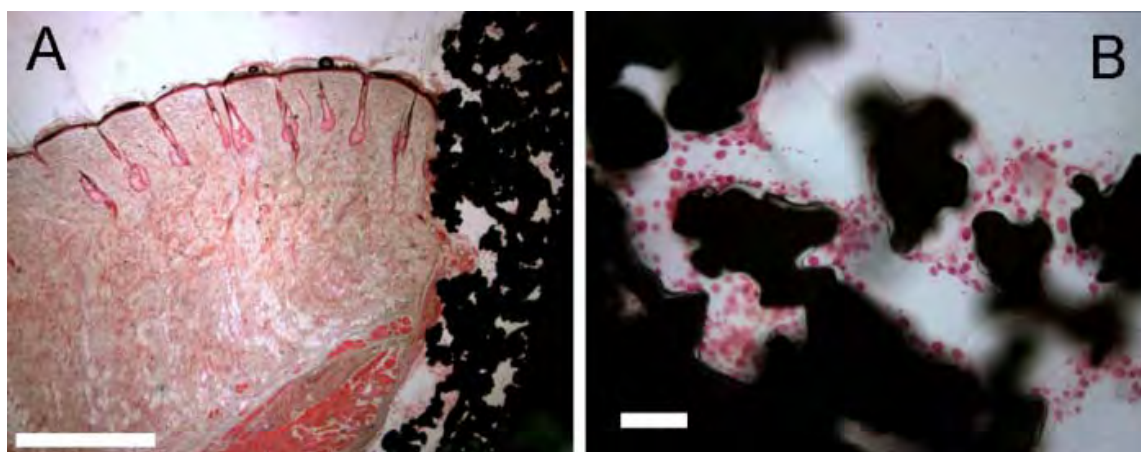
Figure 4.4. Tissue and cellular infiltrates of "day 0" implant. (A) Skin and underlying soft tissue interfacing with porous coating (black) of percutaneous component on implant (scale bar is 1mm; 4x original magnification; H&E). (B) Macrophage infiltration, along with red blood cells, into porous coating (black) (scale bar is 100 μm; 20x original magnification; H&E).
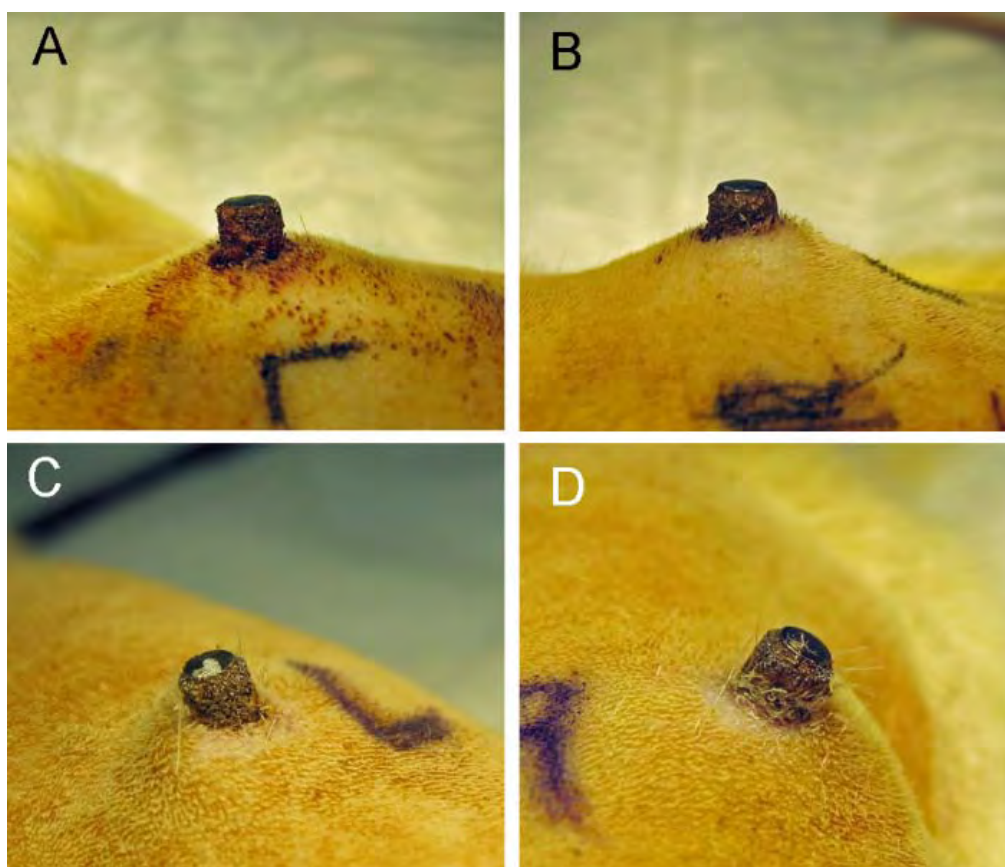
Figure 4.5. Porous titanium percutaneous implants at 3 days and 28 days post-transplantation. (A and B) Implants at 3 days with residual blood clot at skin-implant interface on both treated (A) and untreated (B) implants. (C and D) Implants at 28 days showing the skin more settled around the post and appearing healthy around treated (C) and untreated (D) implants.
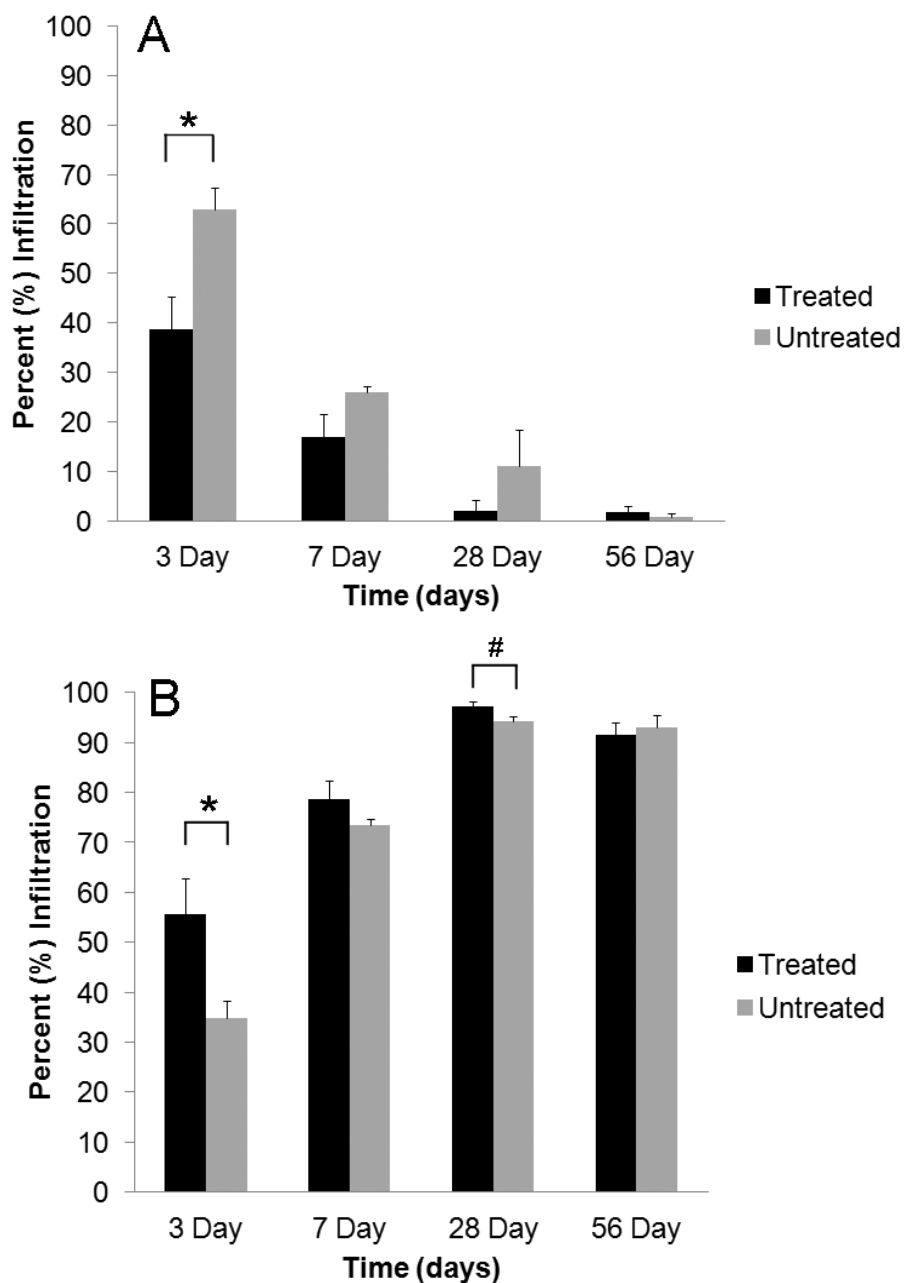
Figure 4.6. Tissue infiltration throughout 56 days. (A) Percent infiltration of fibrin/serum into the porous coating of treated and untreated implants. At 3 days, treated implants had significantly less fibrin/serum compared to untreated implants (*$p < 0.05$). (B) Percent infiltration of collagen matrix into the porous coating of treated and untreated implants. Treated implants had significantly more collagen at 3 days (*$p = 0.05$) and at 28 days (# $p < 0.05$) compared to untreated implants. Data are represented as means + SEM, n=5-6.
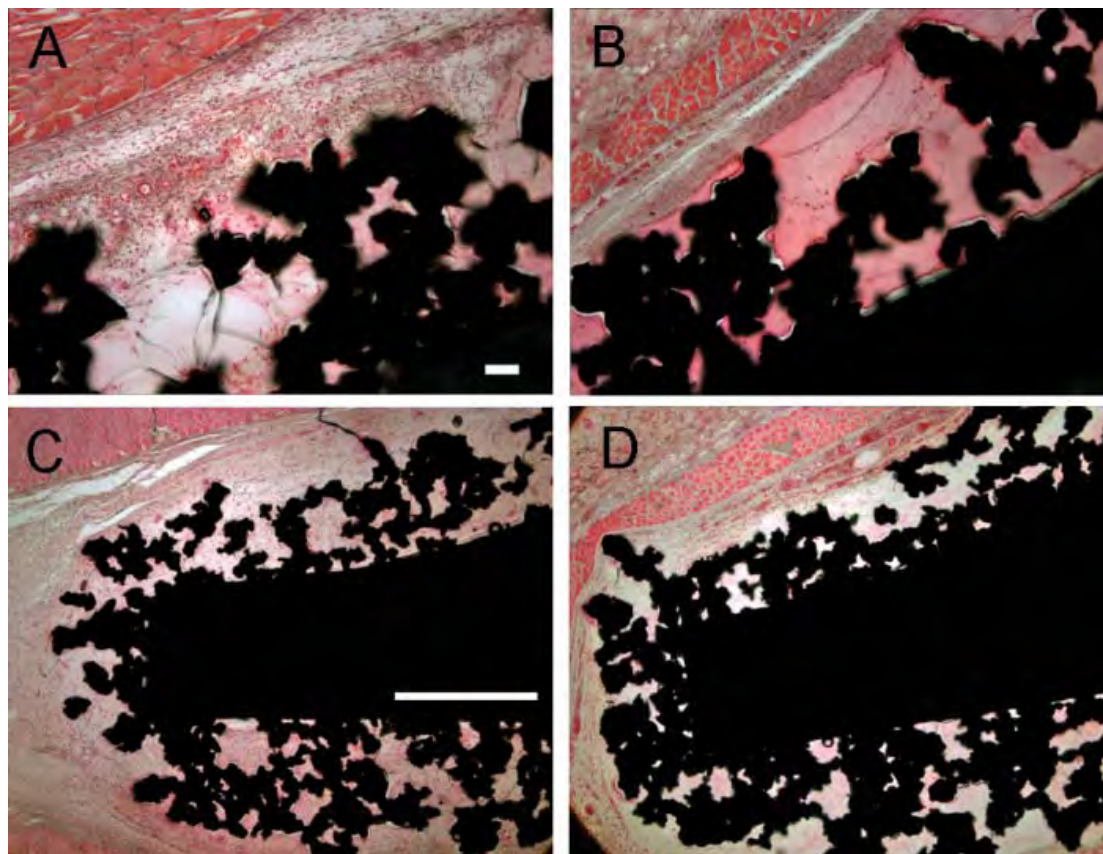
Figure 4.7. Tissue reactions to treated and untreated implants at 3 and 7 days. (A) Treated implant from a 3-day animal showing increased cellular infiltration, increased collagen matrix, and decreased fibrin/serum compared to untreated implant (scale bar is 100 µm; 10x original magnification; H&E). (B) Untreated implant from a 3-day animal showing increased fibrin/serum infiltration in porous coating, with little cellular infiltration and little collagen matrix deposition (10x original magnification; H&E). (C) Granulomatous inflammation tissue infiltrating and surrounding a treated implant from a 7-day animal. Tissue contained many macrophages, fibroblasts, collagen matrix, and vasculature (scale bar is 1mm; 4x original magnification; H&E). (D) Very few fibroblasts infiltrating porous coating of untreated implant from a 7-day animal. Early collagen matrix deposition with fewer inflammatory cell infiltrates (4x original magnification; H&E).
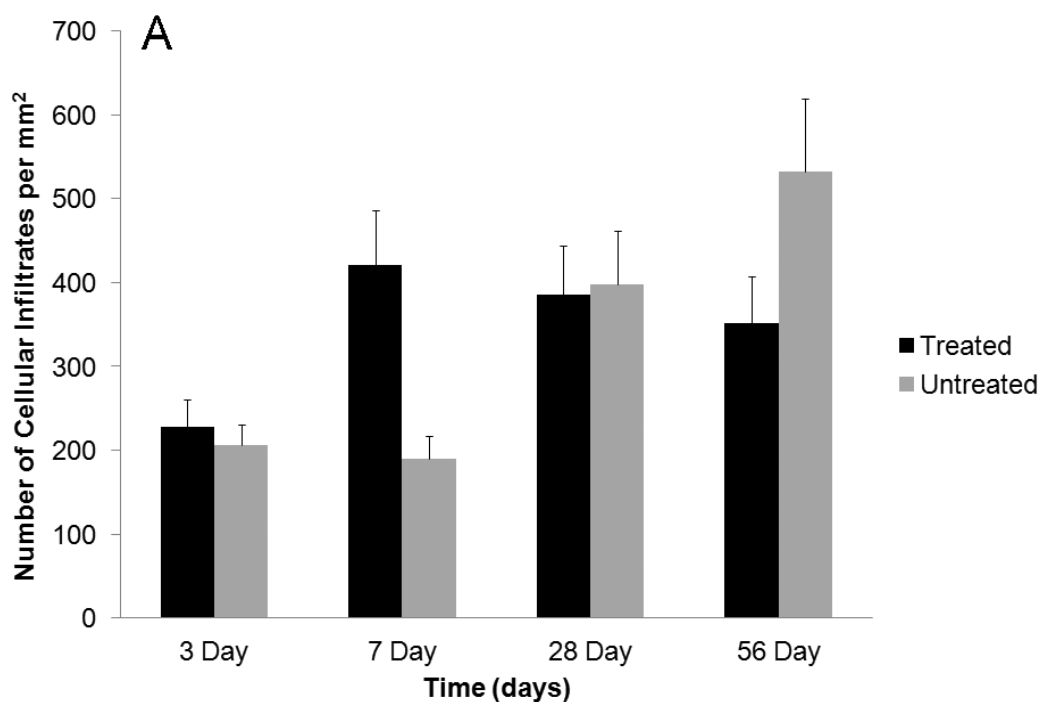
Figure 4.8. Cellular infiltrates and neovascularation over the 56-day period. (A) Cellular infiltrates over the 56-day period in treated and untreated implants. The total number of cells peaked at 7 days for the treated and thereafter slowly decreased. The cell numbers increased throughout time for the untreated implants, peaking at 56 days. (B) The individual cells comprising the cellular infiltrates over 56 days between the treated and untreated implants. Notice the trend in macrophages as they peak at 7 days for treated implants and then slowly decrease; however, for the untreated implants they substantially increase throughout 56 days. (C) Neovascularization between the treated and untreated implants throughout the 56-day period. Data are represented as means + SEM, n=5-6.
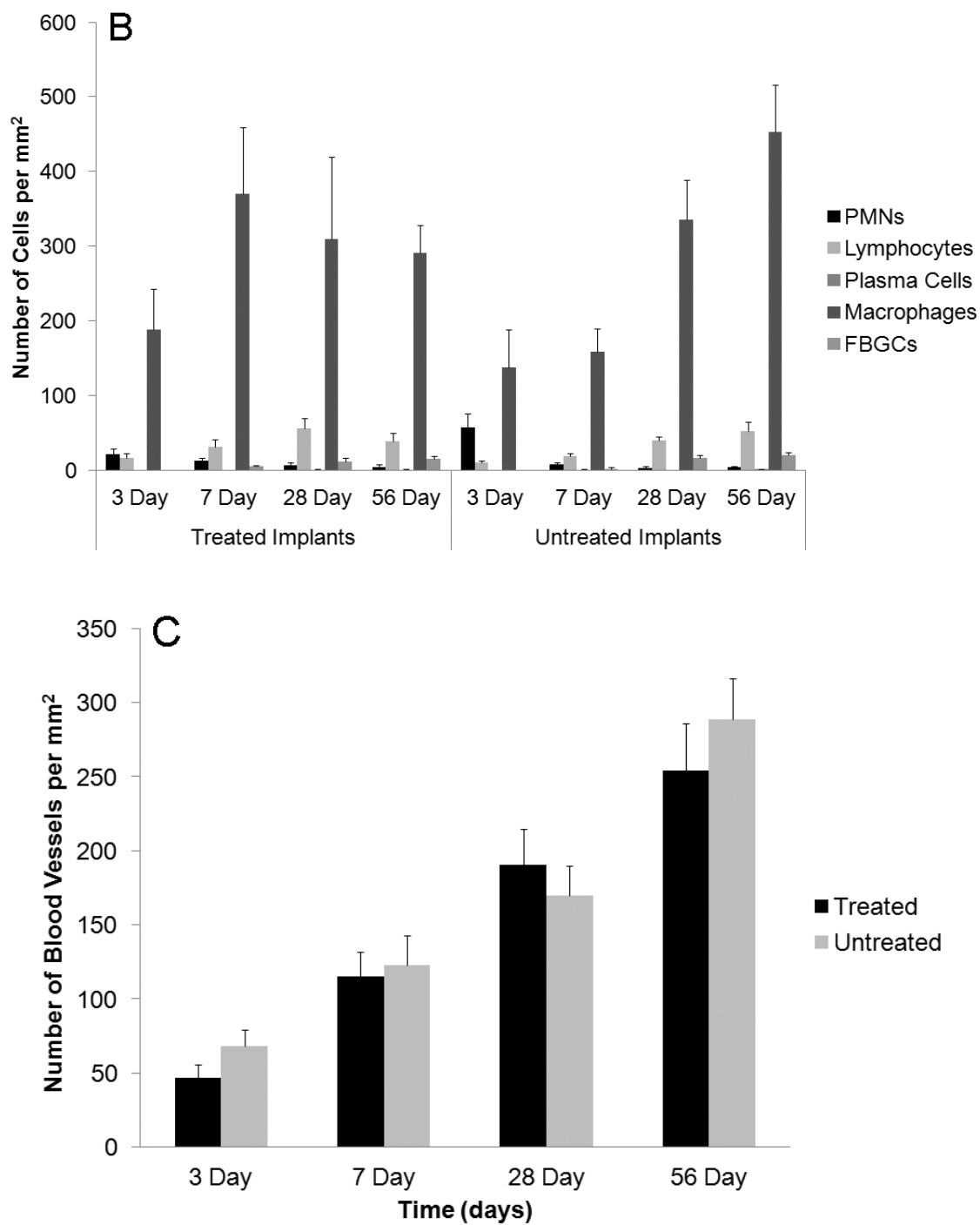
Figure 4.8 continued.
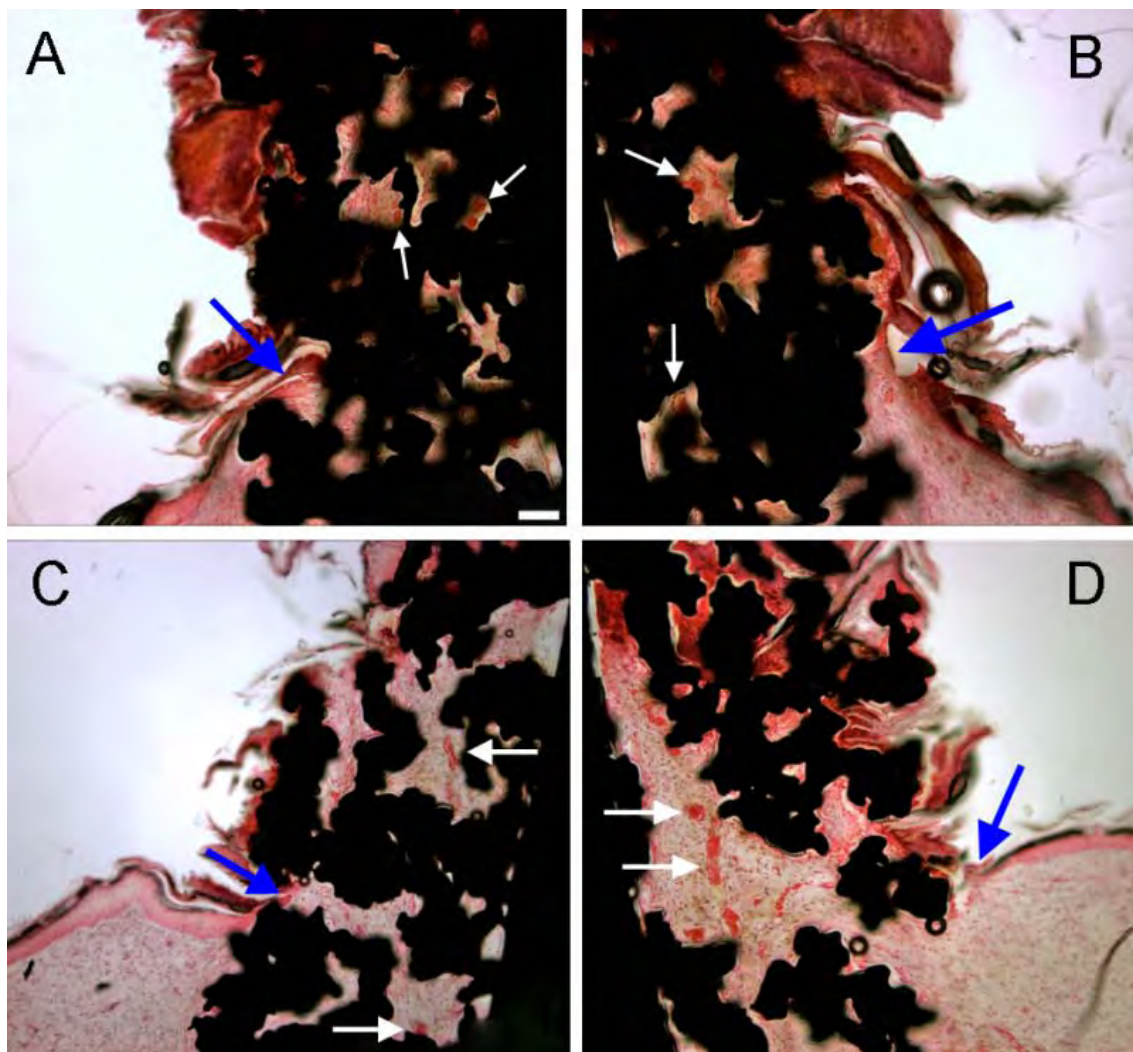
Figure 4.9. Epidermal attachment with treated and untreated implants at 28 days. (A and B) Epidermal integration (blue arrows) with porous coating (black) on percutaneous component of **treated** implant. There was vascularized (white arrows), viable tissue in pores where epidermis appeared to be integrating (scale bar is 100 μm; 10x original magnification; H&E). (C and D) Epidermal integration (blue arrow) with porous coating (black) on percutaneous component of **untreated** implant. Note viable tissue with blood vessels (white arrows) in pores above where epidermis appeared to be integrating (10x original magnification; H&E).
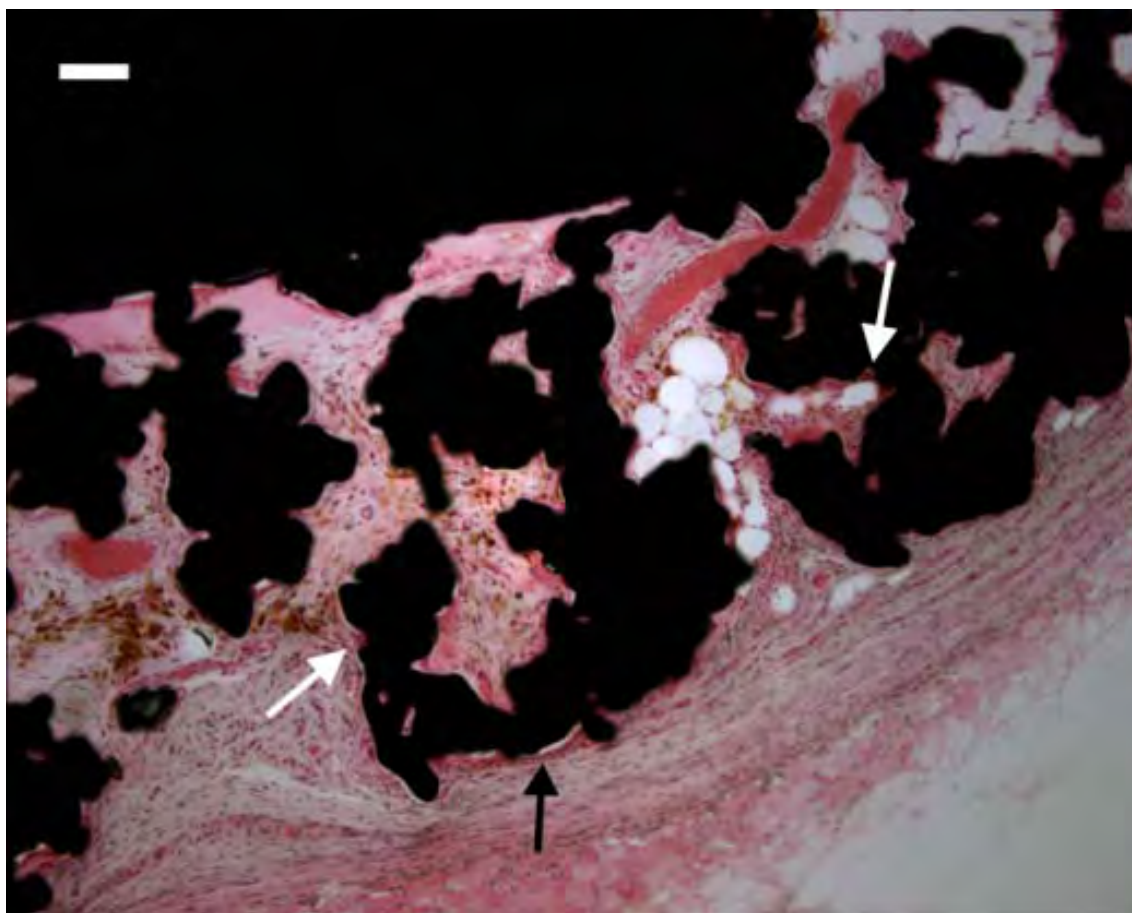
Figure 4.10. Untreated implant at 56 days demonstrating increased inflammatory cell influx in porous coating. Foreign body giant cells (white arrows) and macrophages (black arrow) lining implant surface in untreated implant (scale bar is 100 µm; 10x original magnification; H&E).

CHAPTER 5

MESENCHYMAL STEM CELL THERAPEUTICS IMPROVE TISSUE

INTEGRATION WITH POROUS METAL PERCUTANEOUS

IMPLANTS AND DECREASE INFECTION RISK

5.1 Abstract

Percutaneous devices serve an important role in the clinic; yet, their short- and long-term success is dependent on an impenetrable seal between the skin and the device such that microbial invasion is inhibited and infection prevented. This study evaluated the capacity of mesenchymal stem cells (MSCs) to stimulate an improved and rapid tissue-implant seal thus conferring protection from infection in a bacterial challenge environment. Two porous coated titanium percutaneous implants were implanted on the dorsum of a Lewis rat. One implant was treated with MSCs, the other was untreated. Beginning 2 weeks after surgery, animals received weekly bacterial inoculations of *Staphylococcus aureus* at the implant site until consistent symptoms of clinical infection presented. Presentation of clinical symptoms of infection, microbiological analyses, and histological analyses were used to confirm device infection. Our results showed the untreated implants were significantly at a higher risk of infection compared to the MSC-treated implants. The MSC-treated implants had significantly greater tissue infiltration

into the porous coating, with an overall decreased cellular presence, reflecting a later stage of wound healing. The untreated implants presented with mild inflammation, granulation tissue, and an overall increased cellular presence compared to the treated implants. In conclusion, our data suggest that when in a bacterial challenged environment, MSCs have the capacity to promote a fortified seal with porous metal percutaneous implants, thus serving as a barrier to microbial invasion.

5.2 Introduction

Many clinical conditions require a medical device to exit through the skin for the lifetime of the individual; these devices are commonly referred to as percutaneous implants. Some common percutaneous devices used in the clinic include, bone-anchored hearing aids (BAHAs), dental implants, intravascular devices, glucose sensors, and, of particular interest to our work, osseointegrated percutaneous prosthetics. Osseointegrated percutaneous prosthetics attach directly to the skeleton serving as an artificial limb for amputees but, like other percutaneous devices, are susceptible to infection due to their skin-breaching nature. In these instances, the device is a physical barrier to natural skin closure, and as such, the skin must create and maintain a permanent seal with the device. Unfortunately, if a seal is not formed between the skin and device, an avenue for microbial invasion is created and places the device at increased risk for infection.

Osseointegrated percutaneous prosthetics currently have a reported 18% infection rate, typically presenting within the first 3 years of implantation [1]. BAHAs currently have a 23.9% failure rate, consisting of device infections and other soft tissue problems that arise within the first year of implantation [2, 3]. Several factors are involved that

may determine when a percutaneous device will become infected, for example, improper surgical implantation, poor healing abilities, lack of routine cleaning of the device, misuse of the device, etc. In any case, early development of an impenetrable seal between the skin and device is critical for short- and long-term functional success of percutaneous implants.

To improve the skin seal to the implant, previous work has evaluated several modalities, some of which include surface texturing to increase cellular adhesion and surface area for tissue attachment [4-9]; collagen, laminin, and fibronectin coatings to provide a natural and recognizable surface for cellular adhesion [10-14]; alterations in implant shape and design to increase surface area for soft tissue attachment and to accommodate for skin and soft tissue stresses at the implant interface [15-19]; and different materials that more closely resemble the mechanical properties of the skin and soft tissue [20-24]. Yet, to more accurately evaluate infection susceptibility and the integrity of the skin-implant seal, few investigations actively create infectious environments for the percutaneous implant [25, 26]. This is important because small animal models, especially rodents and rabbits, heal more rapidly and through different mechanisms than humans, and often times it is very difficult to see natural infection develop with percutaneous implants [27, 28].

We previously evaluated commercially pure titanium porous coatings and smooth titanium surfaces on percutaneous implants in a bacterial challenge rabbit model to determine infection risk [29]. We showed that porous coatings on percutaneous implants had a 7-fold reduced risk of infection compared to smooth polished surfaces [29]. However, a simple porous coating was not sufficient in providing a skin-implant seal that

could completely eliminate the risk of infection. Poor skin attachment was manifested by epidermal downgrowth and marsupialization. As previous work has investigated several static treatments (e.g., porous coatings, implant materials, implant coatings, etc.) to improve a skin-implant seal, we postulate that a dynamic approach involving wound healing signaling mechanisms, encompassed in regenerative medicine approaches, could better stimulate and promote an effective skin-implant seal.

Recently, we evaluated the contributions of mesenchymal stem cells (MSCs) delivered on porous commercially pure titanium percutaneous implants to improve and stimulate a rapid integration of the skin with the implant [30]. MSCs were investigated as they have been shown to accelerate cutaneous wound closure [31-34], increase collagen content in wounds which subsequently increases the wound strength [31, 34, 35], increase cellularity for enhanced tissue repair [32-34], and to increase neovascularization, which provides oxygen and nutrients to healing tissue [32-34]. We found that, when compared to untreated implants, MSCs accelerated collagen deposition within the porous coating, and accelerated the inflammatory healing response with an earlier presentation of granulation tissue within the porous coating [30]. These data provided encouraging results reflecting the capacity of MSCs to stimulate a rapid and improved barrier between the skin and implant.

To further explore the use of MSCs in stimulating a rapid and improved skin-implant barrier, this study sought to evaluate the infection risk of MSC-treated porous metal percutaneous implants in an implant infection animal model. We hypothesized that *MSC treated implants would have a reduced infection risk compared to untreated implants*. We tested this hypothesis by challenging MSC-treated and untreated implants

with weekly bacterial inoculations two weeks after implantation to determine if the MSC-treatment prevented infection development. A *Staphylococcus aureus* strain (S. *aureus*, ATCC 49230) was used for inoculations as S. *aureus* is part of the commensal microbial population on rat and human skin [36], and being a serotype 8, this microencapsulated strain accounts for ~50% of clinical isolates [37-40].

5.3 Materials and Methods

5.3.1 Ethical statement

All animal studies were performed according to the *Guide for the Care and Use of Laboratory Animals* [41] and all protocols were approved by the University of Utah Institutional Animal Care and Use Committee (IACUC).

5.3.2 Study design

The study consisted of 11 animals that were randomly assigned to two groups: Group 1 – bacteria challenged animals (n=6), and Group 2 – control animals (n=5). Each animal in both groups received two metal implants: (1) treated with 6 x 10^6 MSCs and (2) untreated (control). The two implants were randomly assigned placement on the rat dorsum to accommodate for placement-specific biases. Randomization was performed using simple computerized randomization procedures. The Lewis rat served as our animal model and bone marrow mesenchymal stem cell (BMMSC) source. At two weeks after surgery, Group 1 animals received weekly inoculations of 1.5 x 10^8 colony forming units (CFU) of S. *aureus* (ATCC# 49230, Manassas, VA, USA). Weekly inoculations

continued until clinical symptoms of infection presented, at which point the animals were euthanized. The control animals were euthanized at 8 weeks following surgery.

5.3.3 Implant fabrication

The percutaneous implant consisted of a Ti6Al4V substrate fabricated by the School of Medicine Machine Shop (University of Utah, Salt Lake City, UT, USA). These substrates then received a commercially pure titanium porous coating (P^2 Thortex, Inc., Portland, OR, USA) that was 1mm thick on the substrate. The porous coating had a ~55% porosity that was previously determined using microCT (Xradia MicroXCT system), and had an average pore size of ~360um that was previously determined using scanning electron microscopy (SEM, Hitachi S3000-N). The percutaneous portion of the implant was cylindrical with a 5mm diameter. At 3mm from the implant top, the implant surface gradually sloped outward to a final subcutaneous base diameter of 17mm. The implant height was 12mm (Figure 5.1).

5.3.4 Endotoxin testing, passivation, and sterilization

Each porous titanium percutaneous implant was passivated according to ASTM F86 standards. Briefly, the implants were sonicated in distilled water, then in acetone (Sigma-Aldrich, St. Louis, MO, USA), followed by a distilled water wash before being soaked in 49% nitric acid (Macron Chemicals, Center Valley, PA, USA) for 2 hours. They were then sonicated in distilled water and allowed to air dry overnight.

Prior to each experiment all implants were sterilized as routinely performed using an autoclave (NAPCO 8000-DSE, Winchester, VA, USA).

All implants were tested for endotoxin before and after sterilization using the LAL QCL-1000® Assay (Lonza, Walkersville, MD, USA), according to manufacturer's directions. Endotoxin levels were found to be below detection level (< 0.05 EU/ml).

5.3.5 Bone marrow-derived mesenchymal stem cell culture and scale-up

The bone marrow-derived mesenchymal stem cells (BMMSCs) were derived from a 4-month old male Lewis rat, and were purchased from Texas A&M University System Health Science Center. The BMMSCs were cultured in complete growth medium, consisting of MEM α with L-glutamine (Gibco-Invitrogen, Carlsbad, CA, USA), 20% FBS (Premium select, Atlanta Biologicals, Lawrenceville, GA, USA), 2% L-glutamine (200 mM, Gibco-Invitrogen, Carlsbad, CA, USA), and 1% antibiotic/antimycotic (Gibco-Invitrogen, Carlsbad, CA, USA). Cells were seeded at 100 cells/cm^2 density, cultured in T-75 tissue culture flasks (Falcon, BD Biosciences, Bedford, MA, USA), and passaged at 80% confluency using 0.25% Trypsin/EDTA (Gibco-Invitrogen, Carlsbad, CA, USA).

To scale-up the number of BMMSCs needed for *in vivo* transplantations, the BMMSCs were seeded at a density of 1000 cells/cm^2 and cultured in HYPER*Flask*™ Cell Culture Vessels (Corning Inc., Lowell, MA, USA). Passage 8 BMMSCs were then cryopreserved in aliquots of 9×10^6 cells for *in vivo* transplantation. All implants, excluding control implants, were treated using one single lot of P.8 BMMSCs.

5.3.6 Characterization of BMMSCs

To verify a consistent multilineage differentiation potential, passages 6-9 of BMMSCs were differentiated into adipogenic and osteogenic lineages over a 3-week period using a commercial kit according to manufacturer's directions (StemPro®, Invitrogen, Carlsbad, CA, USA). To confirm differentiation, Oil Red O (Sigma-Aldrich, St. Louis, MO, USA) was used to stain lipid droplets of adipogenic cultures, and Alizarin Red S (Sigma-Aldrich, St. Louis, MO, USA) was used to stain calcium deposits of osteogenic cultures. Dermal fibroblasts (CRL-1414, ATCC, Manassas, VA, USA) and epidermal cells (CCL-68, ATCC, Manassas, VA, USA) were used as controls.

To confirm the immunophenotype of the BMMSCs, the cells were stained for a panel of cell surface markers, according to Harting et al [42] and Dominici et al [43]. The BMMSCs (passages 6-8) were stained with the following fluorescent-conjugated antibodies: CD90-PerCP/Cy5.5 (BioLegend, San Diego, CA, USA), CD29-FITC (LifeSpan BioSciences, Seattle, WA, USA), CD45-APC/Cy7 (BioLegend, San Diego, CA, USA), CD34-PE/Cy7 (Santa Cruz Biotechnology, Santa Cruz, CA, USA), CD79α-PE (Santa Cruz Biotechnology, Santa Cruz, CA, USA), and CD11b-AF647 (AbD Serotec, Raleigh, NC, USA). Isotype controls included the following: APC Mouse IgG1, κ (BioLegend, San Diego, CA, USA), FITC Armenian Hamster IgG (BioLegend, San Diego, CA, USA), FITC Mouse IgG2a, κ (BioLegend, San Diego, CA, USA), and PE Mouse IgG (Santa Cruz Biotechnology, Santa Cruz, CA, USA). Flow cytometry was performed on a FACSCanto-II Analyzer (Becton-Dickinson, San Jose, CA, USA) with appropriate compensation using BD CompBead Plus Particles (BD Biosciences, San Diego, CA, USA), and data were analyzed using FACSDiva software (Becton-Dickinson,

San Jose, CA, USA). Results are expressed as a percent of the total cells gated, which are calculated by subtracting the percent gated of nonlabeled cells from the percent gated of labeled cells.

 5.3.7 Seeding of BMMSCs on porous coated percutaneous implants

The day prior to surgery, an aliquot of cells was thawed and recovered in complete growth medium. Before surgery, 6×10^6 cells were suspended in 100µl of MEM α (Gibco-Invitrogen, Carlsbad, CA, USA), and was carefully added in 10µl droplets onto the porous coated implant. The treated implant was incubated at 37°C with 5-10% CO_2 for 1-2 hours, and then carefully transported to the surgery suite, where transplantation occurred within 4-6 hours after cell seeding. Our prior *in vitro* validation studies showed that maximal cell adherence and cell viability can be achieved if cells were seeded in MEM α and delivered within a 4-12 hour time frame after cell seeding [44].

5.3.8 Animal surgeries

Male Lewis rats (n=11, ~170g and ~6 weeks old) were obtained (Harlan Laboratories, Livermore, CA, USA), and their health was monitored for one week after arrival to ensure fitness of use for surgical procedures. Prior to surgery, animals were housed in groups of three, and after surgery, animals were individually housed (Thoren Caging Systems, Inc., Hazleton, PA, USA). The average room temperature was 71°C with 33% relative humidity, and a 12 hour on/12 hour off light cycle. Animals were fed a standard laboratory diet and water *ad libitum*.

All surgeries were performed under sterile conditions using aseptic technique. Animals were induced with 3-5% Isoflurane (VetOne, Meridian, ID, USA) via inhalation and maintained at 1-3% during operation. Animals were monitored throughout surgical procedures, specifically heart rate, respiratory rate, blink reflex, skin color, temperature, and % Isoflurane setting. The dorsum of the rat was close-shaved using fur clippers, then animal was positioned on a warm circulating water blanket on the surgical table. A routine surgical scrub was performed on the dorsum, consisting of alternating scrubs of Povidone-Iodine Solution (Purdue Products L.P., Stamford, CT, USA) and 70% ethyl alcohol, finished with a final scrub of chlorhexidine (CareFusion, San Diego, CA, USA) [45]. A 4-cm incision was made diagonally across the dorsum. An anterior subcutaneous pocket, created by blunt dissection, was placed 2.5cm lateral to the spine on the right side of the animal, just posterior to the scapula. Similarly, a posterior subcutaneous pocket was placed 2.5cm lateral to the spine on the left side of the animal, just anterior to the ilium. Using a 4.0mm biopsy punch (Robbins Instruments, Chatham, NJ, USA), a hole was placed through each subcutaneous pocket, being 2.5cm from the central incision. The porous titanium percutaneous implants were then carefully inserted into the subcutaneous pockets with the percutaneous components protruding through the holes in the skin. This location provided a 5-cm distance between the two implants. The implants that were untreated (control) were submersed in sterile MEM α (Gibco-Invitrogen, Carlsbad, CA, USA) prior to being inserted in the tissue. Once both implants were placed, the central incision was closed with an interrupted vertical mattress suture using 4-0 Vicryl (Ethicon®, Johnson & Johnson, Somerville, NJ, USA). Upon anesthesia recovery and physical mobility, animals were returned to their cages and administered

Buprenorphine (Hospira, Lake Forest, IL, USA), 0.05mg/kg, subcutaneous, for analgesia, and as necessary twice per day following 72 hours from surgery. Animals were given Rimadyl wafers (Rodent MD's™, Bio-Serv®, Frenchtown, NJ, USA) for continued pain-relief and water *ad libitum* for 24-72 hours following surgical procedure. Once animals were no longer showing signs of pain, they were returned to their standard laboratory diet. Animals were observed daily during the first week after surgery, and every other day thereafter until sacrifice. Signs of clinical infection of the implant, any changes to the implant, and overall animal health and well being were assessed.

5.3.9 Staphylococcus aureus inoculation

Following our previously published work, an inoculation of bacteria was applied to the implants to study implant infection in a small animal model [29]. Two weeks following surgery, Group 1 animals were inoculated weekly with 1.5×10^8 CFU of S. *aureus*. The S. *aureus* was subbed from a frozen stock onto Columbia Blood agar plates (Hardy Diagnostics, Santa Maria, CA, USA) with at least two passages prior to application [25]. From colonies on the plate, a 1.0 McFarland standard was made in 0.9% saline solution. The bacteria were centrifuged and re-suspended in 50ul of saline, which resulted in 1.5×10^8 CFU (~0.5 McFarland) per implant. The bacterial suspension was immediately applied to the skin-implant interface of each implant in Group 1. This was performed once per week until signs of clinical infection presented, including: redness, tenderness, edema, blood, exudate, aggressiveness, and lack of appetite. Once consistent symptoms of infection were observed, the animals were euthanized.

5.3.10 Microbiology procedures

Prior to bacterial inoculation, skin culture swabs (BBL™ CultureSwab™, Becton Dickinson, Sparks, MD) of each implant site recorded the baseline microbial flora on the skin. At sacrifice, skin culture swabs and soft tissue biopsies were obtained from each implant of both Group 1 and Group 2 animals. The swabs from the skin cultures were then streaked onto Columbia blood agar plates (Hardy Diagnostics, Santa Maria, CA, USA) and bacteria growth was recorded. For the soft tissue biopsy, a 2cm x 2cm area at the skin-implant interface was scrubbed, as performed routinely prior to surgery (see description above). A 3mm biopsy punch (Acuderm Inc, Ft. Lauderdale, FL, USA) of soft tissue was obtained from this scrubbed region and placed in fastidious broth (Hardy Diagnostics, Santa Maria, CA). The broth biopsy specimens were incubated at 37°C for 5-7 days, or until broth turbidity was observed. After the 5-7 day culture period, or when broth was turbid, a swab (BBL™ CultureSwab™, Becton Dickinson, Sparks, MD, USA) of the broth suspension was cultured on Columbia blood agar plates to confirm bacterial growth.

5.3.11 Implant harvest and histology processing

Animals were euthanized when consistent signs of clinical infection presented for Group 1 and at 8 weeks following surgery for Group 2. The implant specimens with generous tissue margins were carefully excised from the dorsum and fixed in 10% neutral buffered formalin (Fisher Scientific, Pittsburgh, PA, USA). Specimens were processed for histology according to previously published methods [29, 46].

The histology slides were stained with hematoxylin and eosin (H&E) or Multiple Stain Solution (MSS, Polysciences, Inc., Warrington, PA, USA). For H&E staining, slides were placed in Mayer's Hematoxylin (Electron Microscopy Sciences, Hatfield, PA, USA) at 50-55°C for 2-3 hours, then washed in running tap water for 10 minutes. Slides were placed in Eosin Y-Phloxine (Richard Allan Scientific, Kalamazoo, MI, USA) with Glacial Acetic Acid (Fisher Scientific, Pittsburgh, PA, USA) Solution (3:1) for 10-30 minutes, then rinsed in 100% ethyl alcohol (Fisher Scientific, Pittsburgh, PA, USA). The slides stained with MSS were placed in acid-alcohol (1% hydrochloric acid; 70% ethyl alcohol) for 5-10 minutes, then rinsed in distilled water. The MSS was added drop-wise on the slide to completely cover the section, incubated at 50-55°C on a slide warmer for 8-10 minutes, and then gently rinsed in running tap water.

5.3.12 Histology analysis

Slides were interpreted using a light microscope (Optiphot-2, Nikon, Japan; BX41, Olympus, Center Valley, PA, USA). Images were captured (Retiga 1300, QImaging, Surrey, BC, Canada) and measurements were made using Bioquant Nova Prime software (version 6.9.10MR, Bioquant Image Analysis, Nashville, TN, USA).

All histology slides were de-identified by one author (KJC), and then blindly interpreted and analyzed by two authors (DI and LDM). Thirteen $1mm^2$ boxes were analyzed around the implant (Figure 5.2). A Mertz Graticle was used to standardize the location of the $1mm^2$ box area for cell counting, tissue volume fill, and overall interpretation and analysis. The following five outcomes were analyzed: cellular

infiltrates, neovascularization, quality and quantity of tissue ingrowth, epidermal

downgrowth, and fibrous encapsulation (Table 5.1).

5.3.13 Statistical analysis

To qualify as infected, *a priori* criteria stated that the implant must exhibit (1)

clinical symptoms of infection, (2) positive bacterial growth from the skin-implant

interface swab, (3) positive bacterial growth from the soft tissue biopsy broth, and (4)

histological evidence of infection. If all four criteria were positive, the implant was

deemed "infected."

All data are presented as means ± mean standard error (SE) or means ± standard

deviation (SD). The data of the histological outcomes were tested using a Paired t-Test

($p \leq$ 0.05, two-tailed, 95% CI) (SPSS vs.11.5, Armonk, NY, USA), meaning implants

within each animal were paired. Infection data of the implants were analyzed using

Kaplan-Meier survival analysis, and the infection risk of treated and untreated implants

was analyzed using a Log Rank test ($p \leq 0.05$, two-tailed, 95% CI) (Stata/IC vs.10.1,

Statacorp, College Station, TX, USA).

5.4 Results

5.4.1 Characterization of BMMSCs

The BMMSCs were successfully differentiated into the adipogenic and osteogenic

lineages, as seen by the formation and staining of lipid droplets and calcified extracellular

matrix deposits (Figure 5.3). Differentiation was not observed in the control BMMSCs.

Further, differentiation was not observed in the dermal fibroblasts and epidermal cells

that were cultured in the differentiation media (data not shown). The cell surface markers were detected in consistent proportions on the BMMSC populations, showing greater than 90% positive for CD90 and CD29, and less than or around 10% positive for CD45, CD34, CD11b, and CD79α (Table 5.2).

5.4.2 Clinical observations

All surgical procedures occurred without any complications or infections. Animals in Group 1 healed uneventfully until weekly *S. aureus* inoculations commenced. Animals in Group 2 (control) healed uneventfully, and successfully reached their experimental end point of 8 weeks, with no clinical signs of infection.

5.4.3 Infection risk of MSC-treated and untreated implants

The untreated implants had a significantly higher infection risk ($p < 0.05$) compared to MSC-treated implants, when analyzed with the Log Rank test (Figure 5.4). Fifty percent (50%) of the untreated implants were determined infected, according to the *a priori* infection criteria, while infection was not confirmed in any of the MSC-treated implants (Table 5.3). Majority of the untreated implants presented with symptoms of infection (mainly redness, tenderness, animal lethargy, and animal aggressiveness) much earlier and for a longer duration than treated implants (Table 5.3). All bacterial cultures of the skin-implant interface were positive, and 50% of both treated and untreated implants presented with positive biopsy broth cultures (Table 5.3). Histological evidence of infection was confirmed in 50% (3/6) of untreated implants, and 16.7% (1/6) of treated implants.

5.4.4 Histological observations and histopathology interpretations

5.4.4.1 Group 1 bacteria challenged animals (6/6)

For the MSC-treated implants, the epidermis integrated with the porous surface, often with excellent vascularization in the pores. There was no evidence of an epidermal downgrowth alongside the porous implant (Figure 5.5). There was significantly more tissue infiltration into the pores ($p < 0.05$), consisting of fibrovascular tissue and collagen (Figures 5.6 and 5.7). Neovascularization was slightly higher in the treated implants compared to the untreated, though not significant. Overall, the treated implants demonstrated a late wound healing response, with relatively low cellularity (Figure 5.8).

For the untreated implants, the epidermis integrated into the pores with little evidence of downgrowth (Figure 5.5). In the infected implants, the infection was not septic throughout the entire implant, rather, the infection was localized in pockets scattered in and above the porous coating (Figure 5.7). In the uninfected implants, the cellular infiltrates suggested a chronic wound healing response with some granulomatous inflammation and fibrovascular tissue. The cumulative number of cellular infiltrates in the untreated implants was higher than the treated implants, though no significance was determined ($p = 0.23$) (Figure 5.8). The fibrous capsule was thin and organized around both the treated and untreated implants, with no difference between the two.

5.4.4.2 Group 2 control animals (n=5/5)

At 8 weeks, the skin was very settled around the implant for both treated and untreated implants. For the treated, epidermal and dermal integration was consistent in all implants, including fibrovascular tissue in pores of post above where epidermis was

integrating (Figure 5.9). Minimal inflammation was observed, with granulation tissue present and evidence of tissue reorganization. Mature collagen filled the pores, with a reduced number of cellular infiltrates and neovascularization compared to untreated implants (Figures 5.8 and 5.10). A slight foreign body reaction was observed by evidence of flat macrophages and a few FBGCs lining the metal surface.

For the untreated implants, there was good epithelial integration with the pores, with minimal downgrowth observed (Figure 5.9). The overall tissue reaction throughout the implant consisted of a mild inflammatory response along with fibrovascular tissue (Figure 5.10). The metal surface was lined by macrophages and scattered foreign body giant cells. There was also a higher influx of total cellular infiltrates compared to the untreated implants, though not statistically significant ($p = 0.08$) (Figure 5.8).

The fibrous capsule thickness was slightly higher for the untreated implants, being 69.6 µm (±SD 21.0 µm), and 61.6µm (±SD 21.0 µm) for treated implants. No statistical significance was determined ($p = 0.53$).

5.5 Discussion

Percutaneous device infections can be costly and inconvenient, and with the growing concern of antibiotic resistance, they can also potentially lead to tissue morbidity and in the most severe case, mortality. For percutaneous devices, and particularly osseointegrated percutaneous prosthetics, to be successful in the clinic, an infection-free environment must be created and maintained which requires a complete, stable skin attachment to the device.

We demonstrated that a mesenchymal stem cell treatment significantly decreased the risk of infection compared to untreated implants. Further, we showed that a mescenchymal stem cell treatment significantly increased the amount of tissue integration within the porous coating compared to untreated implants. These results suggest that MSCs possess the capacity to promote a more pronounced tissue integration that can serve as a barrier to infecting microorganisms.

Our unpublished work demonstrated that over time, MSCs significantly increased collagen deposition at 4 days and 4 weeks after transplantation, and overall, accelerated the wound healing response in porous titanium percutaneous implants [30]. The results presented in this study confirm those results, in addition to previously published work [31, 34, 35]. In this current study, we suggest that an increased collagen infiltration in the porous coating at an earlier time point provided a stable seal to invading microorganisms, of which the untreated implants could not prevent. We postulate that MSCs, through paracrine signaling mechanisms, stimulated resident cellular activity and subsequent deposition of the extracellular matrix into and around the porous coating [47-49]. As soluble signaling molecules are known to play an important role in wound healing through direct secretion from MSCs and other resident cells (e.g., fibroblasts, macrophages, etc.), we believe this may have contributed to the improved skin-implant seal [50, 51]. Recently, Maggini et al. demonstrated that around subcutaneously implanted glass cylinders, macrophage infiltration was significantly increased at two weeks around cylinders inoculated with MSCs compared to the cylinders that were not inoculated with MSCs [52], similar to what we found in our previous unpublished work [30]. After additional experimentation, they concluded that MSCs can direct

macrophages into a wound-healing-like profile and a regulatory-like profile [52]. What this means in context of this study, is that the MSC treatment may have induced an early and more pronounced recruitment of macrophages (as found in our previous unpublished work) which were then altered to become more of a wound healing effector resulting in an increase in granulation tissue and overall a more robust ECM barrier to develop within the treated implants.

It is difficult to assess whether the MSCs had any influence, either encouraging or suppressing, on the inflammatory response to the bacterial challenged environment. Studies have shown MSCs to have a dampening effect on excessive inflammation through interactions with T cell populations [53], secretion of prostaglandin E_2 (PGE2) [54], secretion of sTNFR1 [55], expression of IL-1 receptor antagonist [56], among other suggested mechanisms [57]. Observing that there was a decreased infiltration of inflammatory cells within the treated implants in Groups 1and 2, it is possible that this was an MSC-induced attenuation in inflammation; however, this cannot be proven with our results as we were not able to investigate the above suggested signaling mechanisms within the inflammatory cellular milieu. Regarding antimicrobial properties, Krasnodembskaya et al demonstrated *in vitro* that MSCs through release of an antimicrobial peptide LL-37 inhibited bacterial growth of *Escherichia coli* (E. *coli*) and *Pseudomonas aeruginosa*; and further, they showed *in vivo* that MSCs decreased bacterial numbers in a murine model of *E. coli* pneumonia through secretion of the same peptide [58]. Though we did not investigate antimicrobial peptides, this is a possible mechanism for the reduced infection rate observed in the MSC-treated implants. Thus, potential mechanisms underlying the observed decreased infection risk of the MSC-

treated implants may include interactions between MSCs and the resident cell populations, and/or possible interactions with the bacterial populations through secretion of antimicrobial peptides.

In light of the encouraging results in this study, we would like to discuss some limitations. First, there was an inability to control for the bacteria inoculations to reside at the skin-implant interface. A few factors influenced that, including animal licking, which was observed, and occasional loss of bacterial suspension, as it would run off the implant-interface. Future work should optimize a smaller volume (<50 ul) of bacterial suspension that can better reside at the implant interface. A second limitation was the presentation of ambiguous signs of infection at the skin-implant interface. Though the tissue would swell and become pink/red, this would eventually dissipate, despite the animal showing symptoms of tenderness, lethargy, and aggressiveness. Thus if a similar rat model is used to study percutaneous device infections, we recommend that inoculations occur prior to two weeks after surgery, or increase the bacteria concentration, or increase the number of weekly inoculations such that stronger infection symptoms can be observed. The third limitation involves the culture results of the biopsy punch in that these results were dependent on the size of the punch (3mm) and the location of the punch. Though each punch was consistent in size and location, there is the possibility that bacteria could have been in the tissue in different areas where the punch was not taken.

Herein we have demonstrated that MSCs can play a role in stimulating a more effective integration of the epidermal and dermal tissues with percutaneous implants thus providing a seal that can decrease infection risk when in a bacterial challenged

environment. Future work should optimize both the delivery of the MSCs and the bacterial inoculations in a percutaneous implant animal model. Furthermore, future studies should also attempt to elucidate interactions of MSCs with the resident cellular milieu when in an implant infection model, and further, potential interactions, if any, with a developing biofilm on the implant surface. In summary, we have demonstrated that mesenchymal stem cell therapeutics hold potential in promoting a robust, long-term skin-implant seal that can result in a functional and infection-free environment of porous metal percutaneous devices.

5.6 Acknowledgements

5.7 References

1.   Tillander J, Hagberg K, Hagberg L, Branemark R. Osseointegrated titanium implants for limb prostheses attachments: infectious complications. Clin Orthop Relat Res 2010;468(10):2781-2788.

2.   Badran K, Arya AK, Bunstone D, Mackinnon N. Long-term complications of bone-anchored hearing aids: a 14-year experience. The Journal of Laryngology and Otology 2009;123(2):170-176.

3.   Hobson JC, Roper AJ, Andrew R, Rothera MP, Hill P, Green KM. Complications of bone-anchored hearing aid implantation. The Journal of Laryngology and Otology 2010;124(2):132-136.

4.   Walboomers XF, Jansen JA. Effect of microtextured surfaces on the performance of percutaneous devices. J Biomed Mater Res A 2005;74(3):381-387.

5.   Chehroudi B, Gould TR, Brunette DM. A light and electron microscopic study of the effects of surface topography on the behavior of cells attached to titanium-coated percutaneous implants. J Biomed Mater Res 1991;25(3):387-405.

6.   Chehroudi B, Brunette DM. Subcutaneous microfabricated surfaces inhibit epithelial recession and promote long-term survival of percutaneous implants. Biomaterials 2002;23(1):229-237.

7.   Jain R, von Recum AF. Effect of titanium surface texture on the cell-biomaterial interface. J Invest Surg 2003;16(5):263-273.

8.   Clubb FJ, Jr., Clapper DL, Deferrari DA, Hu SP, Seare WJ, Jr., Capek PP, et al. Surface texturing and coating of biomaterial implants: effects on tissue integration and fibrosis. Asaio J 1999;45(4):281-287.

9.   Puckett SD, Lee PP, Ciombor DM, Aaron RK, Webster TJ. Nanotextured titanium surfaces for enhancing skin growth on transcutaneous osseointegrated devices. Acta Biomater 2010;6(6):2352-2362.

10.   Gordon DJ, Bhagawati DD, Pendegrass CJ, Middleton CA, Blunn GW. Modification of titanium alloy surfaces for percutaneous implants by covalently attaching laminin. J Biomed Mater Res A 2010;94(2):586-593.

11.   Chimutengwende-Gordon M, Pendegrass C, Blunn G. Enhancing the soft tissue seal around intraosseous transcutaneous amputation prostheses using silanized fibronectin titanium alloy. Biomedical Materials 2011;6(2).

12.   Middleton CA, Pendegrass CJ, Gordon D, Jacob J, Blunn GW. Fibronectin silanized titanium alloy: a bioinductive and durable coating to enhance fibroblast attachment in vitro. J Biomed Mater Res A 2007;83(4):1032-1038.

13.   Pendegrass CJ, Middleton CA, Gordon D, Jacob J, Blunn GW. Measuring the strength of dermal fibroblast attachment to functionalized titanium alloys in vitro. J Biomed Mater Res A 2010;92(3):1028-1037.

14.   Okada T, Ikada Y. Surface modification of silicone for percutaneous implantation. J Biomater Sci Polym Ed 1995;7(2):171-180.

15.   Pendegrass CJ, Goodship AE, Blunn GW. Development of a soft tissue seal around bone-anchored transcutaneous amputation prostheses. Biomaterials 2006;27(23):4183-4191.

16.   Paquay YC, De Ruijter AE, van der Waerden JP, Jansen JA. A one stage versus two stage surgical technique. Tissue reaction to a percutaneous device provided with titanium fiber mesh applicable for peritoneal dialysis. ASAIO J 1996;42(6):961-967.

17.   Jansen JA, van der Waerden JP, de Groot K. Development of a new percutaneous access device for implantation in soft tissues. J Biomed Mater Res 1991;25(12):1535-1545.

18.   Grosse-Siestrup C, Affeld K. Design criteria for percutaneous devices. J Biomed Mater Res 1984;18(4):357-382.

19.   Tramaglini D, Powers DL, Black J. The influence of flange compliance and mechanical loading on the tissue response to percutaneous devices. J Appl Biomater 1993;4(2):183-194.

20.   Fukano Y, Knowles NG, Usui ML, Underwood RA, Hauch KD, Marshall AJ, et al. Characterization of an in vitro model for evaluating the interface between skin and percutaneous biomaterials. Wound Repair Regen 2006;14(4):484-491.

21.   Knowles NG, Miyashita Y, Usui ML, Marshall AJ, Pirrone A, Hauch KD, et al. A model for studying epithelial attachment and morphology at the interface between skin and percutaneous devices. J Biomed Mater Res A 2005;74(3):482-488.

22.   Underwood RA, Usui ML, Zhao G, Hauch KD, Takeno MM, Ratner BD, et al. Quantifying the effect of pore size and surface treatment on epidermal incorporation into percutaneously implanted sphere-templated porous biomaterials in mice. J Biomed Mater Res A 2011;98(4):499-508.

23.   Smith CM, Roy TD, Bhalkikar A, Li B, Hickman JJ, Church KH. Engineering a titanium and polycaprolactone construct for a biocompatible interface between the body and artificial limb. Tissue Engineering 2010;16(2):717-724.

24.   Isenhath SN, Fukano Y, Usui ML, Underwood RA, Irvin CA, Marshall AJ, et al. A mouse model to evaluate the interface between skin and a percutaneous device. J Biomed Mater Res A 2007;83(4):915-922.

25.   Williams D, Bloebaum R, Petti CA. Characterization of Staphylococcus aureus strains in a rabbit model of osseointegrated pin infections. J Biomed Mater Res A 2008;85(2):366-370.

26.   Chou TG, Petti CA, Szakacs J, Bloebaum RD. Evaluating antimicrobials and implant materials for infection prevention around transcutaneous osseointegrated implants in a rabbit model. J Biomed Mater Res A 2010;92(3):942-952.

27.   Davidson JM. Animal models for wound repair. Archives of Dermatological Research 1998;290 Suppl:S1-11.

28.   Dorsett-Martin WA. Rat models of skin wound healing: a review. Wound Repair Regen 2004;12(6):591-599.

29.   Isackson D, McGill LD, Bachus KN. Percutaneous implants with porous titanium dermal barriers: an in vivo evaluation of infection risk. Med Eng Phys 2011;33(4):418-426.

30.   Isackson D, Cook KJ, McGill LD, Bachus KN. Mesenchymal Stem Cells Increase Collagen Infiltration and Improve Wound Healing Response to Porous Titanium Percutaneous Implants. Medical Engineering and Physics pending(In Submission and Under Review).

31.   McFarlin K, Gao X, Liu YB, Dulchavsky DS, Kwon D, Arbab AS, et al. Bone marrow-derived mesenchymal stromal cells accelerate wound healing in the rat. Wound Repair Regen 2006;14(4):471-478.

32.   Wu Y, Chen L, Scott PG, Tredget EE. Mesenchymal stem cells enhance wound healing through differentiation and angiogenesis. Stem Cells 2007;25(10):2648-2659.

33.   Badiavas EV, Falanga V. Treatment of chronic wounds with bone marrow-derived cells. Arch Dermatol 2003;139(4):510-516.

34.   Fu X, Fang L, Li X, Cheng B, Sheng Z. Enhanced wound-healing quality with bone marrow mesenchymal stem cells autografting after skin injury. Wound Repair Regen 2006;14(3):325-335.

35.   Jeon YK, Jang YH, Yoo DR, Kim SN, Lee SK, Nam MJ. Mesenchymal stem cells' interaction with skin: wound-healing effect on fibroblast cells and skin tissue. Wound Repair Regen 2010;18(6):655-661.

36.   Baker DG. Natural pathogens of laboratory mice, rats, and rabbits and their effects on research. Clin Microbiol Rev 1998;11(2):231-266.

37.   Darouiche RO. Device-associated infections: a macroproblem that starts with microadherence. Clin Infect Dis 2001;33(9):1567-1572.

38.   Coldren FM, Palavecino EL, Levi-Polyachenko NH, Wagner WD, Smith TL, Smith BP, et al. Encapsulated Staphylococcus aureus strains vary in adhesiveness assessed by atomic force microscopy. J Biomed Mater Res A 2009;89(2):402-410.

39.   O'Riordan K, Lee JC. Staphylococcus aureus capsular polysaccharides. Clin Microbiol Rev 2004;17(1):218-234.

40.   Hochkeppel HK, Braun DG, Vischer W, Imm A, Sutter S, Staeubli U, et al. Serotyping and electron microscopy studies of Staphylococcus aureus clinical isolates with monoclonal antibodies to capsular polysaccharide types 5 and 8. J Clin Microbiol 1987;25(3):526-530.

41.   Institute of Laboratory Animal Research CoLS, National Research Council. Guide for the Care and Use of Laboratory Animals. Washington, D.C.: National Academy Press, 1996.

42.   Harting M, Jimenez F, Pati S, Baumgartner J, Cox C, Jr. Immunophenotype characterization of rat mesenchymal stromal cells. Cytotherapy 2008;10(3):243-253.

43.   Dominici M, Le Blanc K, Mueller I, Slaper-Cortenbach I, Marini F, Krause D, et al. Minimal criteria for defining multipotent mesenchymal stromal cells. The International Society for Cellular Therapy position statement. Cytotherapy 2006;8(4):315-317.

44.   Isackson D, Cook KJ, Bachus KN. In Vitro Investigation of Mesenchymal Stem Cell Cytotoxicity and Adherence to Porous Titanium Surfaces in Various Delivery Solutions for In Vivo Transplantation Studies. Cytotechnology pending(In Submission and Under Review).

45.   Darouiche RO, Wall MJ, Jr., Itani KM, Otterson MF, Webb AL, Carrick MM, et al. Chlorhexidine-Alcohol versus Povidone-Iodine for Surgical-Site Antisepsis. N Engl J Med 2010;362(1):18-26.

46.   Emmanual J, Hornbeck C, Bloebaum RD. A polymethyl methacrylate method for large specimens of mineralized bone with implants. Stain Technology 1987;62(6):401-410.

47.   Kim WS, Park BS, Sung JH, Yang JM, Park SB, Kwak SJ, et al. Wound healing effect of adipose-derived stem cells: A critical role of secretory factors on human dermal fibroblasts. J Dermatol Sci 2007;48(1):15-24.

48.   Liu Y, Dulchavsky DS, Gao X, Kwon D, Chopp M, Dulchavsky S, et al. Wound repair by bone marrow stromal cells through growth factor production. J Surg Res 2006;136(2):336-341.

49.   Chen L, Tredget EE, Wu PY, Wu Y. Paracrine factors of mesenchymal stem cells recruit macrophages and endothelial lineage cells and enhance wound healing. PLoS One 2008;3(4):e1886.

50.   Singer AJ, Clark RA. Cutaneous wound healing. N Engl J Med 1999;341(10):738-746.

51.   Gurtner GC, Werner S, Barrandon Y, Longaker MT. Wound repair and regeneration. Nature 2008;453(7193):314-321.

52.   Maggini J, Mirkin G, Bognanni I, Holmberg J, Piazzon IM, Nepomnaschy I, et al. Mouse bone marrow-derived mesenchymal stromal cells turn activated macrophages into a regulatory-like profile. PLoS One 2010;5(2):e9252.

53.   Gonzalez-Rey E, Gonzalez MA, Varela N, O'Valle F, Hernandez-Cortes P, Rico L, et al. Human adipose-derived mesenchymal stem cells reduce inflammatory and T cell responses and induce regulatory T cells in vitro in rheumatoid arthritis. Ann Rheum Dis 2010;69(1):241-248.

54.   Bouffi C, Bony C, Courties G, Jorgensen C, Noel D. IL-6-dependent PGE2 secretion by mesenchymal stem cells inhibits local inflammation in experimental arthritis. PLoS One 2010;5(12):e14247.

55.   Yagi H, Soto-Gutierrez A, Navarro-Alvarez N, Nahmias Y, Goldwasser Y, Kitagawa Y, et al. Reactive bone marrow stromal cells attenuate systemic inflammation via sTNFR1. Mol Ther 2010;18(10):1857-1864.

56.   Prockop DJ, Youn Oh J. Mesenchymal stem/stromal cells (MSCs): role as guardians of inflammation. Mol Ther 2011.

57.   Singer NG, Caplan AI. Mesenchymal stem cells: mechanisms of inflammation. Annu Rev Pathol 2011;6:457-478.

58.   Krasnodembskaya A, Song Y, Fang X, Gupta N, Serikov V, Lee JW, et al. Antibacterial effect of human mesenchymal stem cells is mediated in part from secretion of the antimicrobial peptide LL-37. Stem Cells 2010;28(12):2229-2238.

Table 5.1. Histology outcomes and procedures for analysis and interpretations. Refer to Figure 5.2 for implant locations. Each box was 1mm^2 and covered the implant porous coating. Polymorphonuclear leukocytes = PMNs; Foreign body giant cells = FBGCs.

Outcomes	Locations	Analysis
Cellular Infiltrates (PMNs, Lymphocytes, Plasma Cells, Macrophages, FBGCs)	Boxes 1-13	Each cell type was counted at 200x magnification
Neovascularization	Boxes 1-13	Number of blood vessels ($\geq$7µm) were counted at 200x magnification
Tissue Ingrowth	Boxes 1-13	Determined % fill of collagen; % fill of fibrin/serum; and total % fill of tissue at 100x magnification
Epidermal Downgrowth	~Boxes 1 and 13; 3 measurements taken per side	Measured distance (µm) between leading edge of epidermis and starting location of downgrowth at 200x magnification
Fibrous Capsule	Boxes 2-12; 3 measurements taken per box	Measured distance (µm) of fibrous capsule thickness at 200x magnification

Table 5.2. Cell surface marker expression determined by flow cytometry on P.8 BMMSCs. Data are represented as percent of the gated population.

Cell Surface Marker	Percent Positive	Percent Negative
CD29	100	0
CD90	100	0
CD34	3.3	96.7
CD45	0.2	99.8
CD11b	1.1	98.9
CD79a	13.8	86.9

Table 5.3. Infection data of treated (T) and untreated (U) implants from Group 1 animals. In the columns, a (+) indicates a positive result and a (-) indicates a negative result. Data are sorted by the number of days consistent inflammation was observed. The shaded rows signify infected implants.

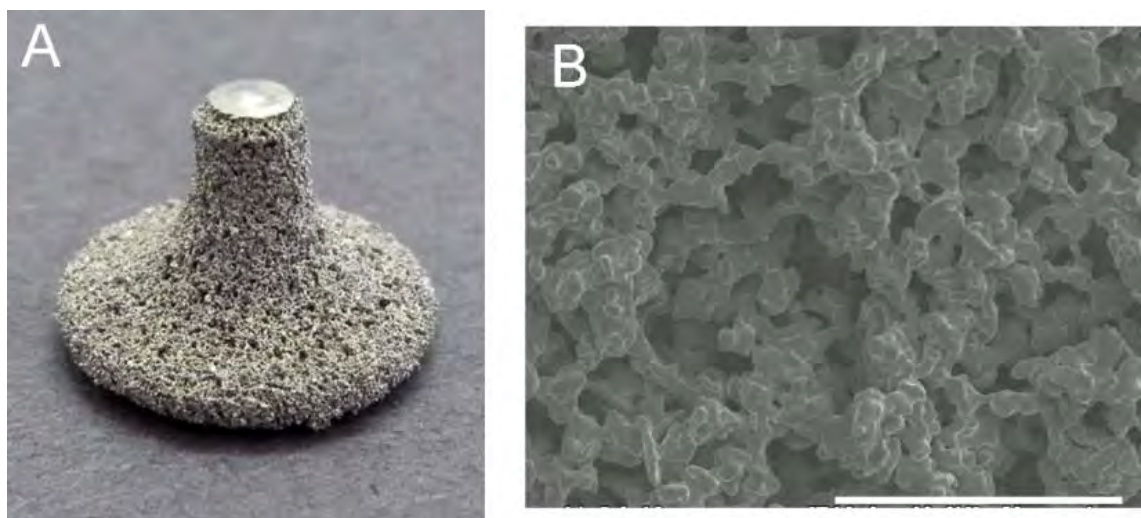| Group 1 Specimens	Days in Study	Days of Consistent Inflammation	Skin-Implant Interface Swab	Soft Tissue Biopsy	Histopathology Infection	Infected
U – 35	69	50	+	+	+	+
U – 31	61	37	+	+	+	+
U – 33	61	37	+	-	-	-
T – 32	78	36	+	-	+	-
U – 32	78	16	+	-	-	-
U – 36	69	13	+	+	+	+
T – 35	69	11	+	+	-	-
T – 31	61	5	+	+	-	-
T – 33	61	5	+	+	-	-
U – 34	61	5	+	-	-	-
T – 34	61	5	+	-	-	-
T – 36	69	4	+	-	-	-

Figure 5.1. Porous titanium percutaneous implant. (A) Photo of implant with a commercially pure titanium porous coating. (B) Scanning electron microscopy image (SEM) of titanium porous coating with ~360μm pore size and ~55% porosity (magnification: 50x; accelerating voltage: 20.0kV). Scale bar is 1mm in length.
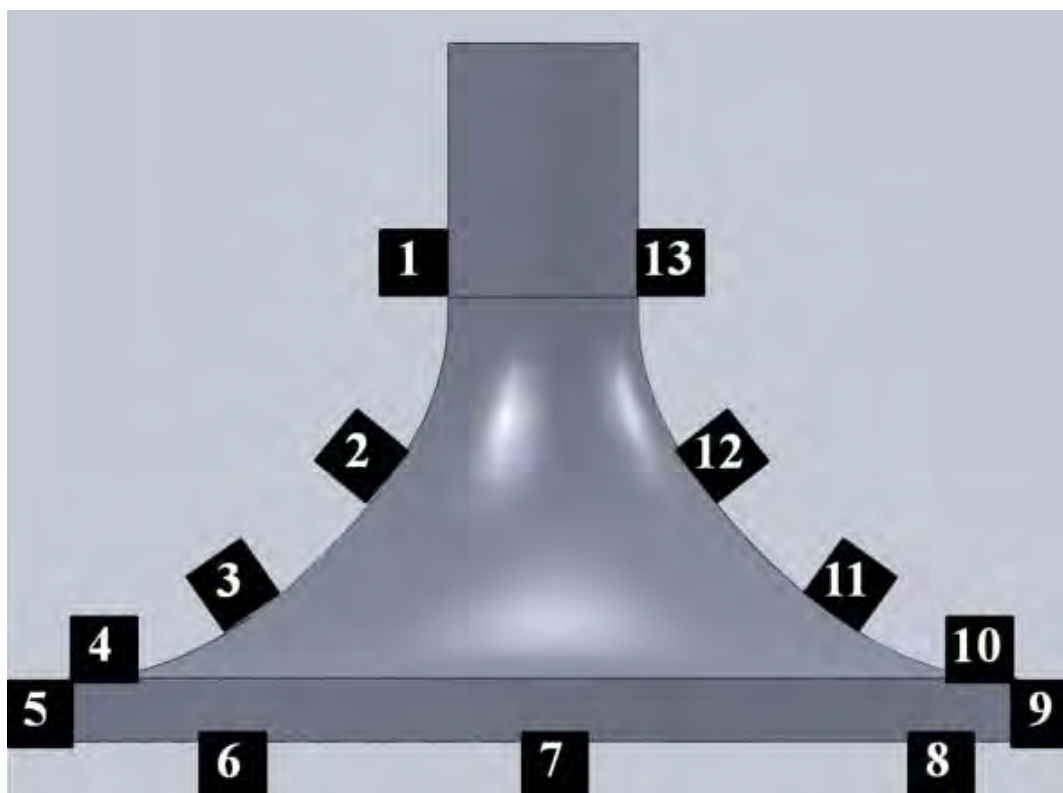
Figure 5.2. Histology analysis template. Analysis was performed in the 13, 1mm^2 boxes around the implant surface. This is a cartoon graphic of the titanium substrate, thus the boxes are positioned over the 1mm porous coating.
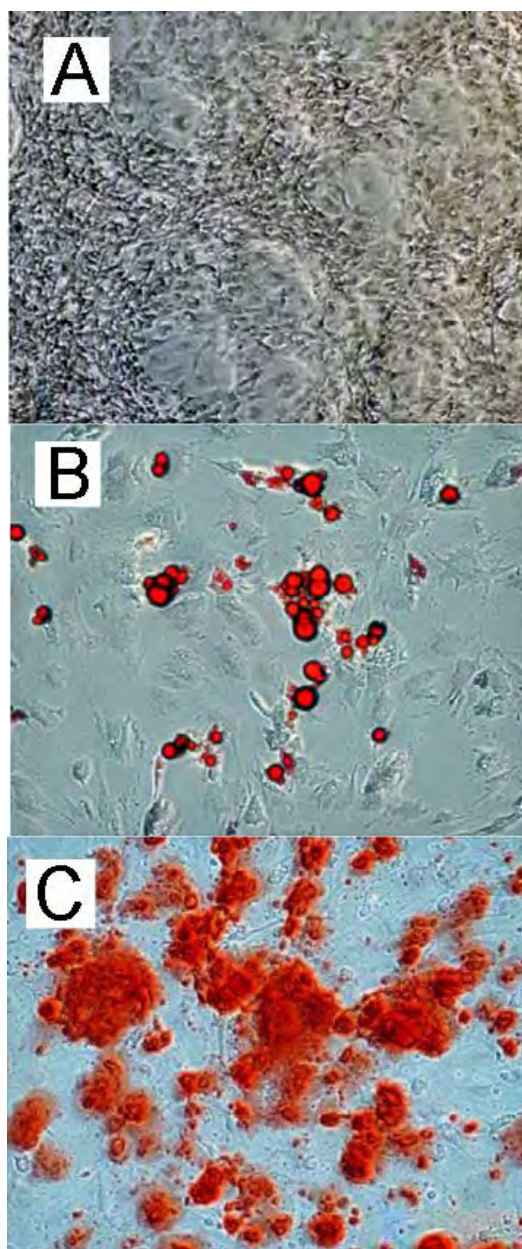
Figure 5.3. Differentiation of P.8 BMMSCs. (A) Control cells in complete growth medium (4x magnification). (B) Adipogenic differentiation and Oil Red O staining of lipid droplets (10x magnification). (C) Osteogenic differentiation and Alizarin Red S staining of calcium deposits (10x magnification).
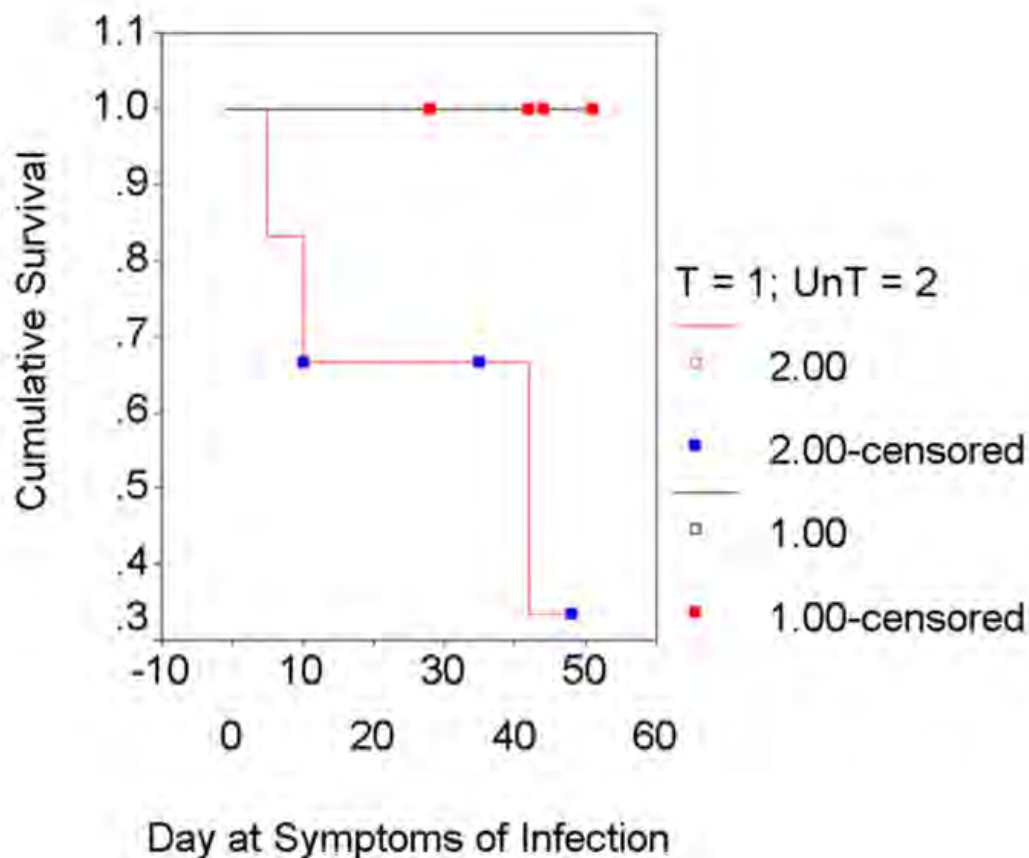
Figure 5.4. Kaplan-Meier survival estimate of treated and untreated implants. The black line with red squares represents treated implants (T), and the red line with blue squares represents untreated implants. The untreated curve drops at the day when consistent symptoms of infection were observed and implant was later confirmed infected. Each dot represents censored data in which consistent symptoms of infection were observed, though no infection was later confirmed. The untreated implants had a significantly ($p < 0.05$) higher risk of infection.
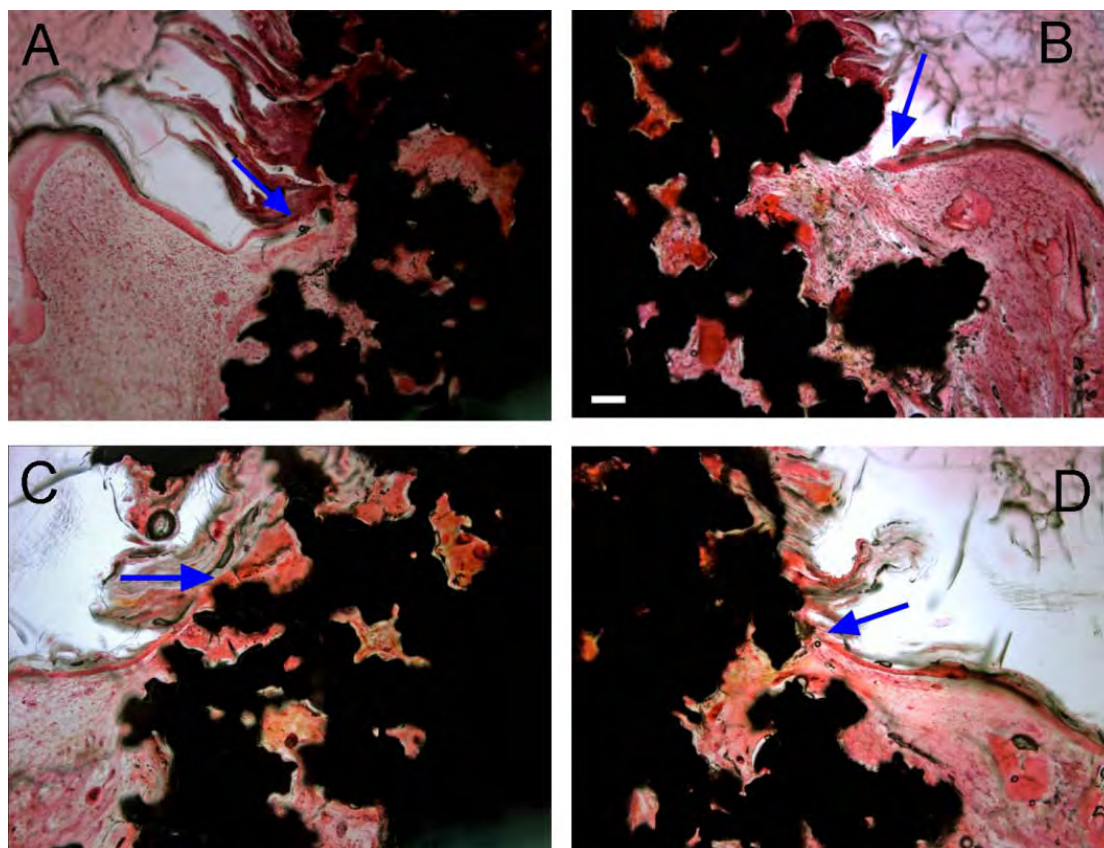
Figure 5.5. Epidermal integration in Group 1 animals. (A and B) Epidermal integration in an untreated implant that was infected. Note leading edge of epidermis (arrow) and high influx of inflammatory cells in tissue. (C and D) Epidermal integration in a treated implant that was not infected. Notice leading edge of epidermis (arrow) and decrease in inflammatory cells in tissue. Images are 10x original magnification; scale bar is 100 μm; H&E stain.
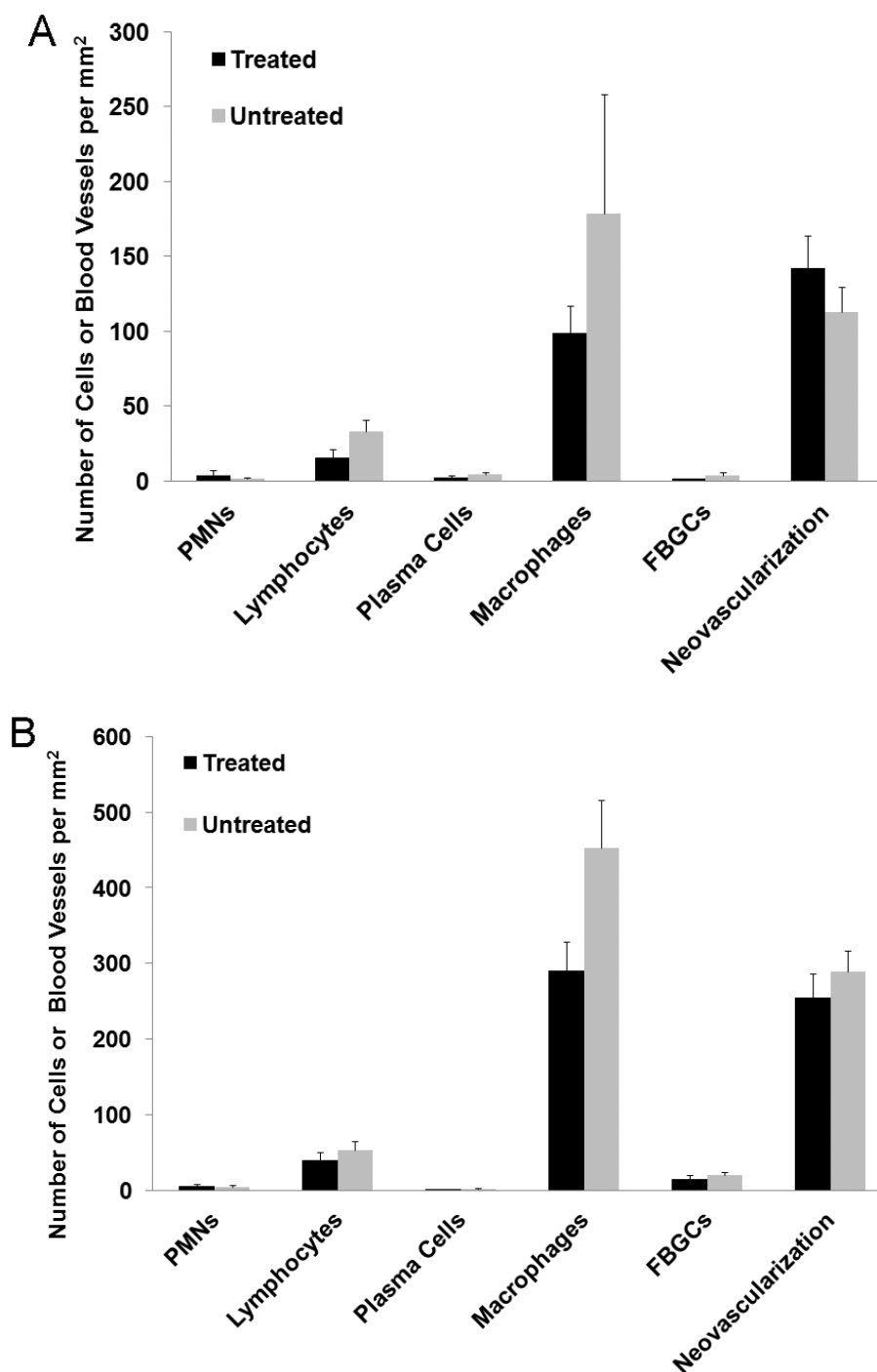
Figure 5.6. Cell and tissue infiltrates into porous coating of percutaneous implants. Cellular and neovasculature infiltration in treated and untreated implants in (A) Group 1 animals and (B) Group 2 animals. Tissue infiltration into porous coating of treated and untreated implants in (C) Group 1 animals and (D) Group 2 animals. * $p < 0.05$ between treated and untreated implants in Group 1 animals. All data are represented as means + SEM, n=5-6.
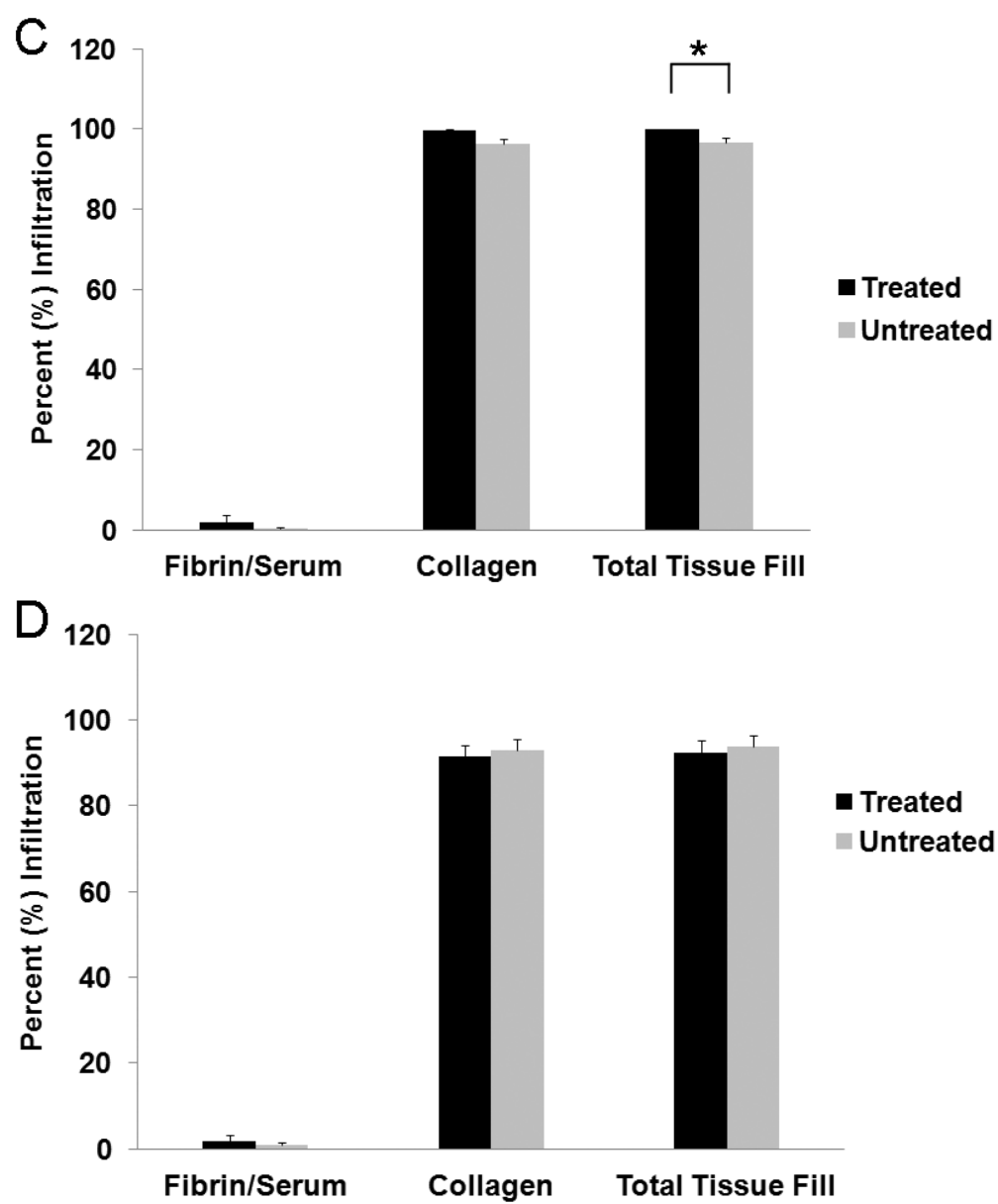
Figure 5.6 continued.
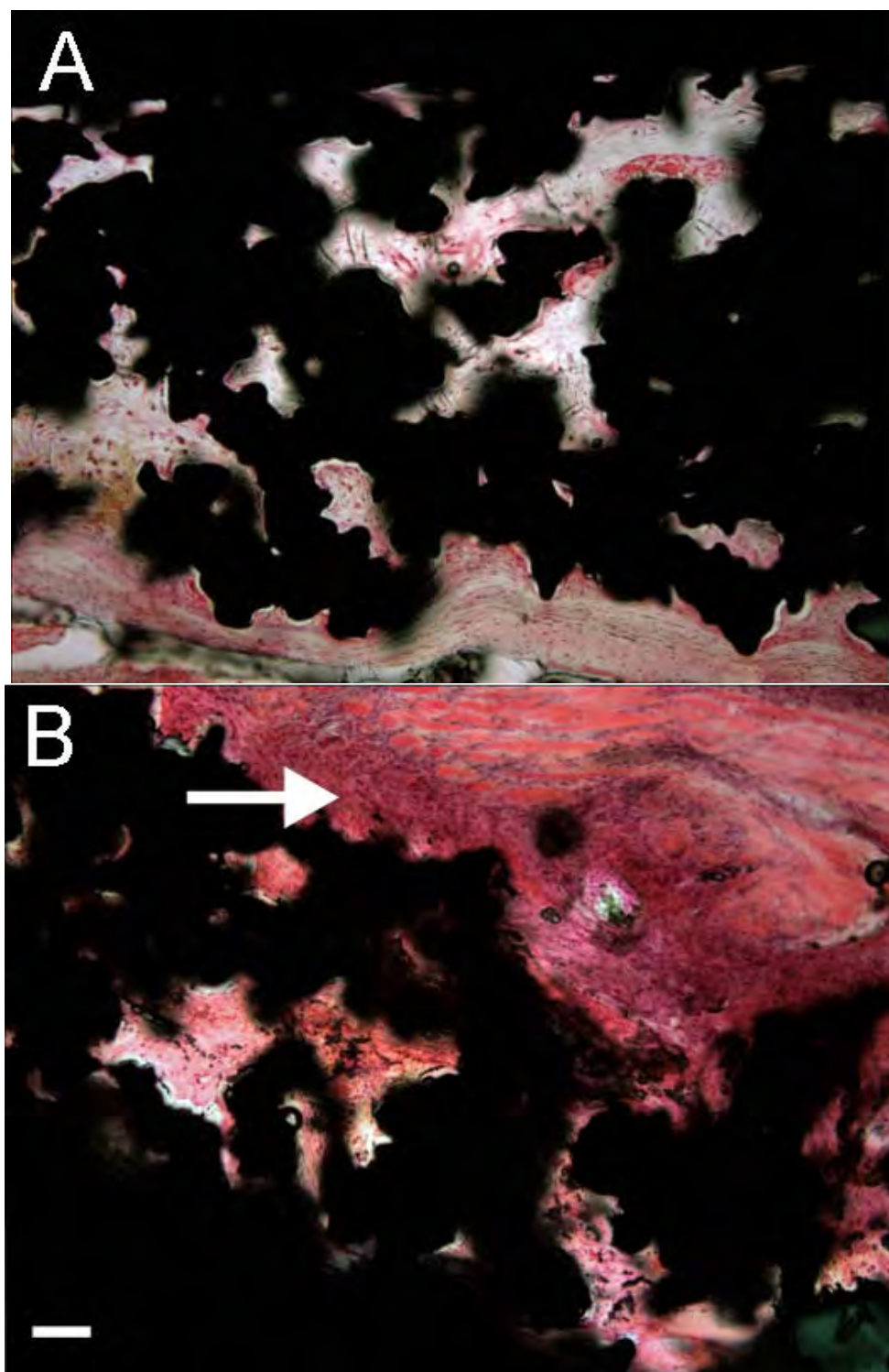
Figure 5.7. Tissue infiltration of Group 1 implants. (A) Uninfected fibrovascular tissue in porous coating of treated implant. (B) Infected tissue of untreated implant. Note high influx of inflammatory cells (arrow), mostly PMNs, outside of porous coating (black). Scale bar is 100 μm; images are 10x original magnification; H&E stain.
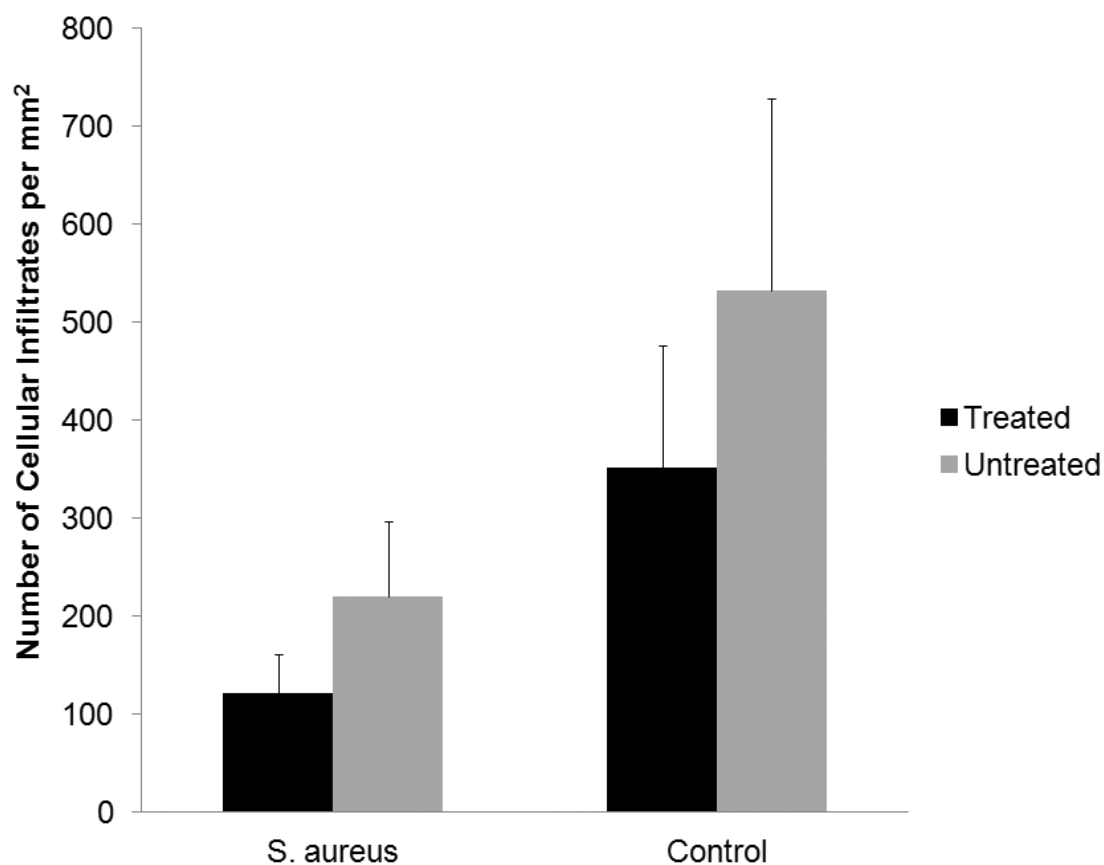
Figure 5.8. Total number of cellular infiltrates in porous coating of MSC-treated and untreated implants in Group 1 (S. aureus) and Group 2 (Control) animals. Data are represented as means + SEM, n=5-6.
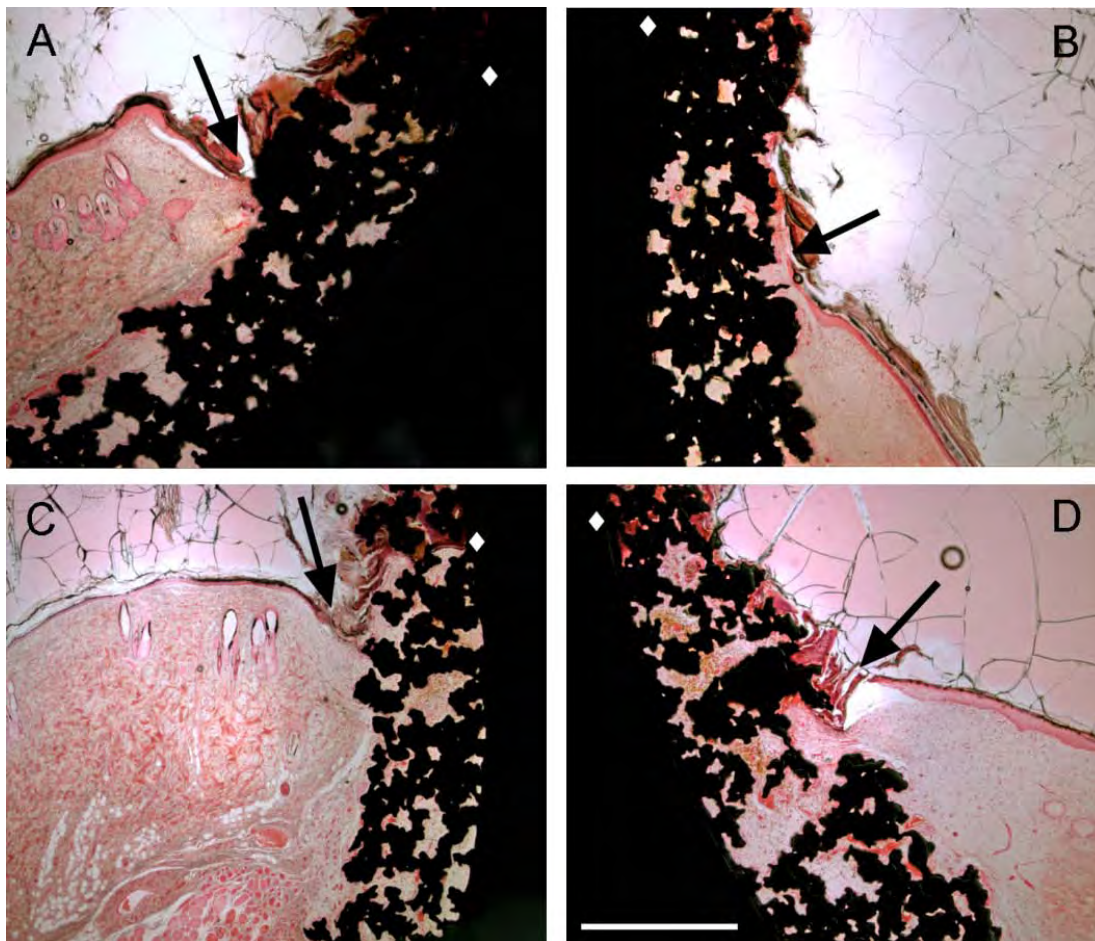
Figure 5.9. Skin-implant interface of treated and untreated implants. (A and B) Epidermal integration (arrow) into porous coating of a treated implant in Group 2. White diamonds on titanium implant (black) designate the uppermost part of viable, vascularized tissue in pores. (C and D) Epidermal integration (arrow) into porous coating of an untreated implant in Group 2. There was vascularized tissue in pores above where epidermis was integrating (white diamonds). All images are 4x original magnification; scale bar is 1mm; H&E stained.
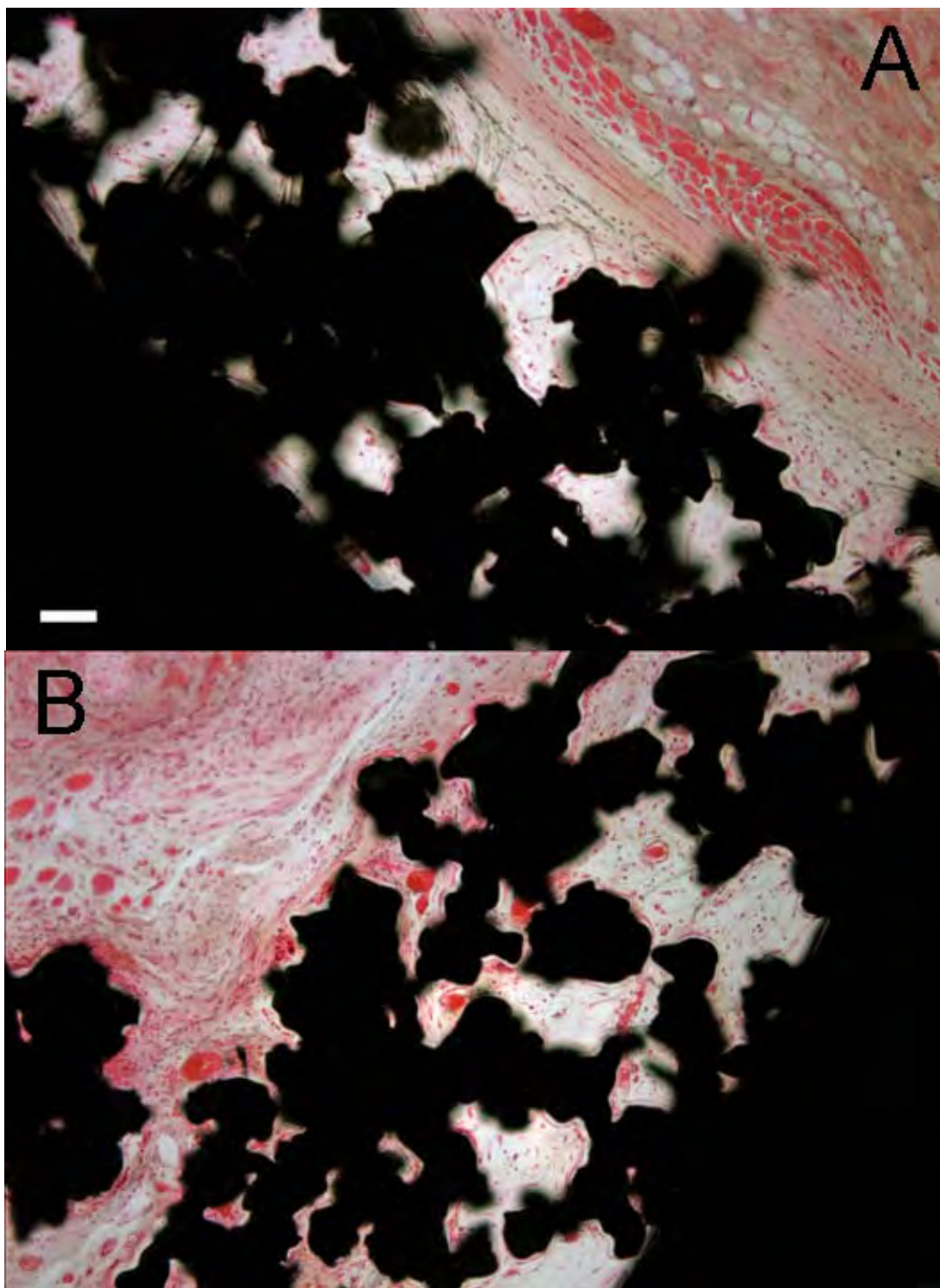
Figure 5.10. Tissue infiltration into treated and untreated implants from Group 2. (A) treated implant was less cellular and had less vasculature compared to (B) the untreated which had more inflammatory cells and vasculature in the porous coating (black). Images are 10x original magnification; scale bar is 100 µm; H&E stain.

CHAPTER 6

CONCLUSIONS, CHALLENGES, AND FUTURE DIRECTIONS

Percutaneous devices are of great value to healthcare professionals and to patients who use them. These devices serve as the connection between the external environment and internal environment, providing data, as in the case of glucose monitors; restoring hearing, as in the case of bone anchored-hearing aids; or restoring physical mobility, as in the case of osseointegrated percutaneous prosthetics. The aim of the research presented in this dissertation was to improve the integration and seal between the skin and the percutaneous device such that a barrier to infection was established. This dissertation work investigated smooth polished and porous titanium surfaces, and transplantation of mesenchymal stem cells to promote a dermal barrier to infection. Overall, this work showed that both porous surfaces and MSC transplantations were effective in decreasing the infection risk of percutaneous implants. This work, to the author's knowledge, was the first to evaluate stem cell transplantation in this type of application with percutaneous implants.

In the next section, brief conclusions pertaining to each individual chapter are presented. Following these conclusions, overall challenges with respect to this dissertation work are discussed along with future directions of research.

6.1 Chapter Conclusions

<u>6.1.1 Chapter 2: infection risk of porous and smooth surface</u>

<u>percutaneous implants in a rabbit model</u>

The rabbit model investigated infection risk of porous and smooth titanium surfaces on percutaneous implants, and demonstrated that porous surfaces significantly decreased infection risk. We postulated that this was due to the increase in surface area for tissue integration, resulting in a tissue attachment and a physical "lock" between the tissue and implant surface. Histology analyses revealed that a common failure mechanism, "epidermal downgrowth," was evident in most every implant section, meaning that the tissue integration on the subcutaneous flange, as opposed to the percutaneous post, served as the primary barrier to infection. Despite infection risks being decreased with porous coatings (note: infection was NOT eliminated), an absence of tissue integration with the percutaneous component of the implant is a concern, most especially for the long-term functionality of the implant. Chapter 2 conclusions are as follows:

♦ Porous coatings contributed to a significantly decreased infection risk of titanium percutaneous implants in a rabbit model

♦ Tissue integration in the percutaneous component was poor; result was epidermal downgrowth and marsupialization

♦ Supra-physiological inoculations of bacteria were necessary to induce implant infection

♦ Was this a clinically relevant percutaneous device infection model? Yes and no; this is debatable

6.1.2 Chapter 3: in vitro cytotoxicity and cellular adherence of

MSCs on porous titanium surfaces

Basic *in vitro* techniques were employed to assess MSC adherence and viability on porous titanium surfaces in various solutions. These studies showed that within a 12-24 hour period, a serum-free cell culture medium was sufficient in retaining cell viability above 90%, and cellular adherence near 90%. As expected, serum-supplemented medium was superior in retaining viability and promoting cellular adherence, while phosphate buffered solutions were inferior to the other solutions. Chapter 3 "take home messages" are as follows:

♦ Serum-free cell culture medium is a satisfactory solution in which to suspend and deliver cells onto porous titanium surfaces

♦ Cell delivery must occur within 12-24 hours after cell seeding on titanium surface, if using serum-free medium

♦ Phosphate buffered solutions significantly decreased cell viability over 24 hours

♦ Serum-supplemented, or protein-laden solutions would be ideal for cell attachment and viability, if an *in vivo* immunogenic response could be prevented

6.1.3 Chapter 4: in vivo assessment of MSCs to improve tissue

integration with percutaneous implants in a rat model

Incorporating the knowledge gained from Chapter 3 (*in vitro* cytotoxicity and cell adherence study), and aiming to show improvements over Chapter 2 (rabbit model evaluating percutaneous implant infection susceptibility), a rat model was used to study effects of MSC treatments on tissue integration with percutaneous implants. This study

not only changed the animal model from rabbit to rat, but also modified the implant design, going from a two-piece percutaneous implant with a right angle to a one-piece implant with a sloped surface (Figure 6.1). The decision to change animal model was based on the following primary reasons: (1) a need to use a syngeneic species for MSC transplantations between animals, (2) the availability of antibodies for characterizing the MSCs as opposed to that available for rabbit, (3) a smaller animal size and ease in handling, (4) fur not as thick as in rabbit, and (5) the opportunity to perform immunohistochemistry staining due to increased availability of antibodies for rat than that for rabbit. To determine efficacy of MSC treatment, implant histology was analyzed at several time points throughout an 8-week period. Chapter 4 study conclusions are as follows:

- MSCs significantly increased rate of collagen infiltration in treated implants

- MSCs increased cellular infiltrates at early time points and promoted an early inflammatory resolution of treated implants

- MSCs possibly decreased foreign body response but additional data is necessary

- MSCs appeared to not affect epidermal downgrowth as it was not observed in most treated and untreated implants

- It is possible that a sloped surface as opposed to a perpendicular surface allowed for epidermal attachment

- Rat model limitations, including presence of fur, differences in skin anatomy and healing mechanisms, differences in cellular metabolism in the skin, make clinical translation difficult

- Transplantation of MSCs on the porous titanium surface needs optimization

♦ Future investigations should elucidate possible mechanisms of MSCs in

improving tissue ingrowth

6.1.4 Chapter 5: in vivo assessment of MSCs to prevent infection

of percutaneous implants in a rat model

As the ultimate goal of the MSC therapy was to stimulate a rapid and robust skin-

implant seal such that infection was prevented, this study replicated the rabbit model

methods to investigate percutaneous implant infection through use of bacterial

inoculations. Based on literature and personal experience, if left to natural

circumstances, implant infection may not develop in small animals. Thus, infection was

induced by inoculating the skin-implant interface with an exogenous bacterial

suspension.

One important lesson learned from this rat model was that these animals are

extremely resilient and physically flexible and agile (considering this is a rodent, this

should not be a surprise!). Inflammation of the implant would fluctuate, and this might

have been partly because they took great care of their implants by contorting their head to

routinely licking them and the bacterial solutions on the skin-implant inteface. It is

widely known that saliva has antimicrobial peptides, wound healing growth factors, and

acts as a physical cleansing mechanism [1-4]. Due to these properties of saliva, it is

possible that the consistent animal licking of the implants impeded infection

development. This was surprising as the rabbits did not act in this manner, to our

knowledge. Very obvious implant infection (gross swelling with exudate) in the rabbit

model was evident after 6 weeks of bacterial inoculations, but this was not the case with

the rat model. The most blatant signs of infection observed included pink/red skin color, tenderness, aggressive behavior, and lethargy. Some of the implants displayed slight swelling, but the swelling would fluctuate along with changes in skin color.

It has been noted that rabbits are more susceptible to *Staphylococcus aureus* infections, compared to other bacterial species [5], and thus this could also explain differences in presence and severity of infection symptoms between the rat and rabbit models. Nonetheless, infection of untreated implants did eventually develop according to the defined implant infection criteria as stated in Chapter 5. The "take home messages" for Chapter 5 are as follows:

- ♦ Infection development was prevented in MSC-treated implants

- ♦ Tissue infiltration was significantly increased in MSC-treated implants

- ♦ Implant infection development in the Group 1 animals proved to be challenging in the rat model, compared to what was observed in the prior rabbit study

- ♦ Mechanisms contributing to the decreased infection risk are unknown and need to be further elucidated

- ♦ MSCs appear to be a promising therapeutic for tissue integration, though there are many unanswered questions regarding mechanisms between the MSCs and the local cellular milieu, and regarding the appropriate delivery regimen (number of dosages, timing of dosages, etc.)

- ♦ Translation to the clinic? Debatable; results prompt investigation into models, such as a porcine model, that are more clinically relevant

6.2 Challenges and Future Directions

6.2.1 Mesenchymal stem cell culture and clinical scale

manufacturing limitations

In this dissertation, the author primarily sourced the mesenchymal stem cell population from the bone marrow of a male Lewis rat. However, within the MSC research community, another commonly used source for MSCs is adipose tissue. The question arises how these two MSC populations differ with respect to animal species, animal age, and passage of cells used for experimental purposes. BMMSCs from commonly used rat strains (Fisher, Lewis, Sprague-Dawley, and Wistar) share similar characteristics with respect to cell-surface phenotype, expansion rates, and differentiation capacities [6]. Several studies have successfully employed the therapeutic use of BMMSCs from animal models including rat [7], rabbit [8], murine [9, 10], equine [11], porcine [12], non-human primate [13], and human [10, 14]. It has been shown that with respect to cell yield, growth kinetics, cell senescence, and multi-lineage difference capacity, both ASCs and BMMSCs behave similarly, though ASCs do exhibit a higher cell yield at harvest [15]. As for the ASC population, Arrigoni et al. demonstrated slight differences between rat, rabbit, and porcine ASCs with regards to population doubling time and clonogenic ability [16]. The ASCs from all three animals displayed similar and suitable osteogenic differentiation potential [16].

With regards to animal age and passage number influencing MSC phenotype and functionality, it is generally agreed that with increasing animal age and passage number, MSCs exhibit decreasing ability to differentiate into multiple lineages, along with a decreasing clonogenic ability (personal communication with Roxanne Reger, Senior

Research Scientist, Tulane University and the Darwin Prockop Research Group at Texas A&M University) [17, 18]. For practical purposes, it is recommended that cells do not undergo more than 50 population doublings [19] and/or be used after 10 passages (personal communication with Roxanne Reger). For additional information on MSC isolation and culture, the reader is referred to the following relevant publications [9, 19-26].

Many challenges exist to successfully achieve large-scale expansion of MSCs in ex vivo culture conditions; and an optimum, standardized protocol for clinical scale production of MSCs has yet to be developed. An important element in culturing MSCs for clinical application is using a growth medium that retains MSC phenotype and functionality, but that does not elicit differentiation or immunogenic responses *in vivo* or introduce bacterial, fungal, or other zoonotic diseases within the transplant recipient. In the work presented in this dissertation, all MSC expansion was performed using fetal bovine serum (FBS). However, alternative cell culture media have been investigated and a promising alternative is platelet lysate [27]. Platelet lysate presents with decreased risk of transmission of disease to the recipient, it can be an autologous source, and it is effective in expanding MSCs while retaining phenotypic and functional characteristics [27]. Thus, future work should seek to optimize culture expansion conditions using an alternative growth supplement, such as platelet lysate, that has fewer risks compared to FBS. However, caution must be taken as, like MSC sources, platelet lysate can be quite variable in composition, variable between species, and variable upon donor age and health.

6.2.2 MSC characterization after culture on porous titanium surfaces

In Chapter 3, we evaluated cell delivery solutions that were commonly used in clinical and animal model studies reported in literature. A few questions were not addressed, but should be addressed in future studies. First, we did not address the functional and phenotypic characteristics of the MSCs cultured during and after the 24-hour culture in the different solutions. Future studies could repeat the methods described previously, then detach the cells from the surface and place them in differentiation conditions or stain them for cell surface marker expression at the defined timepoints during the 24-hour period.

Second, we did not evaluate an optimal holding temperature of the cell-seeded construct. Previous work has shown that cell viability is increased when cells are kept below 37°C [28-30]; therefore, future studies could repeat the described methods though at lower temperatures, such as 4° and 20°C, then provide optimal temperature recommendations based on cellular adherence, proliferation, phenotypic and functional preservation, and cytotoxicity results.

6.2.3 Optimization of MSC adherence and *in vivo* delivery methods

Cells adhere to surfaces through focal adhesion sites, integrin receptors, and adhesion proteins. The choice of analyzing serum-supplemented cell culture medium, serum-free cell culture medium, and phosphate buffered solutions was primarily due to the fact that they are commonly used cell delivery vehicles, and as they are commercially available, they are well characterized and consistency can be achieved by using a single lot. The work presented in this dissertation used an FBS from a single lot to eliminate

lot-to-lot variability. The data generated from Chapter 3 provided basic groundwork with which future studies could compare and future work could be expanded. With that said, a possible next step in optimization of MSC delivery on porous titanium surfaces would be to use a matricellular protein (such as collagen, fibronectin, or laminin) surface modification that could possibly increase the number of adherent cells, and the strength of cellular attachment. The protein modification would need to be non-immunogenic, and optimal concentration and attachment method would need to be determined.

On the other hand, separately or in addition to modifying the implant surface, a different cell carrier could be evaluated. For example, a more viscous and enriching medium such as platelet rich plasma [31-34], a collagen gel [35, 36], or fibrin matrix[10] could be used. Though these suggested carriers have been used in diverse tissue repair applications reported in literature, further analysis of cell number delivery, viability, and characterization in a 24- or 48-hour period would need to be performed prior to *in vivo* applications.

6.2.4 Percutaneous implant geometry: perpendicular versus sloped

As mentioned a few times previously, a simple but important study needs to determine, in either a rabbit or rat model, whether or not implant geometry affects skin ingrowth (Figure 6.1). This is important because we experienced opposite results regarding epidermal downgrowth in the rat and rabbit models (see Figures 2.3 and 2.4 in Chapter 2, Figure 4.9 in Chapter 4, and Figures 5.5 and 5.9 in Chapter 5). Though this could be due to species-specific differences, this is unlikely as both animals have relatively similar skin physiology and healing mechanisms. Differences could also be

related to *in situ* residence time; however, the rabbit implants were harvested after 10-14 weeks and the rat implants were harvested after 9-11 weeks of implantation. Though there is a 1-3 week difference, it is highly unlikely that the epidermis would travel a couple millimeters in that short amount of time. Thus, head-to-head comparisons between the two implant designs should be performed either in the rat or the rabbit model.

6.2.5 Implant infection animal model and infection diagnosis

Inducing implant infection through bacterial inoculations was challenging in the rat model due to animal licking, instability of bacteria solution droplets at the implant interface, and/or robust host immunity to *S. aureus*, among other potential contributing factors. The differences observed between the rat and rabbit models of implant infection highlight the issue that choice of animal model and bacterial strain can easily bias the study results. The following paragraphs further discuss this in relation to the work presented in this dissertation.

The native physical activity of the animal species having a potential interference with results (i.e., animal licking wound or implant site) is a point to keep in mind when selecting an animal model for a percutaneous implant infection study. If future studies warrant the use of an animal model that does not lick their implants, the rabbit model may be a better choice as, to this author's experience, the rabbits did not lick their implants. On the other hand, animal licking of the implant site is a form of implant care, which somewhat mimics the care of an implant site that humans might have with their own percutaneous implants, though in the human case there would be a cleansing of the

implant as opposed to licking the implant. Thus, rats might then be a more appropriate animal model if there is a desire to incorporate host care of an implant site.

Regarding choice of bacterial strain used to induce implant infection, several strains of *Staphylococcus aureus are* available from ATCC for experimental use. Some of these strains have very weak virulence properties while others exhibit stronger virulent properties. The strain used for the studies outlined in this dissertation was the ATCC 49230 strain (also referred to as CDC 587 or UAMS-1), a *Staphylococcus aureus* clinical isolate from a human patient that had osteomyelitis in Little Rock, USA. As for virulence, this particular isolate is reported to be a **serotype 8** *S. aureus* strain which produces an extracellular capsular polysaccharide that aids in resisting phagocytosis, and is equipped with adhesins for binding ECM proteins, cells, body fluids, and implant surfaces [37-39]. **Serotype 8** *S. aureus* strains account for ~50% of isolates recovered from humans, and are prevalent among isolates from clinical infections as well as from commensal sources. Thus, according to literature, this is a relevant clinical strain as it has the virulence properties (i.e., capsular production and adherence factors) deployed in majority of human infections.

This strain was selected for use in the Chapter 2 rabbit study as it successfully produced strong infection symptoms in a previous rabbit study that Dr. Roy Bloebaum's group had conducted [40].With no previous experience working with *S. aureus* strains, this author thought it was a reasonable strain to use. This author chose to use this same strain for the rat study based on (1) the strong infection data achieved with the Chapter 2 rabbit study[41], and (2) the information stated in the previous paragraph regarding its clinical relevance.

Though the bacterial strain used in these studies is a relevant clinical strain important in human infections, the use of this strain as was presented in Chapters 2, 4, and 5 to predict human infections, specifically those acquired in hospital settings, is somewhat difficult to make. Other more virulent strains are present in hospital settings and may compete with commensal microorganisms in causing infection. Further, it has been demonstrated that the hospital environment can exert a selective pressure on commensal strains, causing them to become more virulent [42]. Nosocomial infections are commonly caused by *S. aureus*, *S. epidermidis, P. aeruginosa*, and *Enterococcus* species, in addition to more resistant microorganisms, such as methicillin-resistant *S. aureus* [43]. Device-related infections are commonly caused by *S. aureus* and *S. epidermidis* [44, 45]. Though the presented studies used a common microorganism responsible for nosocomial skin and soft tissue infections and device-related infections, realistically a nosocomial device-related infection is profoundly influenced by other commensal microorganisms and the hospital environment.

Host response to microbial invasion is different between rat and rabbit, as it is known that rabbits are more susceptible to *S. aureus* infections [5]. The predictability of the rat and rabbit response to that of the human response is somewhat difficult to assess. Rabbits do not possess neutrophils like humans and rats, but instead possess heterophils. This difference in the inflammatory cell population may coincide with differences in host response to microbial invasion, and therefore hamper infection predictability in humans. In addition, (a) rats and rabbits reside in very different environments and are exposed to different antigens compared to humans; (b) they are smaller in body mass and thus their physiological requirements are very different than that for humans; and (c) both of these

small animals have a thick coat of fur, which humans do not have. This author cannot

find literature to back up her assertion that these listed differences may ultimately at some

point result in a species-specific immune response to bacterial infection, and thereby may

produce little predictability or translation to human infection.

If future investigations require use of a rat model as used in these studies,

incorporating one of the following recommendations may improve implant infection

development. (A) Based on rate of tissue integration from the histology data in Chapter 4,

microbial inoculations may be more effective if given prior to two weeks after

transplantation, preferably at one week or less. (B) Increase concentration of bacterial

inoculum (>1.5 x 10^8 CFU), though with the disclaimer that even though increased

concentrations of bacteria inoculums are documented in literature, it does not improve

clinical relevance, but merely increases likelihood of observing stronger infection

symptoms. (C) Increase frequency of inoculations, such as twice per week. (D) Use a

more virulent bacterial strain to which rats are susceptible or to which rats natively

succumb to infection, taking caution that this may not improve clinical relevance. (E) Use

a rat strain more susceptible to infection, such as an immunodeficient strain, being aware

that with an immunodeficient strain, wound healing response will be compromised and

again, this does not improve overall clinical relevance.

In addition to optimizing bacterial infection development, it would be beneficial

to incorporate molecular methods in confirming implant infection more quantitatively.

This is very important in light of evidence that cultures from infected implants with

biofilms rarely produce positive growth on agar plates due to phenotypic differences in

planktonic bacteria as opposed to biofilm microcolonies [46]. As contaminated, infected

wounds typically host a diverse population of microorganisms, of which not all will grow in the same media conditions. Hence, sophisticated and sensitive techniques should enable more accurate detection of these complex bacterial isolates [47]. Relatively "newer" techniques exist such as polymerase chain reaction (PCR), reverse transcription-PCR [48], and PCR coupled with electrospray ionization/mass spectrometry (e.g., Ibis Systems from Abbott Laboratories) [49] are examples. Use of molecular biology techniques like PCR in similar studies as presented in this dissertation will require additional tissue from the implant for analysis, but also it would be advantageous to sonicate the implant to dislodge biofilm colonies [46, 50]. A potential limitation in using these techniques is that this will decrease the amount of tissue available for other histology analysis. Thus, the researcher will need to consider increasing the sample number to accommodate for both tissue infection analysis and histology analysis.

In light of this limitation and the potential need to increase animal number, another relatively newer avenue in quantifying bacterial colonization in tissue is the use of bioluminescent bacterial strains (Bioware™ Microorganisms, Caliper Life Sciences, Inc.). These strains allow one to monitor *in vivo* bacterial growth using optical imaging technology (Xenogen IVIS, Caliper Life Sciences, Inc.) [51-53]. An advantage to using bioluminescent bacterial strains is that this may eliminate the need to harvest tissue specimens to detect bacterial growth, thus allowing histology analysis to be performed and also potentially decreasing the animal number needed in studies. However, some limitations exist including potentially weaker virulence capacity of the bioluminescent strains, reduced imaging resolution due to increased tissue mass, and optical interference if metals are being investigated. Other possible routes of analyzing and visualizing

bacterial colonization in tissue include green fluorescent protein (GFP) markers [54, 55], bioluminescent markers [56, 57], fluorescence *in situ* hybridization (FISH) with probes for RNA or DNA [58], and immunohistochemistry analysis [59].

One last point regarding analysis of tissue infection includes the recent discovery that soft tissue sites adjacent to the primary biomaterial-associated infection may harbor bacteria [60, 61]. If these bacterial colonies in these remote soft tissue sites are not eradicated, this may be a potential source of "re-seeding" the bacterial infection at the original site [60, 61]. Thus, analysis of tissue infection should occur at the biomaterial-tissue interface and in the surrounding soft tissue depots. The use of the above bioluminescent bacteria, or BrdU-labeled bacteria, or even GFP-labeled bacteria may assist the researcher in identifying these surviving bacterial colonies in the surrounding soft tissue.

6.2.6 Animal model limitations and clinical relevance

In the author's opinion, an animal model that has useful clinical relevance to the human model is the "Achilles heel" of most all animal studies. Murine and rodent models are the two most commonly used animal models, yet differences in skin physiology and anatomy can hamper relevant comparisons between these two species and with humans [62]. Further, the location of the implants is very important because skin physiology (e.g., cell turnover, metabolism, and vascular density) and subsequently healing can be quite different in different anatomical locations [63]. For example, since the skin is tightly adhered to underlying tissues in the cranium, healing occurs more by epithelialization than that in the dorsum where contraction predominates, as the skin is

not tightly adhered to underlying muscle, fascia, and bone [64, 65]. With that said, as often times the decision to use a small animal (such as a mouse, rabbit, or rat) is greatly influenced by factors such as ease of handling, limited funding, commercially available antibodies, ability to have higher sample numbers, etc. one must be cautious in designing an appropriate animal model for experimental study. It is difficult to state that one small animal is better than another small animal as all of them are quite different than humans in many aspects that are still quite not fully understood. Thus, it is the researcher's responsibility to select an animal species and an implant anatomical location that appropriately answers their experimental question. If satisfactory results are obtained, then a more human relevant model, such as a porcine model, should be used to evaluate the same experimental question.

To this author's knowledge, there is not a published study on species-related differences regarding metal percutaneous device healing among "loose-skinned" and "tight-skinned" animals. It would be beneficial to conduct a head-to-head comparison performing the exact same treatments, surgery, and implant location in rat, rabbit, and pig. Since rat and rabbit are similar, this author expects similar results from those two. Since both are quite different than pig, this author would expect different results. Sullivan and colleagues reported that pig studies have a 78% correlation with human studies when evaluating the same physiological mechanism, research question, or therapy [66]. On the other hand, small animal studies only had a 53% correlation with human studies [66]. As pig has been shown to be the most similar wound healing model to human healing [66, 67], it is necessary to validate studies in the pig model prior to human trials.

6.2.7 Limitations of histology processing and suggestions for

future work

The studies outlined in the previous chapters use metal implants that are,

relatively speaking, very large. This large mass of metal creates great difficulty in

histology staining methods, as not only are the resulting sections very thick (~150 μm)

but the section surfaces are often severely uneven. If these implants were not composed

of a large mass of metal, these histology limitations could be avoided. If a metal implant

is of interest, one possible option is to use a polymeric substrate and coat the surface with

a metal coating. An implant mainly composed of a polymer with only a thin metal

coating could then be ground down to thinner sections (<50 μm) with more evenly

polished surfaces.

This author hoped to perform immunohistochemistry (IHC) staining on the

histology sections, but for practical purposes this could not be performed. Researchers

intending to perform routine histology staining or IHC staining on

polymethylmethacrylate (PMMA) sections are encouraged to read the work of Quentin et

al. [68], Rammelt et al. [69], Vertenten et al. [70], and Willbold et al. [71] for helpful

methods in performing IHC staining on PMMA histology sections.

6.2.8 Future of percutaneous osseointegrated prosthetic technology

As the motivation for this dissertation is the development of infection-free

percutaneous osseointegrated prosthetic technology for amputees, it is only appropriate

that it ends with this topic. Patients with these prosthetics in Europe surprisingly are

quite satisfied with their prosthesis, despite infectious problems. Branemark's team

reports an 18% infection rate of percutaneous osseointegrated prosthetics [72]; yet, other groups in Europe implanting these prosthetics are reporting very little infectious complications [73, 74]. The differences in infection rates could be attributed to improvements in surgical implantation and rehabilitation regimen. Though it must not go left unsaid that one advantage to implanting these prosthetics in humans is that humans will, for the most part, diligently care for their prosthesis or they will reap very serious consequences – physically, emotionally, and financially.

With respect to providing improved prosthetics for the amputee population, if percutaneous osseointegrated prosthetic technology does not become a FDA-approved medical device, all hope is not lost as the improvement of conventional socket prosthetics continues at a rapid pace. Some examples can be seen in the labs at Vanderbilt with the bionic leg [75], or at Northwestern where Todd Kuiken is developing myoelectric prostheses [76]. Whether amputees receive a socket prosthetic or a percutaneous osseointegrated prosthetic, the skin-implant interface is still a problem. In the former, patients are encumbered by skin irritation, blistering, unevenly distributed stresses leading to skeletal pathologies; and in the latter, poor implant integration with the bone and skin will lead to soft tissue infection, osteomyelitis, and implant removal. Thus, no matter the prosthetic, the interface between the skin and device will be a continual source of challenges to address.

Developing and maintaining a life-long seal between the skin and a percutaneous implant is a formidable task due to the combined complexity existing between the continually, renewing skin and the static, foreign device. Small advancements in knowledge encompassing interactions between skin, biomaterials, cells, proteins, and

bacteria will surely motivate incremental improvements in device design and tissue repair therapeutics. Together this will bring us closer to one day achieving a homeostatic, harmonious relationship between percutaneous devices, specifically percutaneous osseointegrated prosthetics, and the human end-user.

6.3 References

1.   Bodner L. Effect of parotid submandibular and sublingual saliva on wound healing in rats. Comp Biochem Physiol A Comp Physiol 1991;100(4):887-890.

2.   Jahovic N, Guzel E, Arbak S, Yegen BC. The healing-promoting effect of saliva on skin burn is mediated by epidermal growth factor (EGF): role of the neutrophils. Burns 2004;30(6):531-538.

3.   Oudhoff MJ, Bolscher JG, Nazmi K, Kalay H, van 't Hof W, Amerongen AV, et al. Histatins are the major wound-closure stimulating factors in human saliva as identified in a cell culture assay. Faseb J 2008;22(11):3805-3812.

4.   Zelles T, Purushotham KR, Macauley SP, Oxford GE, Humphreys-Beher MG. Saliva and growth factors: the fountain of youth resides in us all. Journal of Dental Research 1995;74(12):1826-1832.

5.   Baker DG. Natural pathogens of laboratory mice, rats, and rabbits and their effects on research. Clin Microbiol Rev 1998;11(2):231-266.

6.   Barzilay R, Sadan O, Melamed E, Offen D. Comparative characterization of bone marrow-derived mesenchymal stromal cells from four different rat strains. Cytotherapy 2009;11(4):435-442.

7.   McFarlin K, Gao X, Liu YB, Dulchavsky DS, Kwon D, Arbab AS, et al. Bone marrow-derived mesenchymal stromal cells accelerate wound healing in the rat. Wound Repair Regen 2006;14(4):471-478.

8.   Zhou W, Han C, Song Y, Yan X, Li D, Chai Z, et al. The performance of bone marrow mesenchymal stem cell--implant complexes prepared by cell sheet engineering techniques. Biomaterials 2010;31(12):3212-3221.

9.   Soleimani M, Nadri S. A protocol for isolation and culture of mesenchymal stem cells from mouse bone marrow. Nat Protoc 2009;4(1):102-106.

10.   Falanga V, Iwamoto S, Chartier M, Yufit T, Butmarc J, Kouttab N, et al. Autologous bone marrow-derived cultured mesenchymal stem cells delivered in a fibrin spray accelerate healing in murine and human cutaneous wounds. Tissue Engineering 2007;13(6):1299-1312.

11.   Smith RKW, Korda M, Blunn GW, Goodship AE. Isolation and implantation of autologous equine mesenchymal stem cells from bone marrow into the superficial digital flexor tendon as a potential novel treatment. Equine Veterinary Journal 2003;35(1):99-102.

12.   Zeng L, Rahrmann E, Hu Q, Lund T, Sandquist L, Felten M, et al. Multipotent adult progenitor cells from swine bone marrow. Stem Cells 2006;24(11):2355-2366.

13.   Izadpanah R, Trygg C, Patel B, Kriedt C, Dufour J, Gimble JM, et al. Biologic properties of mesenchymal stem cells derived from bone marrow and adipose tissue. J Cell Biochem 2006;99(5):1285-1297.

14.   Karaoz E, Okcu A, Gacar G, Saglam U, Yuruker S, Kenar H. A comprehensive characterization study of human bone marrow MSCs with an emphasis on molecular and ultrastructural properties. J Cell Physiol 2010.

15.   De Ugarte DA, Morizono K, Elbarbary A, Alfonso Z, Zuk PA, Zhu M, et al. Comparison of multi-lineage cells from human adipose tissue and bone marrow. Cells Tissues Organs 2003;174(3):101-109.

16.   Arrigoni E, Lopa S, de Girolamo L, Stanco D, Brini AT. Isolation, characterization and osteogenic differentiation of adipose-derived stem cells: from small to large animal models. Cell Tissue Res 2009.

17.   Stolzing A, Jones E, McGonagle D, Scutt A. Age-related changes in human bone marrow-derived mesenchymal stem cells: consequences for cell therapies. Mech Ageing Dev 2008;129(3):163-173.

18.   Wagner W, Bork S, Lepperdinger G, Joussen S, Ma N, Strunk D, et al. How to track cellular aging of mesenchymal stromal cells? Aging 2010;2(4):224-230.

19.   Charbord P. Bone marrow mesenchymal stem cells: Historical overview and concepts. Human Gene Therapy 2010;21(9):1045-1056.

20.   Bunnell BA, Estes BT, Guilak F, Gimble JM. Differentiation of adipose stem cells. Methods in molecular biology. Clifton, NJ 2008;456:155-171.

21.   Bunnell BA, Flaat M, Gagliardi C, Patel B, Ripoll C. Adipose-derived stem cells: isolation, expansion and differentiation. Methods 2008;45(2):115-120.

22.   Dominici M, Le Blanc K, Mueller I, Slaper-Cortenbach I, Marini F, Krause D, et al. Minimal criteria for defining multipotent mesenchymal stromal cells. The International Society for Cellular Therapy position statement. Cytotherapy 2006;8(4):315-317.

23.   Sethe S, Scutt A, Stolzing A. Aging of mesenchymal stem cells. Ageing Res Rev 2006;5(1):91-116.

24.   Torres FC, Rodrigues CJ, Stocchero IN, Ferreira MC. Stem cells from the fat tissue of rabbits: an easy-to-find experimental source. Aesthetic Plastic Surgery 2007;31(5):574-578.

25.   Bieback K, Kinzebach S, Karagianni M. Translating research into clinical scale manufacturing of mesenchymal stromal cells. Stem Cells Int 2011;2010:193519.

26.   Prockop DJ, Phinney DG, Bunnell BA. Methods and protocols. Preface. Methods in molecular biology. Clifton, NJ 2008;449:v-vii.

27.   Doucet C, Ernou I, Zhang Y, Llense JR, Begot L, Holy X, et al. Platelet lysates promote mesenchymal stem cell expansion: A safety substitute for animal serum in cell-based therapy applications. Journal of Cellular Physiology 2005;205(2):228-236.

28.   Pal R, Hanwate M, Totey SM. Effect of holding time, temperature and different parenteral solutions on viability and functionality of adult bone marrow-derived mesenchymal stem cells before transplantation. J Tissue Eng Regen Med 2008;2(7):436-444.

29.   Muraki K, Hirose M, Kotobuki N, Kato Y, Machida H, Takakura Y, et al. Assessment of viability and osteogenic ability of human mesenchymal stem cells after being stored in suspension for clinical transplantation. Tissue Engineering 2006;12(6):1711-1719.

30.   Heng BC, Cowan CM, Basu S. Temperature and calcium ions affect aggregation of mesenchymal stem cells in phosphate buffered saline. Cytotechnology 2008;58(2):69-75.

31.   Formigli L, Benvenuti S, Mercatelli R, Quercioli F, Tani A, Mirabella C, et al. Dermal matrix scaffold engineered with adult mesenchymal stem cells and platelet-rich plasma as a potential tool for tissue repair and regeneration. J Tissue Eng Regen Med 2011.

32.   Blanton MW, Hadad I, Johnstone BH, Mund JA, Rogers PI, Eppley BL, et al. Adipose stromal cells and platelet-rich plasma therapies synergistically increase revascularization during wound healing. Plast Reconstr Surg 2009;123(2 Suppl):56S-64S.

33.   Hadad I, Johnstone BH, Brabham JG, Blanton MW, Rogers PI, Fellers C, et al. Development of a porcine delayed wound-healing model and its use in testing a novel cell-based therapy. Int J Radiat Oncol Biol Phys 2010;78(3):888-896.

34.   Dozza B, Di Bella C, Lucarelli E, Giavaresi G, Fini M, Tazzari PL, et al. Mesenchymal stem cells and platelet lysate in fibrin or collagen scaffold promote non-cemented hip prosthesis integration. J Orthop Res 2011;29(6):961-968.

35.   Kim WS, Park BS, Sung JH, Yang JM, Park SB, Kwak SJ, et al. Wound healing effect of adipose-derived stem cells: A critical role of secretory factors on human dermal fibroblasts. J Dermatol Sci 2007;48(1):15-24.

36.   Shi C, Li Q, Zhao Y, Chen W, Chen B, Xiao Z, et al. Stem-cell-capturing collagen scaffold promotes cardiac tissue regeneration. Biomaterials 2011;32(10):2508-2515.

37.   Blevins JS, Beenken KE, Elasri MO, Hurlburt BK, Smeltzer MS. Strain-dependent differences in the regulatory roles of sarA and agr in Staphylococcus aureus. Infect Immun 2002;70(2):470-480.

38.   Gillaspy AF, Hickmon SG, Skinner RA, Thomas JR, Nelson CL, Smeltzer MS. Role of the accessory gene regulator (agr) in pathogenesis of staphylococcal osteomyelitis. Infect Immun 1995;63(9):3373-3380.

39.   Arciola CR, Visai L, Testoni F, Arciola S, Campoccia D, Speziale P, et al. Concise survey of Staphylococcus aureus virulence factors that promote adhesion and damage to peri-implant tissues. International Journal of Artificial Organs 2011;34(9):771-780.

40.   Williams D, Bloebaum R, Petti CA. Characterization of Staphylococcus aureus strains in a rabbit model of osseointegrated pin infections. J Biomed Mater Res A 2008;85(2):366-370.

41.   Isackson D, McGill LD, Bachus KN. Percutaneous implants with porous titanium dermal barriers: an in vivo evaluation of infection risk. Med Eng Phys 2011;33(4):418-426.

42.   Rohde H, Kalitzky M, Kroger N, Scherpe S, Horstkotte MA, Knobloch JK, et al. Detection of virulence-associated genes not useful for discriminating between invasive and commensal Staphylococcus epidermidis strains from a bone marrow transplant unit. J Clin Microbiol 2004;42(12):5614-5619.

43.   Ki V, Rotstein C. Bacterial skin and soft tissue infections in adults: A review of their epidemiology, pathogenesis, diagnosis, treatment and site of care. Canadian Journal of Infectious Diseases and Medical Microbiology 2008;19(2):173-184.

44.   Barth E, Myrvik QM, Wagner W, Gristina AG. In vitro and in vivo comparative colonization of Staphylococcus aureus and Staphylococcus epidermidis on orthopaedic implant materials. Biomaterials 1989;10(5):325-328.

45.   Harris LG, Richards RG. Staphylococci and implant surfaces: a review. Injury 2006;37 Suppl 2:S3-14.

46.   Trampuz A, Piper KE, Jacobson MJ, Hanssen AD, Unni KK, Osmon DR, et al. Sonication of removed hip and knee prostheses for diagnosis of infection. N Engl J Med 2007;357(7):654-663.

47.   Han A, Zenilman JM, Melendez JH, Shirtliff ME, Agostinho A, James G, et al. The importance of a multifaceted approach to characterizing the microbial flora of chronic wounds. Wound Repair Regen 2011;19(5):532-541.

48.   Kobayashi H, Oethinger M, Tuohy MJ, Hall GS, Bauer TW. Improving clinical significance of PCR: use of propidium monoazide to distinguish viable from dead

Staphylococcus aureus and Staphylococcus epidermidis. J Orthop Res 2009;27(9):1243-1247.

49.   Miclau T, Schmidt AH, Wenke JC, Webb LX, Harro JM, Prabhakara R, et al. Infection. Journal of Orthopaedic Trauma 2010;24(9):583-586.

50.   Costerton JW, Post JC, Ehrlich GD, Hu FZ, Kreft R, Nistico L, et al. New methods for the detection of orthopedic and other biofilm infections. FEMS Immunol Med Microbiol 2011;61(2):133-140.

51.   Kadurugamuwa JL, Sin L, Albert E, Yu J, Francis K, DeBoer M, et al. Direct continuous method for monitoring biofilm infection in a mouse model. Infect Immun 2003;71(2):882-890.

52.   Kadurugamuwa JL, Sin LV, Yu J, Francis KP, Kimura R, Purchio T, et al. Rapid direct method for monitoring antibiotics in a mouse model of bacterial biofilm infection. Antimicrob Agents Chemother 2003;47(10):3130-3137.

53.   Kadurugamuwa JL, Sin LV, Yu J, Francis KP, Purchio TF, Contag PR. Noninvasive optical imaging method to evaluate postantibiotic effects on biofilm infection in vivo. Antimicrob Agents Chemother 2004;48(6):2283-2287.

54.   Franke GC, Dobinsky S, Mack D, Wang CJ, Sobottka I, Christner M, et al. Expression and functional characterization of gfpmut3.1 and its unstable variants in Staphylococcus epidermidis. J Microbiol Methods 2007;71(2):123-132.

55.   Rani SA, Pitts B, Beyenal H, Veluchamy RA, Lewandowski Z, Davison WM, et al. Spatial patterns of DNA replication, protein synthesis, and oxygen concentration within bacterial biofilms reveal diverse physiological states. J Bacteriol 2007;189(11):4223-4233.

56.   Vuong C, Kocianova S, Yu J, Kadurugamuwa JL, Otto M. Development of real-time in vivo imaging of device-related Staphylococcus epidermidis infection in mice and influence of animal immune status on susceptibility to infection. J Infect Dis 2008;198(2):258-261.

57.   Kodjikian L, Burillon C, Roques C, Pellon G, Freney J, Renaud FN. Bacterial adherence of Staphylococcus epidermidis to intraocular lenses: a bioluminescence and scanning electron microscopy study. Invest Ophthalmol Vis Sci 2003;44(10):4388-4394.

58.   Krimmer V, Merkert H, von Eiff C, Frosch M, Eulert J, Lohr JF, et al. Detection of Staphylococcus aureus and Staphylococcus epidermidis in clinical samples by 16S rRNA-directed in situ hybridization. J Clin Microbiol 1999;37(8):2667-2673.

59.   Boelens JJ, Dankert J, Murk JL, Weening JJ, van der Poll T, Dingemans KP, et al. Biomaterial-associated persistence of Staphylococcus epidermidis in pericatheter macrophages. J Infect Dis 2000;181(4):1337-1349.

60.   Zaat S, Broekhuizen C, Riool M. Host tissue as a niche for biomaterial-associated infection. Future Microbiol 2010;5(8):1149-1151.

61.   Broekhuizen CA, Sta M, Vandenbroucke-Grauls CM, Zaat SA. Microscopic detection of viable Staphylococcus epidermidis in peri-implant tissue in experimental biomaterial-associated infection, identified by bromodeoxyuridine incorporation. Infect Immun 2010;78(3):954-962.

62.   Godin B, Touitou E. Transdermal skin delivery: predictions for humans from in vivo, ex vivo and animal models. Advanced Drug Delivery Reviews 2007;59(11):1152-1161.

63.   Dorsett-Martin WA. Rat models of skin wound healing: a review. Wound Repair Regen 2004;12(6):591-599.

64.   Gottrup F, Agren MS, Karlsmark T. Models for use in wound healing research: a survey focusing on in vitro and in vivo adult soft tissue. Wound Repair Regen 2000;8(2):83-96.

65.   Davidson JM. Animal models for wound repair. Archives of Dermatological Research 1998;290 Suppl:S1-11.

66.   Sullivan TP, Eaglstein WH, Davis SC, Mertz P. The pig as a model for human wound healing. Wound Repair Regen 2001;9(2):66-76.

67.   Vodicka P, Smetana K, Jr., Dvorankova B, Emerick T, Xu YZ, Ourednik J, et al. The miniature pig as an animal model in biomedical research. Ann N Y Acad Sci 2005;1049:161-171.

68.   Quentin T, Poppe A, Bar K, Sigler A, Foth R, Michel-Behnke I, et al. A novel method for processing resin-embedded specimens with metal implants for immunohistochemical labelling. Acta Histochem 2009;111(6):538-542.

69.   Rammelt S, Corbeil D, Manthey S, Zwipp H, Hanisch U. Immunohistochemical in situ characterization of orthopedic implants on polymethyl metacrylate embedded cutting and grinding sections. J Biomed Mater Res A 2007;83(2):313-322.

70.   Vertenten G, Vlaminck L, Ducatelle R, Lippens E, Cornelissen M, Gasthuys F. Immunohistochemical analysis of low-temperature methylmethacrylate resin-embedded goat tissues. Anat Histol Embryol 2008;37(6):452-457.

71.   Willbold E, Witte F. Histology and research at the hard tissue-implant interface using Technovit 9100 New embedding technique. Acta Biomater 2010;6(11):4447-4455.

72.   Tillander J, Hagberg K, Hagberg L, Branemark R. Osseointegrated titanium implants for limb prostheses attachments: infectious complications. Clin Orthop Relat Res 2010;468(10):2781-2788.

73.   Aschoff HH, Clausen A, Tsoumpris K, Hoffmeister T. [Implantation of the endo-exo femur prosthesis to improve the mobility of amputees. Oper Orthop Traumatol 2011.

74.   Kang NV, Pendegrass C, Marks L, Blunn G. Osseocutaneous integration of an intraosseous transcutaneous amputation prosthesis implant used for reconstruction of a transhumeral amputee: case report. J Hand Surg Am 2010;35(7):1130-1134.

75.   Varol HA, Sup F, Goldfarb M. Multiclass real-time intent recognition of a powered lower limb prosthesis. IEEE Transactions on Bio-medical Engineering 2010;57(3):542-551.

76.   Hargrove LJ, Simon AM, Lipschutz RD, Finucane SB, Kuiken TA. Real-time myoelectric control of knee and ankle motions for transfemoral amputees. JAMA 2011;305(15):1542-1544.
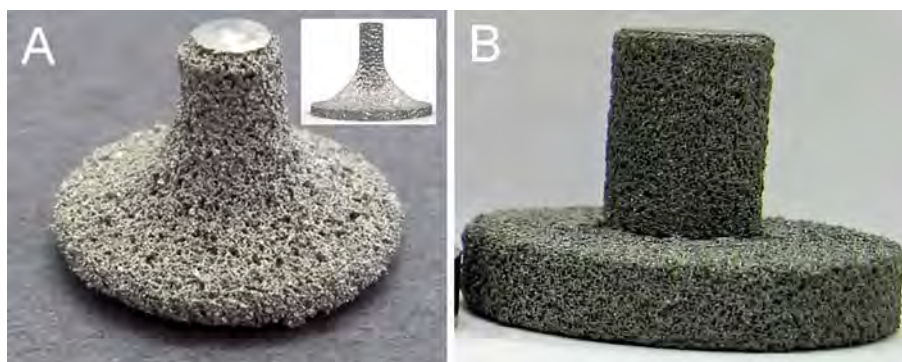
Figure 6.1. Porous titanium percutaneous implants. (A) Percutaneous implant with a sloped surface that was used in rat studies. The inset is the CAD (computer-aided design) representation of the implant. (B) Percutaneous implant with a right angle that was used in rabbit study.